Elucidating Exogenous Stimulation and Molecular Mechanisms for Browning in Pig Adipocytes

2024

KIM Sangwoo

Doctoral Program of
Animal Science and Agriculture
Graduate School of
Animal and Veterinary Sciences and Agriculture
Obihiro University of
Agriculture and Veterinary Medicine

ブタ脂肪細胞の褐色化に関する外因性刺激および分子機構の解明

令和 6 年

(2024)

帯広畜産大学大学院畜産学研究科

畜産科学専攻博士後期課程

金　翔　宇

CONTENTS

Chapter 3

SEASONAL ADAPTATION OF MANGALICA PIGS IN TERMS OF MUSCLE MORPHOLOGY AND METABOLISM

Chapter 4

SEASONAL ADAPTATION OF MANGALICA PIGS IN TERMS OF METABOLIC FUNCTION RELATED TO BROWNING FROM WHITE ADIPOCYTE

Abstract

The beige adipocyte is transformed from white adipocyte with adrenergic stimulation, for example, cold exposure, burn injuries, thyroid hormones, and catecholamine preparations. The transition from white adipocytes to beige adipocytes (browning) alters their metabolic functions, influencing physiological functions in both animals and humans. The browning was focused on human health care and it expected to serve as a new therapy for metabolic diseases such as obesity, diabetes mellitus, and dyslipidemia. However, the molecular mechanism of browning is not clearly understood.

The study of browning has been performed mainly in human or mouse fat tissues and on culture cell lines, such as 3T3-L1, derived from mouse embryonic cells. As ethical issues are posed by the use of human samples, it is difficult to use them for experiments on browning. Furthermore, previous study observed that different expressions between in vivo and in vitro conditions, and reported the result in experiments of adipocyte depend on the animal species. On the other hand, primary cultures of adipocyte can be immensely beneficial for the investigation of adipocyte functions. Therefore, other animal models and primary cultures can be applied to study browning to obtain insights on human metabolic diseases.

Pig shares similar features with human in terms of anatomy, genetics and physiology, making it a valuable animal model for human research. Previous studies have been reported to genetic similarity between pig and human with genome-wide sequencing of various tissues. In addition, the pig lacks functional UCP1 which is related to browning, so pigs are sensitive to cold environment as domesticated animals. This study specifically targeted the Mangalica Pig, a traditional breed in Hungary with unique physiology and characteristics as a lard-type pig. Mangalica has cold tolerance and can live in a grazing environment year-

round. However, it remains unclear whether white adipocytes undergo browning in response to seasonal changes in Mangalica, and the molecular mechanisms by which Mangalica acquires cold tolerance are yet to be revealed.

In this study, I conducted experiments to understand the molecular mechanisms of fat browning. At the cellular level (*in vitro*), I induced browning in adipocytes using primary cultures from a commercial pig breed's fat tissue. At the in vivo level, experiments with Mangalica were carried out to explore cold stimulation in thermogenic physiology, focusing on muscle and fat tissues. The goal was to achieve a comprehensive understanding of the browning process. In the cellular experiment, the administration of 1 μM isoproterenol to pig fat primary cultures significantly increased the gene expression of *PGC-1α* and *UCP3*, which are associated with browning, as well as the COX family genes related to mitochondrial function. Additionally, 1 μM isoproterenol upregulated lipolysis, leading to a significant decrease in the size of lipid droplets and lipid particle content. These results revealed browning in white adipocytes of pigs lacking UCP1. In the in vivo experiment, there was a distinct developmental pattern in fat tissue between Mangalica and a commercial pig breed. The muscle of Mangalica increased the gene expression of *ATP2A1* and *SLN*, and the fat tissue increased the gene expression of *PGC-1α*, *UCP1*, *UCP2*, and *UCP3* in winter compered to summer. The genes upregulated in the fat tissue of Mangalica were consistent with the browning observed in pig fat primary culture. These findings suggest that the fat tissue of Mangalica undergoes browning in winter, contributing to its cold tolerance.

This study is the first study that demonstrate fat browning using fat primary culture from pig, shedding light on the potential for browning in the fat tissue of Mangalica. These findings offer valuable insights into the mechanism of browning in white adipocytes and hold promise for contributing to the therapeutic interventions for human obesity.

要約

白色脂肪細胞は、寒冷刺激、火傷、甲状腺ホルモン刺激、およびアドレナリン作動性のカテコラミンなどの神経刺激によって代謝機能を亢進したベージュ脂肪細胞へと変化（褐色化）する。白色脂肪細胞の褐色化に関連する UCP1 は、主要な熱産生のタンパク質として考えられており、β3 アドレナリン受容体によるシグナル伝達によって活性化される転写因子である PGC-1α や、PRDM16 などによって発現が促進される。また UCP1 タンパク質は、脂肪酸を利用し、ミトコンドリアの電子伝達系にて脱共役作用により熱を産生する。したがって、褐色化は、白色脂肪細胞の代謝機能を大きく変え、哺乳動物およびヒトの生理機能に影響を与え、肥満などの代謝疾患に関する新たな治療方法として着目されている。褐色化研究は、ヒトまたはマウスの脂肪組織およびマウス受精卵から樹立した 3T3-L1 などの培養細胞株が主に使用されている。ヒト脂肪組織を用いた褐色化の研究は、ヒトの組織を使うという点に倫理的な問題が存在し、マウスの脂肪組織はインスリンの感受性がヒトと大きく異なるなど問題点が含まれている。さらに、以前の研究では、生体内（*in vivo*）と培養条件下（*in vitro*）で異なる実験結果が示されるなど、脂肪細胞の褐色化において一致した見解が得られていない。一方で、初代培養は、生体内に生理機能に近く、脂肪細胞の機能メカニズムを調べるために非常に有益ある。したがって、マウス以外の動物モデルの作製と初代培養の利用は、ヒトの代謝疾患に関する洞察を得るため利用でき、より生体に近いモデルとして期待されている。

ブタは、ヒトと解剖学的、遺伝学的および生理学的に類似しており、ヒトの生理機能研究において有益な動物モデルとして期待されている。ブタゲノム全体のシーケンシング結果は、ヒトの様々な組織における遺伝子群の発現パターンに最も類似であることが報告されている。また、ブタは機能的な UCP1 が欠損しており、寒冷環境に不耐性という特徴をもつ家畜である。そこで、本研究はハンガリーの伝統的な品種であるマンガリッツァブタに焦点を当て、研究を行なった。マンガリッツァはラードタイプのブタとし

て知られており、特徴的な生理機能を持っている。また、マンガリッツァは寒冷耐性を有し、一年を通じて放牧飼養が可能である。しかしながら、マンガリッツァが耐寒性を獲得する分子メカニズムは不明であり、白色脂肪細胞が季節の変化に応じて褐色化するかどうかはほとんど解明されていない。

本研究では、脂肪の褐色化の分子メカニズムを明らかにするために細胞（*in vitro*）および生体（*in vivo*）レベルで生理学研究を行った。まず *in vitro* レベルでは、商業用品種のブタの脂肪組織から得た初代培養を使用し、脂肪細胞の褐色化を誘導した。*in vivo* レベルでは、実際にマンガリッツァを用いて、筋肉および脂肪組織に焦点を当て、寒冷刺激による生理機能の変化を調べた。脂肪の初代培養を用いた培養実験では、1 μM のイソプロテレノールを投与することで、*PGC-1α*、*UCP3* およびミトコンドリア機能に関連する COX ファミリー遺伝子の発現が有意に増加した。さらに、1 μM のイソプロテレノールは、脂肪滴のサイズを有意に減少させ、細分化を誘導した。これらの結果は、UCP1 を欠いたブタの白色脂肪細胞においても褐色化を誘導できることを明らかにした。マンガリッツァを用いた生体実験では、成長に伴うマンガリッツァ特異的な脂肪組織の発達の違いを明らかにした。さらに、マンガリッツァは、冬季において筋肉中の *ATP2A1* および *SLN* の遺伝子発現、脂肪中の *PGC-1 α*、*UCP1*、*UCP2*、および *UCP3* の遺伝子発現が夏に比べて有意に増加し、非ふるえ熱産生による体温の上昇を示した。これらの結果は、ブタ脂肪初代培養で観察された褐色化時の遺伝子の発現動態と一致した。したがって、マンガリッツァの脂肪組織は、冬季に褐色化し、耐寒性を獲得している可能性を示唆した。

この研究は、ブタの脂肪初代培養を用いて脂肪の褐色化を初めて実証した。また、マンガリッツァの脂肪組織が冬季にベージュ脂肪細胞へ機能変化する可能性を示し、耐寒性を獲得されるメカニズムを明らかにした。本研究は、白色脂肪細胞における褐色化のメカニズムに関する貴重な知見を提供し、ヒトの代謝疾患の解明に資する基礎研究となった。

GENERAL INTRODUCTION

Fat cells play an important role such as supporting organ structure, attenuation of pressure, and maintenance of body temperature and metabolism (Zwick *et al.* 2018; Song & Kuang 2019). White adipocytes storage triglyceride as lipid and secrete adipokines, which include hormones and cytokines, and are biologically active substances. The brown adipocyte is well known for its physiological functions of high metabolism as it includes many mitochondria and promotes thermogenesis through the uncoupling protein (UCP) in mitochondrial membranes (Bargut *et al.* 2017; Jung *et al.* 2019). Previous studies have reported that the brown adipose tissue (BAT) is abundant in the interscapular and perirenal region in human until the adolescence period, but these gradually disappear (Heaton 1972; Yoneshiro & Saito 2015).

In 2005, the first research has reported that the adipocyte which have multilocular lipid droplets similar to brown adipocyte was discovered in WAT of mouse lacking *RBL1*(*as knowing p107*) expression (Scimè *et al.* 2005). Around 2010, it was increased that studies which investigated transformation of white adipocyte to brown-like adipocyte, and this conversion process from white adipocyte is referred to as “browning” and this brown-like phenotype was knowing as “beige adipocytes” (Spiegelman *et al.* 2009; Petrovic *et al.* 2010; Lshibashi & Seale 2010; Seale *et al.* 2011; Boström *et al.* 2012). Recent studies revealed that the browning was induced by adrenergic stimulation which is induced by cold exposure, burn injuries, thyroid hormones and catecholamine preparations (Patsouris *et al.* 2015; Hu & Christian 2017; Xu *et al.* 2019; Pinto *et al.* 2022). Furthermore, several studies also have been reported that the adipose browning was induced by cytokines related to inflammatory response (Goossens 2017; Reyes-Farias *et al.* 2021). This browning of white adipocyte to

beige adipocyte changed metabolic function in themselves and affected physiological function in animals and humans.

In animals, white adipocyte in mouse was browning to beige adipocyte with cold stimulation (Bal *et al.* 2017; Xu *et al.* 2019), and hamster was induced adipose browning in hibernate condition (Ryu *et al.* 2018). The browning of white adipocyte increased the heat production and related the adaptation to change of environment. In human, the metabolic function in fat tissue related the onset of obesity which the number of the patients has been rapidly increasing in worldwide (Goossens 2017; Longo *et al.* 2019; Reyes-Farias *et al.* 2021). Therefore, the browning, which increased the metabolic function in white adipocyte, was focused on human health care and it expected to serve as a new therapy for metabolic diseases such as obesity, diabetes mellitus, and dyslipidemia. However, the molecular mechanism of browning is not clearly understood.

The study of browning has been performed mainly in human or mouse fat tissues and culture cell lines, such as 3T3-L1 which is derived from mouse embryonic cells. As ethical issues are posed by the use of human samples, it is difficult to use them for experiments on browning. The mouse model exhibits distinct physiological functions compared to humans, including variations in leptin secretion, mitochondrial gene expression, enzyme reactions, and insulin sensitivity (Wang *et al.* 2014). Furthermore, previous study observed that different experimental results between in vivo and in vitro conditions, and reported the result in experiments of adipocyte depend on the animal species (Dufau *et al.* 2021). On the other hand, primary cultures of fat can be immensely beneficial for the investigation of adipocyte functions (Dufau *et al.* 2021). Therefore, other animal models and primary cultures can be applied to study browning to obtain insights on human metabolic diseases.

Pig shares similar features with human in terms of anatomy, genetics and physiology, making it a valuable animal model for human research (Lunney et al., 2021a; Meurens et al.,

2012a). Xenotransplantation using pig organs has been investigated, and recently, pig heart has been successfully transplanted to human (André R. Simon *et al.* 1999; Ibrahim *et al.* 2006; Cooper *et al.* 2018; Wang *et al.* 2022). Furthermore, genome-wide sequencing of various tissues of pig indicated genetic similarity with human (Li *et al.* 2017; Pan *et al.* 2021). Many studies have reported the similarity between adipose tissues of pig and human; therefore, the pig may be an optimal animal model compared to that of the mouse to investigate the functions of human adipose tissue. In addition, the pig lacks functional BAT and UCP1 which is thought the main thermogenesis protein within UCP family (Berg *et al.* 2006; Gaudry *et al.* 2017; Hou *et al.* 2017). A previous study has reported the genetic transfection of mouse UCP1 to pig induced fat browning and indicated the activation of the metabolic function (Zheng *et al.* 2017). Although pigs have been included to study the factors that activate the UCP family, information on the browning of white adipocytes in pigs is scarce.

Then, I focused on Mangalica Pig which is traditional breed in Hungary. Mangalica is thought to have evolved from Alföldi, Bakonyi and Szalontai, which are much older breeds that originated from domesticated Slovenian pigs and wild boars (Egerszegi *et al.* 2003). Mangalica shared a part of its genetic background with Hungarian wild boars and had characteristic features similar to those of wild boars compared to commercial breeds (Frank *et al.* 2017; Bâlteanu *et al.* 2019; Kaltenbrunner *et al.* 2019). Mangalica is classified by the colour of curly hair: red, blond and swallow belly. Furthermore, Mangalica has a unique fat tissue with a high rate of unsaturated fatty acids (Egerszegi *et al.* 2003; Tomović *et al.* 2016). Previous studies have reported that the developmental rate of Mangalica slowly compared to that of commercial breeds (Egerszegi *et al.* 2003; Takatani *et al.* 2021). However, Mangalica has cold tolerance and can be placed in a grazing environment throughout the year. When kept in cold conditions, the daily gain in body weight of Mangalica did not decrease compared to that of commercial breeds (Pârvu *et al.* 2012, 2012). In general, commercial pig

breeds are sensitive to environmental changes, and it was reported that the seasonal changes in temperature reduced their physiological functions such as development rate, metabolism and fertility (Claus & Weiler 1994; Carroll *et al.* 2012; Guo *et al.* 2018; Choi *et al.* 2019; Yu *et al.* 2021; Liu *et al.* 2022). However, it's are unclear that there are seasonal changes in body development, tissue structure and metabolism in Mangalica, and how Mangalica obtain the cold tolerance at grazing environment.

In this thesis, I performed the experiments that to reveal of the mechanism of browning using primary culture (*in vitro*) derived from fat tissue of commercial pig breed, and the cold tolerance physiology between muscle and fat tissues in Mangalica. In first chapter of this thesis, I examined the browning using pig fat primary culture and revealed the mechanism of browning in pig. In second chapter, I indicated the fat development through morphology and gene expression analysis from birth to finishing period in Mangalica. In third and fourth chapter, I examined to the seasonal change of metabolic function in muscle and fat tissue, and revealed the mechanism how Mangalica obtain the cold tolerance during seasonal changes.

I demonstrated that pig white adipocyte may have a potential to undergo browning. Moreover, through physiological studies ranging from primary cultures of pig adipocytes to fat tissue of Mangalica, it was elucidated that pig is a suitable animal model for browning study. This physiological study employing pigs could offer significant insights into the browning of white adipocytes, potentially contributing valuable knowledge for therapeutic interventions in human obesity.

Chapter 1

PIG UCP3 HAS AN ABILITY TO INDUCE ADIPOCYTE BROWNING THROUGH ADRB SIGNALING PATHWAY

1.1. Introduction

Fat cells play an important role in supporting organ structure, attenuation of pressure, and maintenance of body temperature and metabolism in terms of physiological functions (Zwick *et al.* 2018; Song & Kuang 2019). White adipocytes accumulate triglyceride and secrete adipokines, which include hormones and cytokines, and are biologically active substances. The brown adipocyte is well known for its physiological functions of high metabolism as it includes many mitochondria and promotes thermogenesis through the uncoupling protein (UCP) in mitochondrial membranes (Bargut et al., 2017a; Jung et al., 2019a). Previous studies have reported that the brown adipose tissue (BAT) is abundant in the interscapular and perirenal region in human until the adolescence period, but these gradually disappear (Heaton 1972; Yoneshiro & Saito 2015).

Recent research has revealed that nerve stimulation in a cold exposure, burn injuries, thyroid hormones and catecholamine preparations such as adrenaline can induce the transformation of white adipocytes into a brown-like phenotype known as “beige adipocytes”. This conversion process from white to beige adipocytes is often referred to as “browning” (Patsouris *et al.* 2015; Hu & Christian 2017; Xu *et al.* 2019; Pinto *et al.* 2022) . Browning is induced by the pathway that mediates β3 adrenergic receptor (ADRB3) and is activated by transcriptional factors such as peroxisome proliferator-activated receptor γ (PPARγ), PPARγ coactivator 1 alpha (PGC-1α), and PRDI-BF1 and RIZ (PR) domain containing 16 (PRDM16) (Seale *et al.* 2011; Ohno *et al.* 2012; Choi *et al.* 2021; Tabuchi & Sul 2021). The thermogenesis in brown and beige adipocytes are related to UCP, which enhances

the gene expressions of PPARγ, PGC-1α, and PRDM16. UCP induces a proton leak in the mitochondrial electron transport chain. UCP has several subtypes, UCP1 is well known for thermogenesis and expression in brown and beige adipocytes. UCP2 is detected in various tissues such as white adipose tissue, skeletal muscle, and heart. UCP3 is detected in the muscle and adipocyte. UCP4 and UCP5 are present mainly in the brain (Erlanson-Albertsson 2003). In particular, UCP1 is reported to play a critical role in thermogenesis as its expression in the brown adipocyte is more than those of the other members of the UCP family (Erlanson-Albertsson 2003). The UCP family activates the mitochondrial function and decreases the level of reactive oxygen species (Bouillaud *et al.* 2016; Hass & Barnstable 2021). Furthermore, it has been demonstrated that browning reduces body weight and increases lipolysis (Kaisanlahti & Glumoff 2019). Therefore, browning of white adipocytes is expected to serve as a new therapy for metabolic diseases such as obesity, diabetes mellitus, and dyslipidemia as it considerably changes self-metabolic functions. However, the molecular mechanism of browning is not clearly understood.

The study of browning has been performed mainly in human or mouse fat tissues and on culture cell lines, such as 3T3-L1, derived from mouse embryonic cells. As ethical issues are posed by the use of human samples, it is difficult to use them for experiments on browning. The mouse model exhibits distinct physiological functions compared to humans, including variations in leptin secretion, mitochondrial gene expression, enzyme reactions, and insulin sensitivity (Wang *et al.* 2014). Furthermore, it has been reported that 3T3-L1 cells indicate lower UCP1 expression even upon ADRB stimulation compared to prototypical brown adipocyte and transcription factors, such as PPARγ, which induces browning. However, different expressions were observed between in vivo and in vitro conditions, and depend on the animal species (Dufau *et al.* 2021). On the other hand, primary cultures of fat tissue can be immensely beneficial for the investigation of adipocyte functions (Dufau *et al.*

2021). Therefore, other animal models and primary cultures can be applied to study browning to obtain insights on human metabolic diseases.

Pig shares similar features with human in terms of anatomy, genetics and physiology, making it a valuable animal model for human research (Meurens *et al.* 2012; Lunney *et al.* 2021) . Xenotransplantation using pig organs has been investigated, and recently, pig heart has been successfully transplanted to human (André R. Simon *et al.* 1999; Ibrahim *et al.* 2006; Cooper *et al.* 2018; Wang *et al.* 2022). Furthermore, genome-wide sequencing of various tissues of pig indicated genetic similarity with human (Pan *et al.* 2021; Li *et al.* 2023). Many studies have reported the similarity between adipose tissues of pig and human; therefore, the pig may be an optimal animal model compared to that of the mouse to investigate the functions of human adipose tissue. In addition, the pig lacks functional BAT and UCP1 (Berg *et al.* 2006; Gaudry *et al.* 2017; Hou *et al.* 2017). A previous study has reported the genetic transfection of mouse UCP1 to pig induced fat browning and indicated the activation of the metabolic function (Zheng *et al.* 2017). Although pigs have been included to study the factors that activate the UCP family, information on the browning of white adipocytes in pigs is scarce.

In this study, we examined the browning of white adipocytes using pig primary culture. In the pig primary culture, there was an upregulation of gene expression for UCP3, and the lipid droplets were fragmented into smaller particles through ADRB signaling induced by isoproterenol stimulation. These findings suggest that pigs have the potential to induce browning of white adipocytes. Our study offers insights into the mechanism of adipocyte browning using a pig primary culture, which may have potential applications in humans.

1.2. Materials and Methods

1.2.1. Animals and animal ethics

Commercial breed pigs (5-7 mons old) were obtained from a local slaughter house and adipose tissues were used for experiment (n = 4). The study and management of all animals used in this study were conducted in accordance with the Guidelines for the Care and Use of Animals of the Obihiro University of Agriculture and Veterinary Medicine (approval numbers 22-165 and 23-159).

1.2.2 In vitro pig pre-adipocyte isolation and browning

All adipocytes were collected from neck adipose tissues of slaughtered pigs. Isolation of dedifferentiation fat cell (DFAT) from white adipose tissue was performed as described by previous study (Shen *et al.* 2011). Briefly, the adipose tissue was minced, and digested with 1 mg/ml collagenase type I (037-17603, Fujifilm Wako, Osaka, Japan) in Dulbecco's modified Eagle medium (DMEM)/F12 (048-29785, Fujifilm Wako) plus 1% penicillin-streptomycin (168-23191, Fujifilm Wako) for 90 min at 37 °C. After digestion, tissue homogenates were filtrated through 70 μm mesh filter (VCS-70, AS ONE, Osaka, Japan) to remove undigested tissue and centrifuged at 1500 rpm for 10 min. Floating adipocyte in supernatant fluid were collected in a T-flask and filled with DMEM/F12 containing 10% fetal bovine serum (FBS, OAC-001, Japan Bioserum, Fukuyama, Japan) and 1% penicillin-streptomycin. The adipocytes were cultured for 9 days at 37 °C to dedifferentiation. After 9 days, DFAT was collected and used in experiments as primary culture of pig fat tissue.

Browning was induced according to the procedure used for mouse by Miller et al. (2015). Briefly, DFAT was cultured by DMEM/F12 containing 10% FBS and 1% penicillin-streptomycin. For differentiation, confluent DFAT cells (designated as Day 0) were cultured in the induction media (DMEM/F12 medium containing 10 μg/ml human insulin (099-06473,

Fujifilm Wako), 1 nM Triiodothyronine (T3) (T6379-100MG, Sigma-Aldrich, MO, USA), 10 μg/ml transferrin (201-18081, Fujifilm Wako), 1 μM rosiglitazone (180-02653, Fujifilm Wako), and 1 μM dexamethasone (047-18863, Fujifilm Wako)) for 3 days (Day 3). At day 3, the culture medium was switched to the maintenance medium (DMEM/F12 medium containing 10 μg/ml human insulin, 1 nM T3, 10 μg/ml transferrin, and 1 μM rosiglitazone) for 3 days (Day 6). To induce browning, the medium was changed to a new maintenance medium, and isoproterenol (I6504-100MG, Sigma-Aldrich) was administered to the medium at concentrations of 0, 0.01, 0.1, 1, 10, and 100 μM for a duration of 6 h.

1.2.3. RNA preparation and real-time PCR

After inducing browning, cells were harvested and homogenized using EZ beads (No. 76813M, AMR, Inc., Tokyo, Japan). Total RNA was extracted using TRIzol reagent (15596018, Thermo Fisher Scientific, MA, USA). For cDNA synthesis and real-time PCR, we followed the methods described in previous study (Kim *et al.* 2023). In brief, the total RNA concentration was determined using a Nanodrop (Thermo Fisher Scientific). 1 μg of total RNA was treated with DNase and converted into cDNA using Random Primers (48190011, Thermo Fisher Scientific) and SuperScriptTM II (18064022, Thermo Fisher Scientific) with a GeneAtlas thermal cycler 482 (4990902, ASTEC, Fukuoka, Japan).

Real-time PCR was conducted using SsoAdvancedTM Universal SYBR® Green Supermix (1725271, Bio-Rad, CA, USA) and the LightCycler® 96 system (05815916001, Roche, Basel, Switzerland) following the manufacturer's instructions. The PCR conditions included an initial denaturation step at 95 °C for 30 s, followed by 35 cycles of denaturation at 95 °C for 10 s, and annealing/extension at 60 °C for 60 s. The primer sequences used are listed in Table 1. Beta-actin (ACTB) was utilized as the internal control, and the relative gene expression levels were calculated using the $2^{-\Delta\Delta CT}$ method.

1.2.4. Lipid staining after browning

To calculate the number of lipid droplets in browning cells, the cells were visualized using LipiDye II (FDV-0027, FNA, Tokyo, Japan), which is a specific staining reagent. The treatment procedure was according to the instructions of the reagent manufacturer. LipiDye II staining was performed on adipocytes prior to isoproterenol treatment. Cell observations using fluorescein isothiocyanate were conducted on days 6 and 9 after isoproterenol administration. Images of cells were captured over 10 fields using a fluorescence microscope (DMi8, Leica, Wetzlar, Germany) and processed using Leica Application Suite X software (Leica). For each group, 100 adipocytes with lipid droplets were counted to determine the lipid droplet count.

1.2.5. Determination of mitochondrial function and copy number

Total DNA, comprising both genomic and mitochondrial DNA (mtDNA), was extracted from the browning adipocytes. DNA concentration was determined using Nanodrop (Thermo Fisher Scientific). To quantify the relative mtDNA copy number compared to genomic DNA, real-time PCR was performed using the LightCycler® 96 system. The primers used for amplification were as follows: COX-II: forward GGCTTACCCTTTCCAACTAGG, reverse AGGTGTGATCGTGAAAGTGTAG; β-globin: forward GGGGTGAAAAGAGCGCAAG, reverse CAGGTTGGTATCCAGGGCTTCA.

1.2.6. Alignment analysis

The alignment analysis was performed using CLUSTALW (https://www.genome.jp/tools-bin/clustalw) for the following genes and their promoter regions, with a focus on the 1000 bp from the transcriptional start site in the UCP family: UCP1, UCP2, UCP3, PPARγ, and

PGC-1α. Accession numbers of the analyzed nucleotides were obtained from the National Center for Biotechnology Information (https://www.ncbi.nlm.nih.gov) and are as follows:

- Pig chromosome 8 and 9 including UCP1 (XM_021100543.1), UCP2 (NM_214289.1), UCP3 (NM_214049.1), PPARγ (NM_214379.1), and PGC-1α (NM_213963.2)
- Human chromosome 4 and 11 including UCP1 (NM_021833.5), UCP2 (NM_001381943.1), UCP3 (NM_003356.4), PPARγ (NM_138712.5), and PGC-1α (NM_001330751.2)
- Mouse chromosome 7 and 8 including UCP1 (NM_009463.3), UCP2 (NM_011671.6), UCP3 (NM_009464.3), PPARγ (NM_001127330.3), and PGC-1α (NM_008904.3)
- Cattle chromosome 7, 15, and 17 including UCP1 (NM_001166528.1), UCP2 (NM_001033611.2), UCP3 (NM_174210.1), PPARγ (NM_181024.2), and PGC-1α (NM_177945.3)
- Macaca mulatta chromosome 2, 5, and 14 including UCP1 (XM_001090457.4), UCP2 (NM_001195393.1), UCP3 (XM_015115192.2), PPARγ (NM_001032860.1), and PGC-1α (XM_028848369.1)
- Chicken chromosome 1, 4, and 12 including UCP3 (NM_204107.2), PPARγ (NM_001001460.2), and PGC-1α (NM_001006457.2)
- Zebrafish chromosome 1, 7, 10, and 11 including UCP1 (NM_199523.2), UCP2 (NM_131176.1), UCP3 (NM_200353.2), PPARγ (NM_131467.1) and PGC-1α (XM_017357138.2).

1.2.7. Plasmids

A fragment containing a 5′ upstream region of pig UCP3 genes (−911/+90) was amplified using genomic PCR. They were cloned into a pGL4.10 [Luc2] vector (E6651, Promega Corporation, WS, USA). The pcDNA3 that expresses PPARγ was generated by

cloning the open reading frame of rat PPARγ into a pcDNA3.1 vector (V79020, Thermo Fisher Scientific). pcDNA3.1/PGC-1α was prepared as described by previous study (Yazawa *et al.* 2010).

1.2.8. Transfection and luciferase assay

Hela cells were cultured in DMEM (Nacalai Tesque Inc., Kyoto, Japan) supplemented with 10% FBS (Nichirei Bioscience Inc., Tokyo, Japan) and penicillin-streptomycin (Nacalai Tesque Inc.). Transfection of these cells was performed using HilyMax (H357, Dojindo Laboratories, Kumamoto, Japan). One day before lipofection, cells were seeded on 48-well plates and cultured in DMEM supplemented with 10% normal FBS or HyClone charcoal/dextran-treated FBS (GE Healthcare U.K. Ltd., Buckinghamshire, England). Vectors were transfected into Hela cells. One day after transfection, cells were supplemented with 1 μM isoproterenol or 5 μM troglitazone. Luciferase activity was determined using dual luciferase reporter assay system (Progema Corporation, CA, USA) and MiniLumat LB9506 (Berthold Systems, PA, USA) in a single tube, with the first assay of firefly luciferase, followed by the Renilla luciferase assay. Firefly luciferase activities (relative light units) were normalized by Renilla luciferase activities. Each data point represents the mean of at least four independent experiments.

1.2.9. Statistical analyses

Statistical analyses were performed using RStudio Version 1.3.1073 (https://www.rstudio.com/products/rstudio/). Comparisons of multiple groups were analyzed using Tukey and Dunnett's test with multivariate ANOVA. Comparisons between two groups were analyzed using Student's or Welch's *t*-test and *U*-test. Results were depicted as mean ± standard error of the mean (SEM.) and a p value of < 0.05 was considered significant.

1.3. Results

1.3.1. Isoproterenol increased gene expression of PGC-1α and UCP3 in pig DFAT

To examine whether adipocyte browning is induced in DFAT obtained from fat tissue in pig, DFAT was administered with isoproterenol, which is an agonist of beta-adrenergic receptor (ADRB), at concentrations of 0, 0.01, 0.1, 1, 10, or 100 μM, after differentiation. The expression of genes related to thermogenesis and their transcriptional factors was measured using RT-PCR and compared with the control. The administration of 100 μM isoproterenol significantly decreased the gene expression of *PPARγ*, *UCP1,* and *UCP2* ($p < 0.05$, Figure 1A and B). The concentration of 10 μM isoproterenol increased only the gene expression of *PGC-1α*, whereas 1 μM isoproterenol significantly increased the gene expression of *PGC-1*α and *UCP3* ($p < 0.05$, Figure 1A and B). The concentration of 0.1 μM isoproterenol significantly increased the gene expression of *UCP2* and *UCP3*, whereas it did not affect the gene expression of *PGC-1α* ($p < 0.05$, Figure 1A and B). The concentration of 0.01 μM isoproterenol did not affect any gene expression. Furthermore, 1 μM isoproterenol did not affect genes related to apoptosis (Figure 2). Thus, the concentration of 1 μM isoproterenol is suitable for the browning experiment, and was used for subsequent experiments.

1.3.2. PPARγ and PGC-1α activate to pig UCP3 promoter

To investigate whether *UCP3* follows a similar regulation of transcription factor as that of mouse *UCP1*, we conducted a luciferase assay using HeLa cells transfected with *PPARγ*, *PGC-1α*, and a combination of both, and calculated the activation of the *UCP3* promoter region. Interestingly, the transfection of *PPARγ* or *PGC-1α* alone did not significantly increase luciferase activation. However, co-transfection of *PPARγ* and *PGC-1α* expression

vectors markedly induced the luciferase activation compared to that of the control group ($p < 0.05$, Figure 3A and B).

Furthermore, we examined the influence of isoproterenol and troglitazone, a ligand of *PPARγ*, on the activation of the *UCP3* promoter. Remarkably, the luciferase activity was further enhanced by the administration of troglitazone (Figure 3A). In contrast, isoproterenol administration did not affect the luciferase activity (Figure 3B).

1.3.3. Gene alignment: human closer to pig than mouse

The results of luciferase assay indicated that pig *UCP3* promoter is activated by *PPARγ* and *PGC-1α*, similar to the activation mechanism observed for mouse *UCP1*. Following this we conducted an alignment analysis to explore the genetic similarities of UCP family and transcription factors among pig and vertebrates.

In the alignment analysis, we compared the sequences of *PPARγ*, *PGC-1α*, and UCP family across pig, human, mouse, and cattle. Notably, the alignment scores of *PPARγ*, *PGC-1α*, *UCP2*, and *UCP3* were the highest between pig and human (Table 2 and Figures 4, 5, and 6). Although the alignment score of *UCP1* between pig and human was the lowest compared to those with other species, the upstream region of *UCP1* had the same sequence as that of the *PPARγ*-binding site (Table 2 and Figure 3C). Furthermore, the alignment scores for *UCP1* and *UCP3* promoter regions were higher between pig and human than that between mouse and human (Table 3 and Figure 3C). However, the alignment score for *UCP2* was lower between pig and human than that between mouse and human (Table 3).

1.3.4. UCP3 is activated via ADRB signaling

UCP1 is known to be activated via ADRB signaling (Miller *et al.* 2015). In the next experiment, we administered propranolol, an ADRB antagonist, to differentiated DFAT cells

to examine whether *UCP3* activation occurs through ADRB signaling as observed in mouse *UCP1*. This was performed because pig *UCP3* was activated by *PPARγ* and *PGC-1α* as in mouse *UCP1*. The administration of 10 μM propranolol significantly decreased the expression of *PGC-1α* and *UCP3*, both of which were upregulated by isoproterenol (Figure 7).

1.3.5. Isoproterenol induced lipid droplet fragmentation in pig DFAT cells

To investigate whether the activation of pig *UCP3* by isoproterenol administration influences lipolysis in pig DFAT cells, we employed LipiDye II staining to quantify the number of lipid droplets (Figure 8A). On both days 6 and 9, we assessed the average the number of lipid droplets per unit area within cells after the administration of 1 μM isoproterenol and LipiDye II.

On day 6, the average number of lipid droplets in the isoproterenol group was 0.108 ± 0.004 $\times 10^2$/cell/μm^2, showing no significant difference compared to the control group (0.113 ± 0.004 $\times 10^2$/cell/μm^2, Figure 8B). However, on day 9, there was a significant increase in the average number of lipid droplets in the in the isoproterenol group (0.097 ± 0.004 $\times 10^2$/cell/μm^2, Figure 8C, D, and E) compared to the control group (0.079 ± 0.004 $\times 10^2$/cell/μm^2, $p < 0.001$). This reduction in lipid droplets within cells indicates lipid droplet cleavage and the activation of lipolysis, which is a characteristic feature associated with the browning of white adipocytes.

1.3.6. Enhancement of mitochondrial function in pig DFAT by isoproterenol

As the induction of an adipocyte browning phenotype in pig DFAT through isoproterenol stimulation was observed, we proceeded to investigate the mitochondrial functions associated with the browning process. The expression of citrate synthase, which indicates

mitochondrial abundance, was not affected by the administration of 1 μM isoproterenol (Figure 9A). In contrast, the expression of *COX1*, *COX2*, and *COX3*, which are related to mitochondrial function, significantly increased after the administration of isoproterenol ($p < 0.05$, Figure 9B).

1.4. Discussion

This study indicates that pig DFAT isolated from pig fat tissue undergoes browning when exposed to isoproterenol, which activates through the ADRB pathway, similar to that observed in *UCP1*. This stimulation leads to an increase of the expression of *UCP3* and *COX* gene family, and induction to the lipid droplets fragmentation. These results offer valuable insights into the mechanisms underlying the browning of white adipocytes.

Previous studies have reported that isoproterenol concentrations of 1–10 μM increase the expression of *UCP1* and *PGC-1α*, thereby inducing the browning of white adipocytes in primary cultures derived from human and mouse white adipose tissue (Miller *et al.* 2015; Markussen *et al.* 2017; Ng *et al.* 2021). Furthermore, the browning of white adipocytes into beige adipocytes has been associated with enhanced lipid metabolism and a reduction in the size of lipid droplet (Piao *et al.* 2018; Chen *et al.* 2021). Previous studies also reported that lipolysis induced reduction of the size and fragmentation of the lipid droplets (Ducharme & Bickel 2008; Schott *et al.* 2019). Similarly, our study on pig DFAT derived from adipose tissue revealed increased gene expression of *PGC-1α* and *UCP3,* and a reduction in size of lipid droplet caused by the administration of 1 μM isoproterenol. Although previous studies have reported that pigs lacked exon 3 to exon 5 in *UCP1*, and the functional BAT was absent (Berg *et al.* 2006; Gaudry *et al.* 2017; Hou *et al.* 2017), another study demonstrated an increase in *UCP3* expression in pig adipose tissue in response to cold exposure (Lin *et al.* 2017). The results of our study support previous studies on pig adipose tissue that suggested that pig white adipocytes can undergo browning independently of *UCP1*.

It is well known that the expression of *UCP1* in BAT and beige adipocyte is induced by *ADRB3* signaling through PKA and p38 MAPK/ERK pathway and the upregulation of key genes, such as *PPARγ*, *PGC-1α*, and *PRDM16* (Mottillo *et al.* 2014; Cypess *et al.* 2015; Choi *et al.* 2021; Mukherjee & Yun 2022). In this study, results of the promoter assay indicate that

the promoter region of pig *UCP3* was activated by *PPARγ* and *PGC-1α*. This suggests that pig *UCP3* may share a similar thermogenic mechanism with *UCP1*. Notably, pig adipose tissue lacks the expression of *ADRB3* (Li *et al.* 2017). Furthermore, recent human studies have shown that the activation of *ADRB1* using selective agonists significantly increases the gene expression of *UCP1* in brown adipocytes, while selective agonists of *ADRB3* did not have the same effect (Mattsson *et al.* 2011; Riis-Vestergaard *et al.* 2020). These results suggest that pig adipose tissue may serve as an optimal animal model for studying the browning of white adipocytes in humans. In this study, we did not delineate the specific signaling pathway connecting ADRB to p38 MAPK/ERK for *UCP3* activation. Additionally, our luciferase assay indicated that the stimulation of PPARγ using troglitazone may activate the *UCP3* promoter to a greater extent than *PGC-1α* stimulation through ADRB signaling using isoproterenol. Consequently, future experiments should focus on investigating the individual roles of these transcription factors in UCP promoter activation. In this study, we did not delineate the specific signaling pathway that connects ADRB to p38 MAPK/ERK for *UCP3* activation. In addition, the luciferase assay indicates that the stimulation of *PPARγ* using troglitazone may activate the *UCP3* promoter more than *PGC-1α* stimulation through ADRB signaling using isoproterenol. Hence, in future experiments, we should investigate the role of each transcription factor in the activation of the UCP promoter.

The expression of *UCP3* has been reported to be significantly lower by 200–700-fold compared to *UCP1* in BAT, and *UCP3* has a shorter half-life compared to *UCP1* in mice (Erlanson-Albertsson 2003; Pohl *et al.* 2019). Thus, *UCP1* has been regarded as the primary protein involved in thermogenesis. Limited information is available about the function of *UCP3* compared to *UCP1*. Previous studies on mice have shown that the deletion of the *UCP3* did not significantly impact the physiological function (Gong *et al.* 2000; Vidal-Puig *et al.* 2000). In addition, *UCP3* in muscle did not influence the accumulation of intracellular

lipid and mitochondrial function (Nabben *et al.* 2014). However, in human studies, dietary interventions aimed at reducing calorie intake for obesity patients revealed a positive correlation between carbohydrate oxidation and *UCP3* expression (Cortes de Oliveira *et al.* 2018). Overexpression of *UCP3* in primary cultures using human muscle was found to increase both glucose and fatty acid oxidation (García-Martínez *et al.* 2001). Furthermore, avian uncoupling protein (avUCP), which shares high homology with human *UCP3*, has been suggested as an important protein for thermogenesis in avian species such as chicken, hummingbirds, and king penguins (Dridi *et al.* 2004; Emre *et al.* 2007). In other study on chicken, the avUCP, which is orthologous to UCP3, was activated by cold exposure and ADRB stimulation using isoproterenol, contributing to the induction of beige-like adipose tissue (Joubert *et al.* 2010; Sotome *et al.* 2021). Thus, the functional role of *UCP3* appears to be adaptable and may vary based on the presence of BAT or *UCP1* among different animal species.

In summary, our study has revealed that DFAT derived from pig fat tissue may undergo browning, facilitated by a signaling pathway involving ADRB activation and the gene expression of *PPARγ* and *PGC-1α*, similar to that of the *UCP1* pathway observed in humans (Figure 10). Notably, the genetic sequences of *PPARγ*, *PGC-1α*, and *UCP3* in pigs exhibit higher homology with those of humans than with mice. These suggests that pigs may serve as a suitable animal model for the investigation of the molecular mechanisms underlying the browning of white adipocytes, particularly for adult humans, in whom BAT is absent. Our study offers important insights into the mechanisms that govern the browning of white adipocytes and provides valuable information for understanding metabolic diseases in humans.

Figure and captions

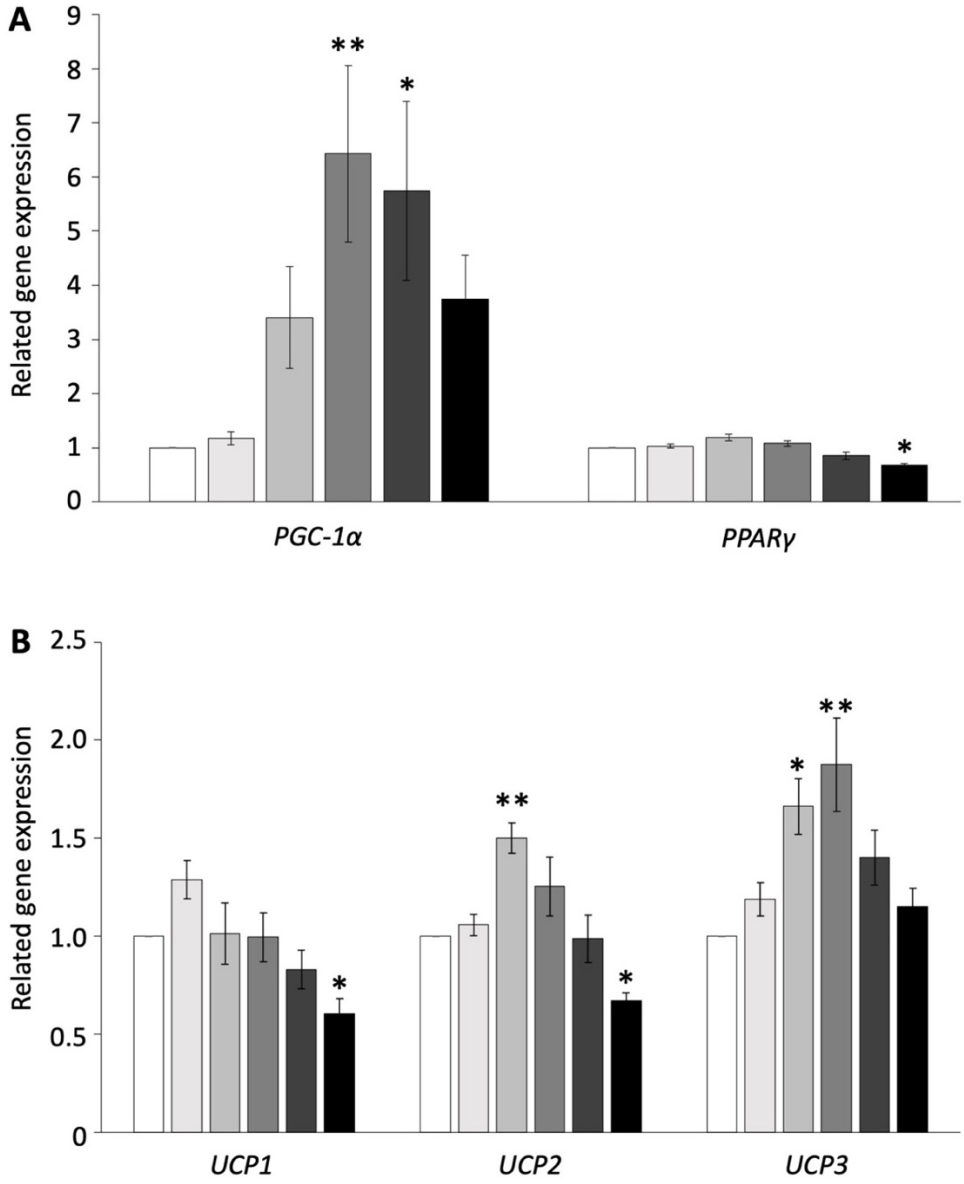

FIGURE 1. Gene expressions of pig DFAT after isoproterenol administration. (A) Gene expression of *PGC-1α* and *PPARγ* related activation of UCP (n = 4). (B) Gene expression of *UCP1*, *UCP2*, and *UCP3*. The experiments were conducted more than twice and values of the treatment and control groups were compared. Each square indicates the concentration of isoproterenol: ( ) control, ( ) 0.01 μM, ( ) 0.1 μM, ( ) 1 μM, ( ) 10 μM, and ( ) 100 μM. The values are shown as mean ± SEM. and * $p < 0.05$, and ** $p < 0.01$.

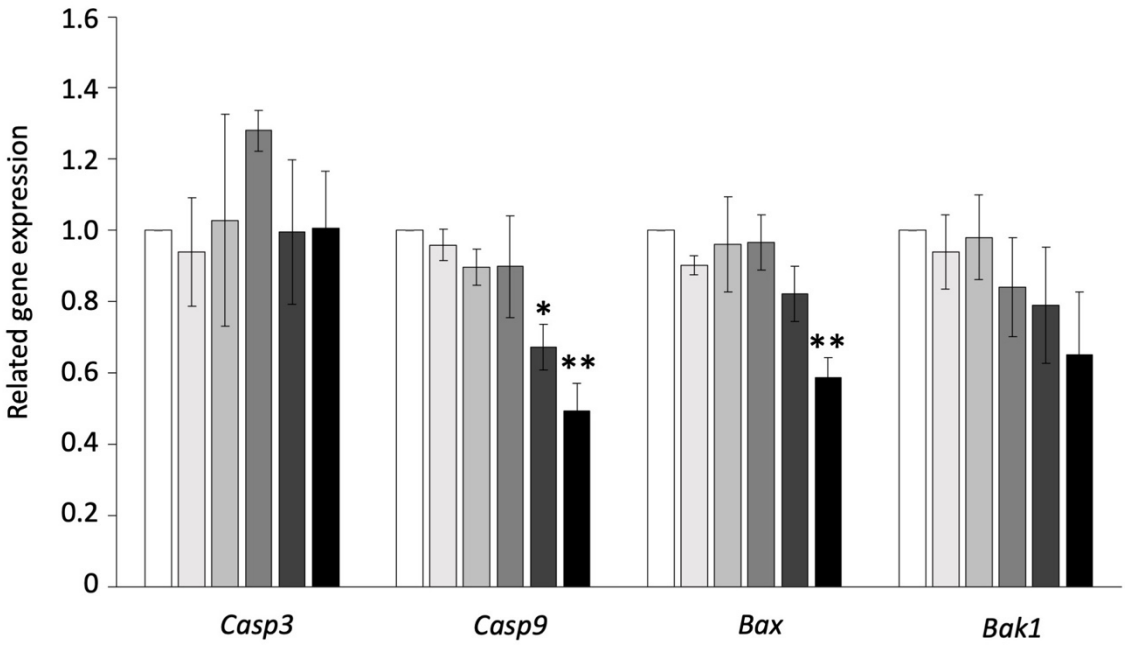

FIGURE 2. Gene expressions related to apoptosis of pig DFAT after isoproterenol administration. Values of the treatment and control groups were compared (n = 4). The experiments were conducted more than two times. Each square indicate concentration of isoproterenol: (□) control, (□) 0.01 μM, (□) 0.1 μM, (□) 1 μM, (■) 10 μM, and (■) 100 μM. The values are shown as mean ± SEM. and * $p < 0.05$, ** $p < 0.01$.

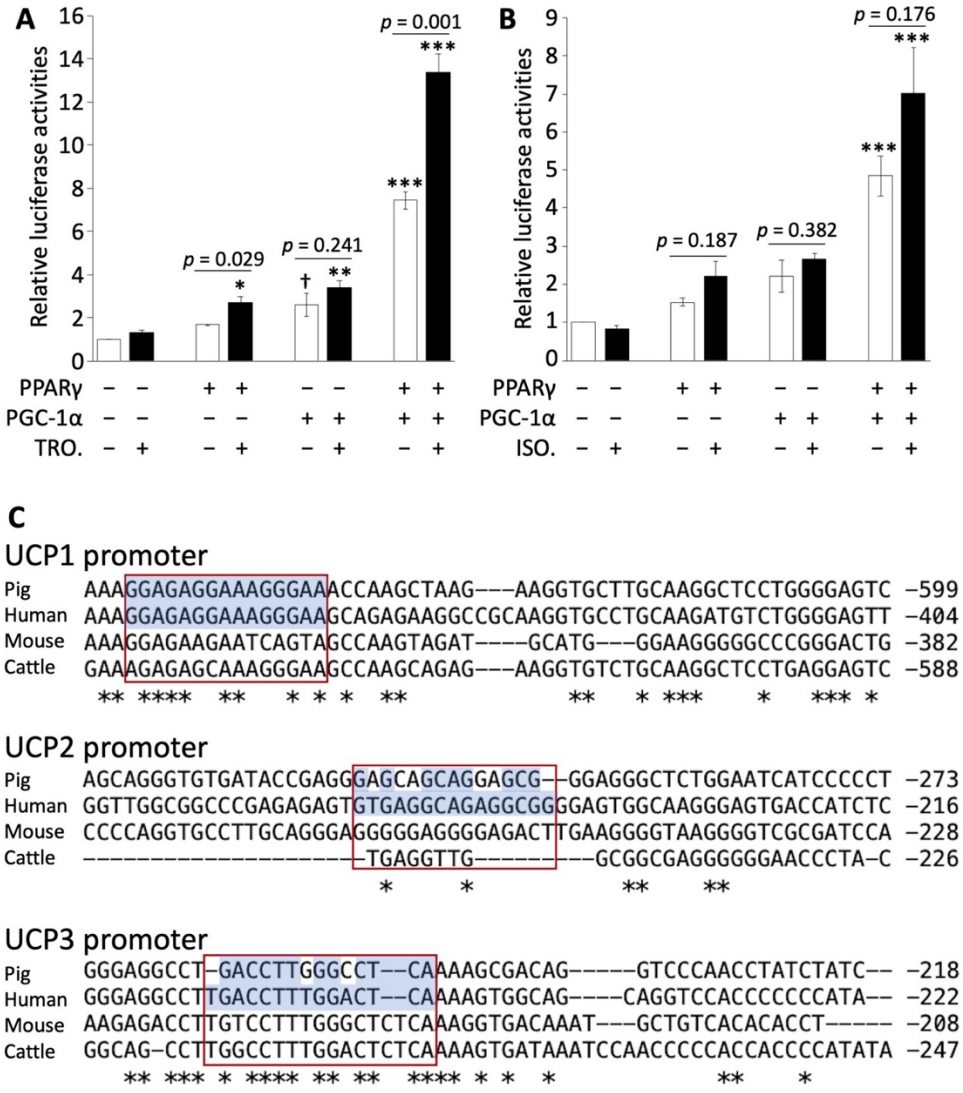

FIGURE 3. Luciferase assay of pig UCP promoter region and alignment analysis. (A) Luciferase assay using Hela cells transfected *PPARγ* or/and *PGC-1α* with/without 1 μM isoproterenol (ISO.) (n = 3). (B) Luciferase assay using Hela cells transfected *PPARγ* or/and *PGC-1α* with/without 5 μM troglitazone (TRO.) (n = 4). (C) Comparison of the sequence of the *PPARγ*-binding site in UCP promoters among several animal species in the promoter region. The asterisks (*) are the conserved nucleotides among all species. The conserved *PPARγ* binding site are shown by redline boxes. The experiments were conducted more than twice and compared to the control. The values are shown as mean ± SEM. and * $p < 0.05$, ** $p < 0.01$, and *** $p < 0.001$.

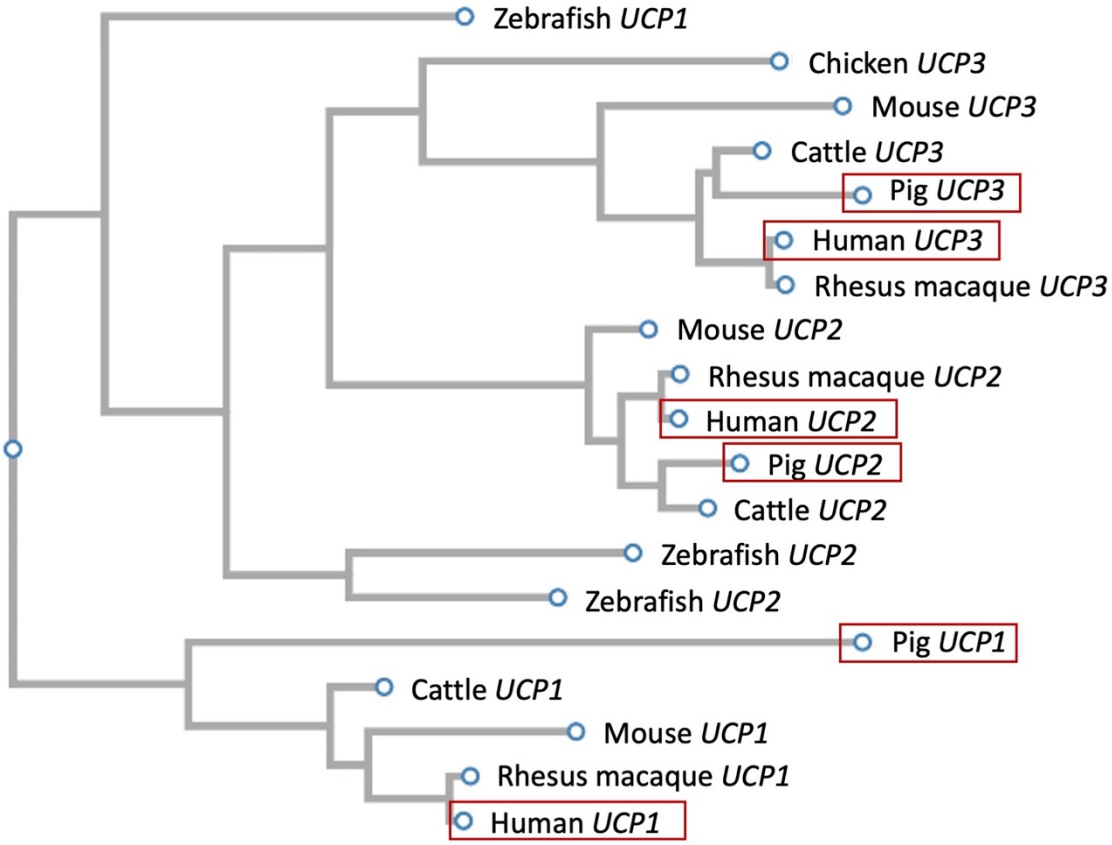

FIGURE 4. Tree diagram of mRNA sequence of UCP family in vertebrates. The redline boxes indicate pig and human genes.

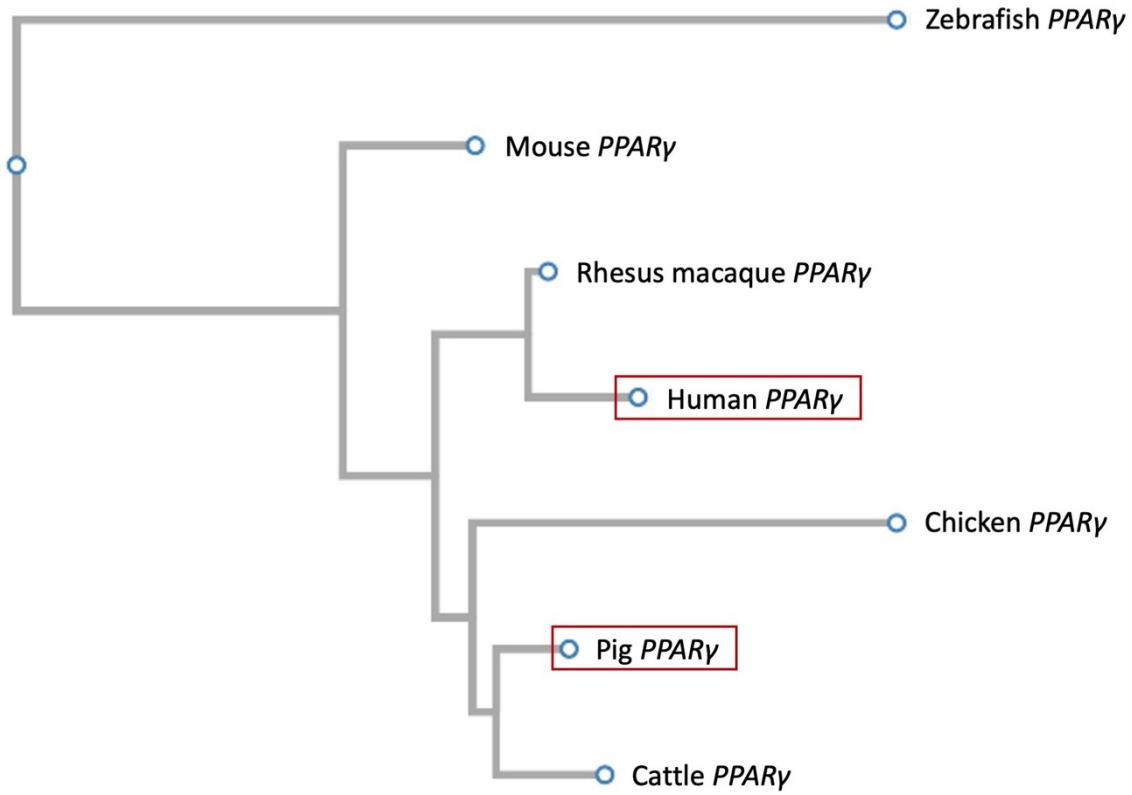

FIGURE 5. Tree diagram of mRNA sequence of *PPARγ* in vertebrates. The redline boxes indicate pig and human genes.

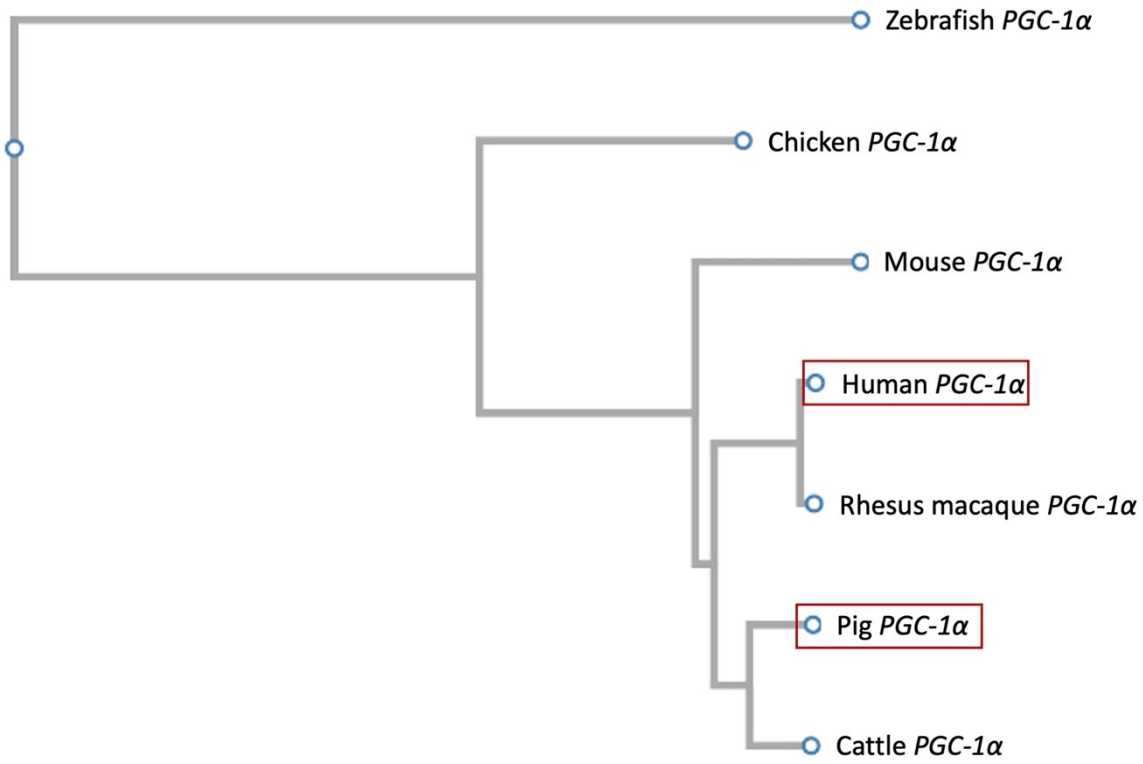

FIGURE 6. Tree diagram of mRNA sequence of *PGC-1α* in vertebrates. The redline boxes indicate pig and human genes.

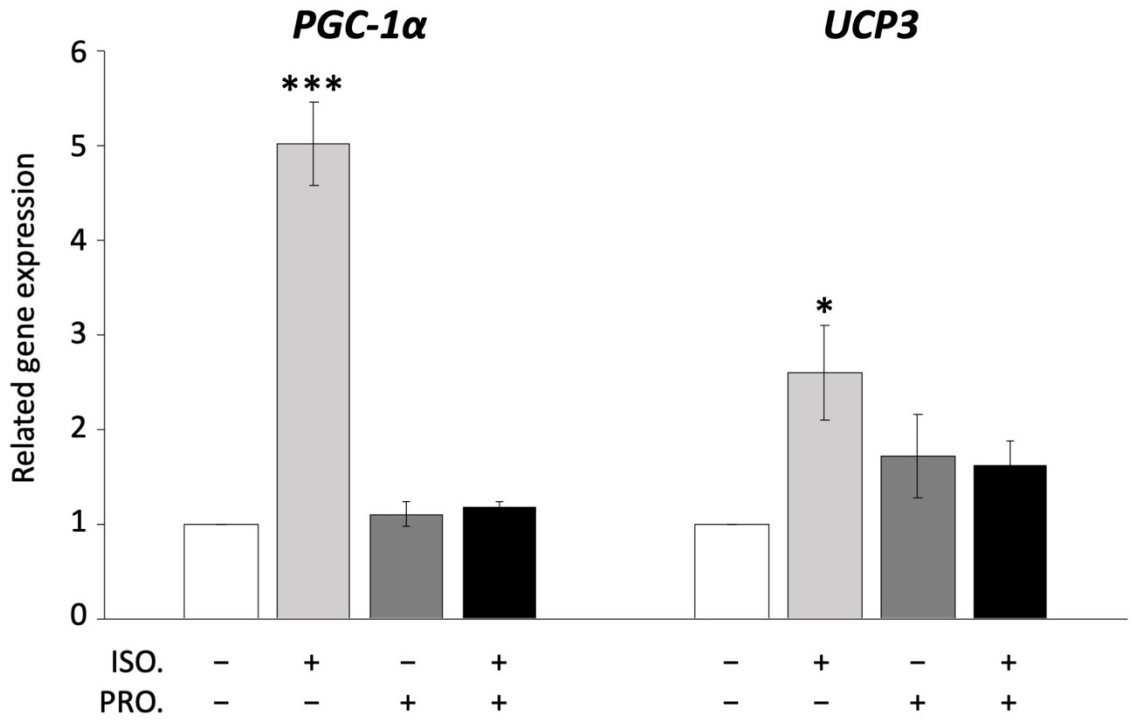

FIGURE 7. Inhibition of ADRB signaling using propranolol in pig DFAT. Experiments using 1 μM isoproterenol (ISO.) and 10 μM propranolol (PRO.) (n = 3). The experiments were conducted more than twice. Gene expression was compared to that of the control and the values of gene expression are shown as mean ± SEM., * $p < 0.05$ and *** $p < 0.001$.

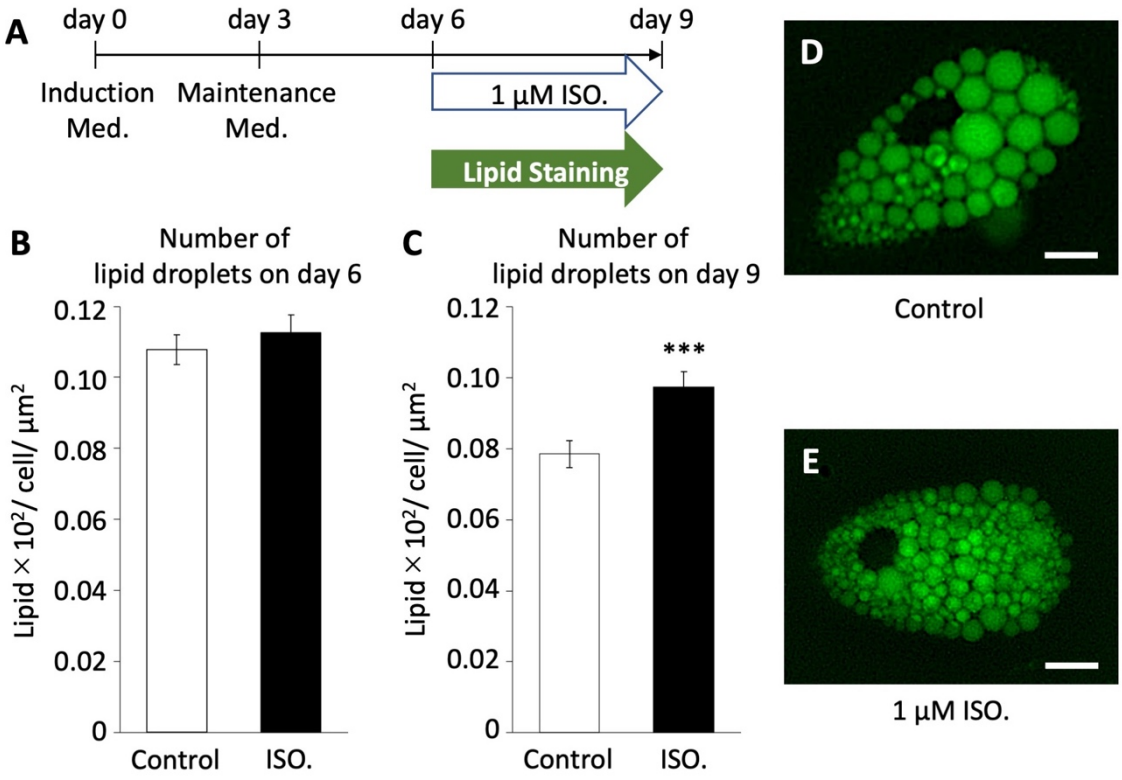

FIGURE 8. Measurement of the number of lipid droplets in pig DFAT. (A) Browning schedule of pig DFAT. (B) Measurement of the number of lipid droplets on day 6 using 100 cells. (C) Measurement of the number of lipid droplets on day 9 using 100 cells. (D and E) Phenotypes of lipid droplets after the administration of isoproterenol (ISO.). The experiments were conducted more than twice. Bar is 10 μm. The values are shown as mean ± SEM. and *** $p < 0.001$.

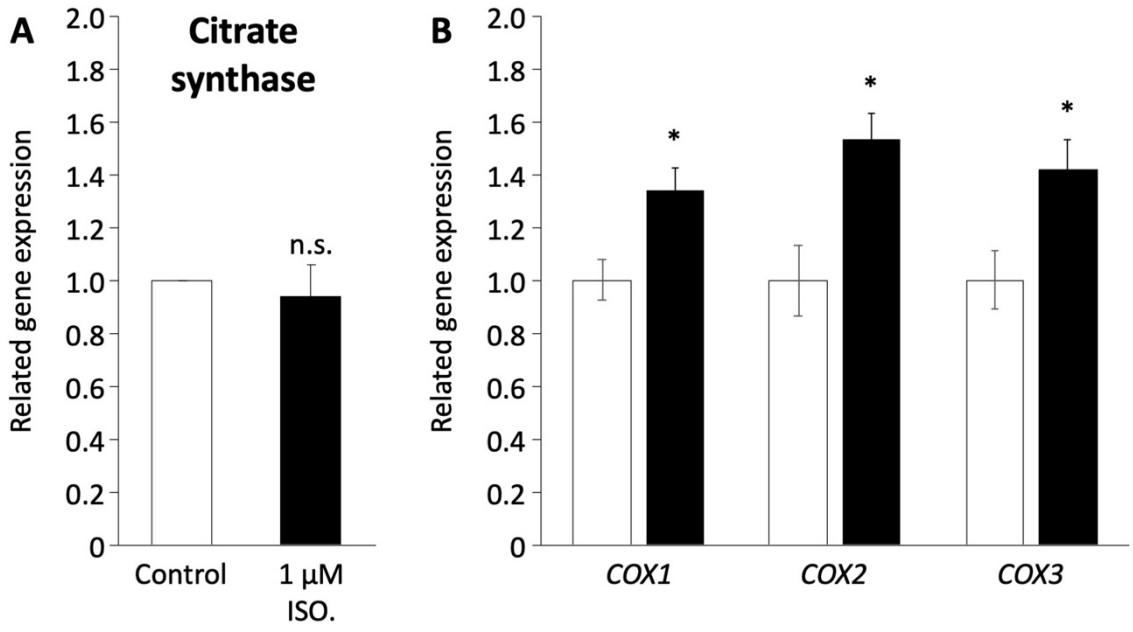

FIGURE 9. Measurement of mitochondria function in pig DFAT. (A) Gene expression of citrate synthase related to mitochondria number (n = 4). (B) Gene expression of *COX1*, *COX2*, and *COX3* related to respiratory chain in mitochondrial membrane. White square indicates control and black square indicates administration of 1 μM isoproterenol (ISO.), and the values are compared to those of the control (n = 3). The experiments were conducted more than twice. The values are shown as mean ± SEM. and * $p < 0.05$.

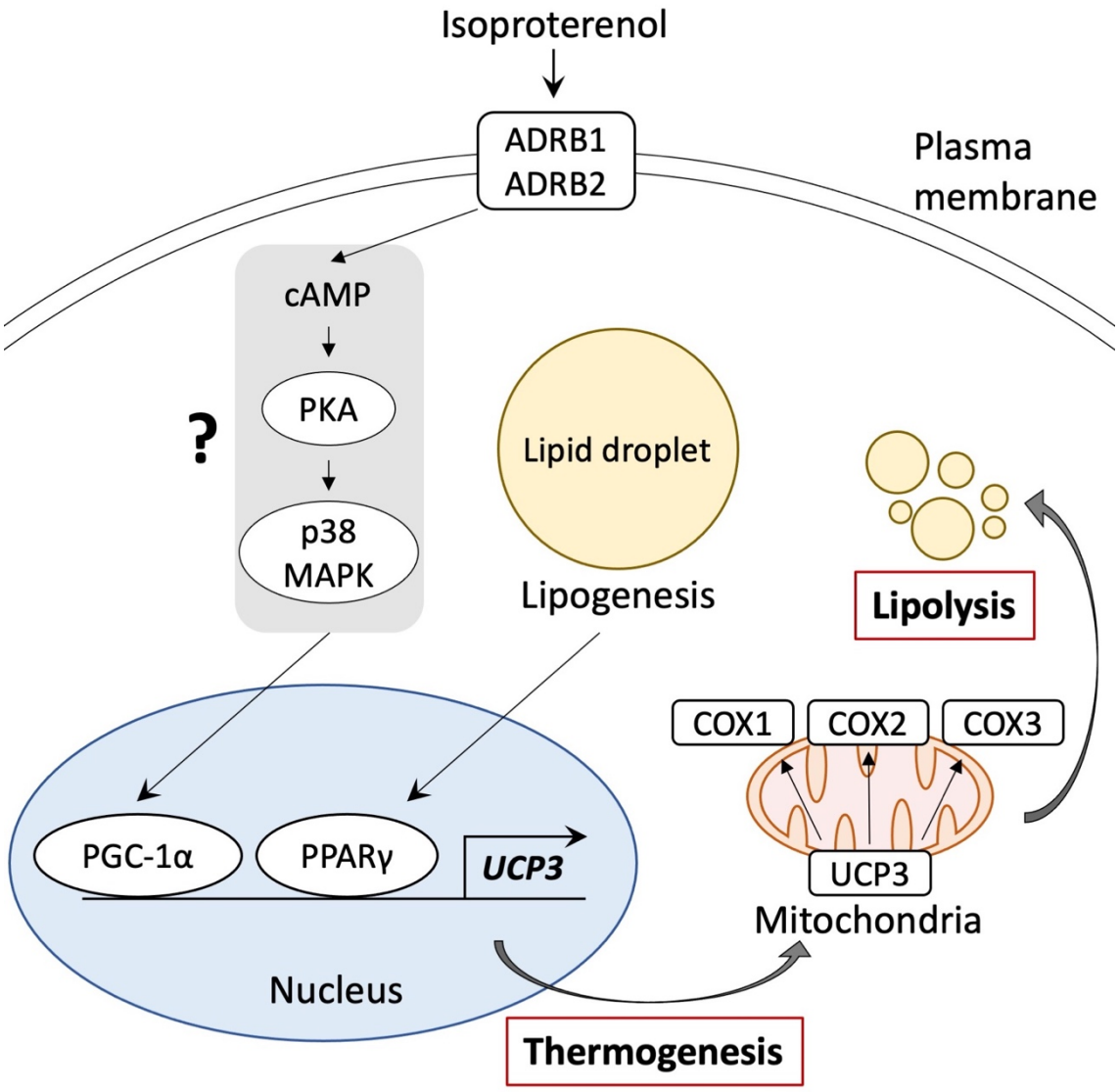

FIGURE 10. Schematic representation of the browning pathway in pig DFAT cells through ADRB signaling and stimulation of *PPARγ* and *PGC-1α*. Isoproterenol activated to *PGC-1α* and *UCP3* gene expressions. *UCP3* activation by isoproterenol enhanced mitochondrial function and lipolysis.

TABLE 1. Primer pairs used in the analysis of gene expressions.

Gene		Primer	Product length (bp)	Annealing temperature (℃)	Accession number
PGC-1α	F	CATGTGCAACCAGGACTCTG	133	60	NM_213963
	R	GCTGTCTGTATCCAAGTCGTTC			
PPARγ	F	AGGACTACCAAAGTGCCATCAAA	142	60	NM_214379
	R	GAGGCTTTATCCCCACAGACAC			
UCP1	F	GCAGGGCAGACAGGTAAGC	134	60	XM_021100543.1
	R	CAAATAGTCCCGCCAAACCA			
UCP2	F	CCTCAGTGTGAGACCTGACGAA	148	60	NM_214289
	R	CTGTGGCCTTGAATCCAACCA			
UCP3	F	ATTCCAGGCCAGCATACACG	165	60	NM_214049
	R	GTCACCATCTCGGCACAGTT			
CS	F	GGCTGACCTTATACCTAAGGAGC	230	60	NM_214276.1
	R	GTTCTTCCCCACCCTTAGCC			
Casp3	F	TGTGGGATTGAGACGGACAG	131	60	NM_214131.1
	R	GATCCGTCCTTTGAATTTCGCC			
Casp9	F	CCAGTGGACATTGGTTCTGGA	247	60	XM_003127618.4
	R	TGGCAGTCAGGTTGCACTTC			
Bax	F	GCCTCAGGATGCATCTACCAA	170	60	XM_003127290.5
	R	AGTTGAAGTTGCCGTCAGCA			
Bak1	F	CTAGAACCTAGCAGCACCATGG	156	60	XM_021098603.1
	R	GGAGGCGATCTTGGTGAAGTAC			
ACTB	F	AGATCAAGATCATCGCGCCTC	159	60	DQ845171.1
	R	AGTCCGCCTAGAAGCATTTGC			

TABLE 2. Alignment scores of thermogenesis genes among mammals.

	Pig Human	Pig Mouse	Pig Cattle	Human Mouse	Human Cattle	Mouse Cattle
PPARγ	85	84	86	84	78	76
PGC-1α	91	90	95	86	90	88
UCP1	30	29	33	70	80	72
UCP2	84	79	86	83	84	80
UCP3	73	52	82	68	86	76

Alignment scores were calculated using mRNA sequence of *PPARγ*, *PGC-1α*, *UCP1*, *UCP2*, and *UCP3* in pig, human, mouse, and cattle. The heights of the alignment scores indicate the homology of mRNA between two species.

TABLE 3. Alignment scores of the promoter regions in the UCP family among mammals.

	Pig Human	Pig Mouse	Pig Cattle	Human Mouse	Human Cattle	Mouse Cattle
UCP1	53	6	66	18	46	5
UCP2	5	3	5	22	53	3
UCP3	23	18	25	21	60	19

The calculation of alignment scores in the promoter region used the sequence until 1000 bp upstream from the transcriptional start site in *UCP1*, *UCP2*, and *UCP3*.

Chapter 2

STUDY OF DEVELOPMENT AND GENE EXPRESSION OF FAT TISSUE IN MANGALICA

2.1. Introduction

Mangalica is a native pig breed in Hungary. It was classified into three lineages based on its curly hair: Red, Blond and Swallow Belly. Mangalica was categorized the lard-type of meat quality, and their dorsal fat tissue reported to contain high concentrates of unsaturated fatty acids such as oleic acid and cholesterol compared to common commercial breeds (Egerszegi *et al.* 2003; Parunovic *et al.* 2015; Tomović *et al.* 2016; Takatani *et al.* 2021).

Mangalica exhibits a slower growth rate than commercial breeds, however Mangalica has highly adaptive function to ambient environment. Furthermore, their developmental rate has not been inferior in cold condition and poor pasture environments compared to commercial breeds (Egerszegi *et al.* 2003; Pârvu *et al.* 2012). Takatani et al. (2021) reported that Mangalica in Tokachi, Japan, displayed growth performance similar to native Hungary Mangalica. It was noted that Mangalica requires more than twice the number of days for slaughter compared to commercial breeds. Additionally, Mangalica has thicker dorsal fat tissue and the different fatty acid composition than commercial breeds (Takatani *et al.* 2021). These results suggested that Mangalica fat tissue indicated specific fat development process compared to commercial breeds. These differences may be generated for the specific growing performance and between meat and fat specific quality in Mangalica.

Generally, fat formation occurs through the proliferation and differentiation of adipocyte and enlargement of adipocyte due to accumulation of lipid within the cells. Metabolic balance between lipogenesis and lipolysis has also been reported to be involved in the formation and maintenance of adipocyte (Ali *et al.* 2013; Albuquerque *et al.* 2020).

Meishan pig, which is a lard-type pig similar to Mangalica, has been reported that size of adipocyte is different to commercial breeds depend on growth period (Nakajima *et al.* 2011). Furthermore, differences of fat gene expression have been reported in the adipose tissue of lard-type fat compared to commercial breeds such as Iberian pigs expressed higher leptin gene related to adipocyte differentiation and lipolysis compared to Duroc (Benítez *et al.* 2018). And Meishan pigs expressed lower adiponectin gene related to fat accumulation compared to Landrace pigs (Nakajima *et al.* 2019). However, studies focusing on Mangalica have been primarily related to its meat quality (Egerszegi *et al.* 2003; Parunovic *et al.* 2015; Tomović *et al.* 2016; Takatani *et al.* 2021), and there is limited research on the dorsal fat tissue formation process and adipocyte development in Mangalica (Tempfli *et al.* 2016).

To understand of the fat tissue developmental process in Mangalica could contribute to improving meat quality, meet production with demands such as the appropriate fat content and control the growing days and establishing appropriate the method of management for growing. Currently, in Tokachi Royal Mangalica Farm is slaughtered over 14 months old when it reaches 130-140 kg, however it is necessary to investigate the growing days and slaughter timing. Therefore, this study examined the histological evaluation of fat tissue and the expression of genes related to fat formation in Mangalica compared to Camborough as commercial cross breed (LWD: Landrace, Large White and Duroc) using slaughter age (14 months old) and slightly earlier slaughter age (8 months old). This research sheds light on the specific fat development and accumulation process in Mangalica.

2.2. Material and Methods

2.2.1. Animals and Ethics

The study and management of all animals used in this study were conducted in accordance with the Guidelines for the Care and Use of Animals of the Obihiro University of Agriculture and Veterinary Medicine (approval numbers 19-26, 20-29 and 21-19).

Mangalica that were raised at the Tokachi Royal Mangalica Farm during 2019-2021, were used for the experiment. The experiments were performed to use 8 months old (n = 3, around 100 kg) and 14 months old (n = 3, 130-140 kg) of Mangalica and these animals were slaughtered at the Hidaka Meat Processing Center (Ni-kap, Hokkaido). Camborough as commercial breed LWD (n = 3) that was raised inside at the Obihiro University of Agriculture and Veterinary Medicine (Obihiro, Hokkaido) until 7-8 months old and these animals were slaughtered at meat processing facility in the University. To perform histological and genetic analyses, fat tissue samples were collected from dorsal fat tissue in thoracic area of Mangalica and LWD after slaughtered with electrical stunning. The collected fat samples were soaked immediately to 10% formalin (066-06921, Fuji Film Wako, Japan) and TRIzol regent (15596018, Thermo Fisher Scientific, USA) to use experiments.

The measurement of fat thickness was conducted using randomly selected Mangalica pigs aged 0-14 months, totaling 42 individuals, from the Tokachi Mangalica Farm. The dorsal fat thickness of LWD were measured at 1-6 months, totaling 28 individuals, from Dream Pork Co., Ltd. (Memuro, Hokkaido).

2.2.2. Measurement of dorsal fat tissue thickness and construction of growth curve

The thickness of dorsal fat tissue was measured using an animal-specific ultrasound imaging device (HS-102 V, Fujihei Industry Co., Ltd., Japan) as echo in Mangalica and LWD. The thickness of dorsal fat tissue was measured at the point of P2 where was the point of

approximately 6-8 cm neighboring from the spine (Figure 1A), following previous studies (Irie & Nishimura 1987; Takatani *et al.* 2021). The images of the fat tissue from echo were analysed with ImageJ Fiji (https://imagej.net/software/fiji/downloads).

Growth curves for Mangalica and LWD fat tissue were constructed using measurement data of thickness in dorsal fat tissue. Furthermore, the end point of growth curves was estimated the data of sow in each breed. Suitability of growth curves were compared based on the Brody, Logistic, Gompertz, and Bertalanffy models (Shi *et al.* 1985). The model equations for each growth curve are provided in Table 1. The root mean square error (RMSE) was used as an index of the accuracy of each growth curve.

2.2.3. Preparation of dorsal fat tissue for histological analysis

For hematoxylin and eosin (H&E) staining, the fat tissue samples were collected from dorsal fat tissue from Mangalica and LWD after slaughter, fixed in 10% formalin, dehydrated in an ethanol series and embedded in paraffin. Multiple sections (4 μm) were prepared using an SM2000R microtome (Leica) and stained with H&E. Images were obtained using an Optiphot-2 stereomicroscope (Nikon) with a Digital Sight 1000 camera (Nikon), and the area of adipocyte was calculated using more than 120 cells in more than three visual fields of each sample using ImageJ Fiji (https://imagej.net/software/fiji/). To prepare Oil Red O staining, fixed fat samples were washed with phosphate-buffered saline (PBS) and replaced with 30% sucrose with over nights. In turn, samples were embed using O.C.T. compound (4583, Sakura FineTech Japan, Co., Ltd., Japan) and storaged in −80℃ until using experiment. Then, the frozen sections were prepared using a Leica CM1900 Cryostat (Leica) and stained with Oil Red O for 2-3 minutes at 37℃.

2.2.4. Analysis of gene expression in fat tissue

Total RNA was extracted from the fat tissue samples using TRIzol reagent (Thermo Fisher Scientific). The total RNA concentration was measured using a NanoDrop spectrophotometer (Thermo Fisher Scientific). Total RNA (1 μg) was treated with DNase and converted to cDNA using Random Primers (48,190,011, Thermo Fisher Scientific) and SuperScript II (18,064,022, Thermo Fisher Scientific) on a GeneAtlas thermal cycler 482 (4,990,902, ASTEC, Fukuoka, Japan).

Real-time PCR was performed using the SsoAdvanced Universal SYBR Green Supermix (1,725,271, Bio-Rad) and LightCycler 96 (05815916001, Roche), according to the manufacturers' instructions. Each PCR reaction was performed at 95°C for 30 s for denaturation, 95°C for 10 s and 60°C for 60 s for 35 cycles for amplification. Table 1 lists the primer sequences used. We used actin beta (ACTB) for internal control, and the relative expression levels of genes were calculated using the $2^{-\Delta\Delta CT}$ method.

2.2.5. Statistical Analysis

All statistical analyses were performed using the RStudio free software version 1.3.1073 (https://www.rstudio.com/products/rstudio/). The results compared to various groups using multiple comparison with Tukey test after one-way analysis of variance (ANOVA). All data are presented as the mean ± standard error of the mean (SEM). $p < 0.05$ was considered significant (* $p < 0.05$, ** $p < 0.01$, *** $p < 0.001$).

2.3. Results

2.3.1. Mangalica has specific development manner of dorsal fat tissue

The development of dorsal fat tissue in Mangalica and LWD were indicated in Figure 1.

The growth curves were constructed from the results of thickness in dorsal fat tissue and each model equations. The value of RMSE was minimized with the logistic model in Mangalica and LWD (Table 3). From growth curves of dorsal fat tissue, Mangalica had thicker dorsal fat tissue than LWD at birth. However, around 100 days of age, dorsal fat tissue of LWD was thicker than Mangalica. In around 150 days age, the growth rate of dorsal fat tissue was decreased in LWD. In contrast, Mangalica's fat tissue was increased growth rate around 150 days age and continued to increase thickness and thickness was reached approximately 45 mm (Figure 1B).

2.3.2. Adipocyte of Mangalica is larger than LWD

The comparison of area in adipocyte was indicated in Figure 2.

The result of staining was indicated that collected samples were adipocyte (Figure 2A). The average area of adipocyte was 7293 ± 229 μm^2 in 8 months old Mangalica, 9751 ± 254 μm^2 in 14 months old Mangalica and 5895 ± 157 μm^2 in LWD. The area of adipocyte in 14-month-old Mangalica was largest and LWD was smallest compared to each group ($p < 0.05$, Figure 2B).

2.3.3. Gene expression in dorsal fat tissue of Mangalica

The gene expression of dorsal fat tissue was compared to 8 months old, 14 months old Mngalica and LWD (Figure 3).

The gene expression related to differentiation of adipocyte was showed in Figure 3A. The expression of Kruppel-like factor 4 (*KLF4*), a marker gene of undifferentiated cells, was

significantly decreased in LWD compared to 8 months old Mangalica (Figure 3A). The expression of Peroxisome Proliferator-activated receptor gamma (*PPARγ*), an upstream gene related to differentiation of adipocyte, was significantly increased in 14 months old Mangalica and LWD (Figure 3A). Whereas, the expression of CCAAT-enhancer-binding protein alpha (*C/EBPα*), the gene related to adipose differentiation similar to *PPARγ*, and peroxisome proliferator-activated receptor alpha (*PPARα*), is a gene related to oxidation and metabolic of fatty acids, was significantly increased in LWD compared to Mangalica (Figure 3A).

The gene expression related to lipolysis and lipogenesis were shown in Figure 3B. The expression of adipose triglyceride lipase (*ATGL*), which resolve triglyceride, was not affected between Mangalica and LWD, however hormone sensitive lipase (*HSL*), which resolve diglyceride, was significantly increased in LWD compared to Mangalica (Figure 3B). Furthermore, the expression of fatty acid synthase (*FASN*), related to lipogenesis, and adipose protein 2 (*aP2*), related to transport of fatty acids, was significantly increased in LWD compared to Mangalica (Figure 3B).

2.4. Discussions

In this study, I revealed differences of growth mechanisms of dorsal fat tissue between Mangalica and LWD, and demonstrated to the specificity of dorsal fat growing manner in Mangalica.

The measurement of thickness in dorsal fat tissue was indicated that the development rate was lower than LWD in Mangalica. However, Mangalica have been continued to grow their dorsal fat tissue and maximum value of thickness was higher than LWD. Furthermore, these results were corresponded to previous study reported that the thickness of dorsal fat tissue in carcass of Mangalica was approximately twice than commercial breed (Takatani *et al.* 2021). It was reported that the development of fat tissue is influenced not only genetic factors but also rearing conditions (Ooishi *et al.* 2006). This study used the Mangalica which was raising outside through a year and LWD which was raising inside, so it may be necessary to conduct the experiment with same raising environment.

It was reported that the cross-sectional area of adipocyte was affected from pig breed, and the diameter of adipocyte was larger than commercial pig breed in lard type pig breed such as Meishan and Wuzhishan pigs (Zhao *et al.* 2009; Nakajima *et al.* 2011). Similarly, in Mangalica pigs, I observed larger area of adipocyte in dorsal fat tissue and confirmed the feature of fat development in lard-type pig breed.

Previous study was reported that knocked out the gene expression of *KLF4* decreased the number of stem cells and progenitor cells, and *KLF4* regulated undifferentiated cells self-renewal (Chen et al., 2019). From the results of RT-PCR, the gene expression of *KLF4* which is a marker of preadipocytes, was higher than LWD compared to Mangalica. The strongly gene expression of *KLF4* suggest that 8 months old Mangalica indicated the higher number of undifferentiated pre-adipocytes and Mangalica has greater potential for the fat accumulation compared to LWD. Furthermore, previous human research had reported that

the number of fat cells is established during early development and the proliferation, and differentiation of preadipocyte is important to development of fat tissue (Longo *et al.* 2019). These data suggested that *KLF4* can be a predict marker for the fat accumulation potential in livestock meat production.

PPARγ and *C/EBPα* were master genes to induce the adipocyte differentiation and reduction of *C/EBPα* was reported to decrease differentiation of adipocyte and fat accumulation (Kim & Nam 2017). Furthermore, PPARα is related to lipid metabolism as β oxidation of fatty acid, which is composed triglyceride, and it was reported that expression of *PPARα* affected the size of fat cells (Goto *et al.* 2011). The gene expression of *PPARγ*, *C/EBPα* and *PPARα* may contribute to slow development and high fat accumulation of dorsal fat tissue in Mangalica.

Previous studies, using mouse and cell culture, were reported that gene expression of *HSL*, *FASN* and *aP2* was correlate with *PPARγ* and *C/EBPα* expression (Cristancho & Lazar 2011; Yang *et al.* 2015) and similar results was obtained in this study. However, Iberian and Meishan, which are lard-type pig breed, were not changed these gene expression compared to commercial breed such as Duroc and Landrace (Benítez *et al.* 2018; Nakajima *et al.* 2019). Another study using Wujin pig of lard-type showed significantly decrease gene expression of *ATGL* and *HSL*, and significantly increase lipogenesis genes involved in *FASN* and *aP2* (Zhao *et al.* 2009). Furthermore, gene expression of *HSL* is related to resolve not only triglyceride but also diglyceride (Lampidonis *et al.* 2011; Wang *et al.* 2013). Triglycerides are known to be related to expansion of adipocyte (Poklukar *et al.* 2020). From these studies and the histological and genetic feature of adipocyte in Mangalica, it may be suggested adipocyte of Mangalica contained high concentration of triglyceride. Previous studies had reported that content of triglyceride and fatty acid composition in Mangalica (Szabó *et al.* 2010, 2010), however it was limited that the knowledge of effect for fat development and fat metabolism.

Hence, I have to perform additional investigations which compared the content of triglyceride in dorsal fat tissue between Mangalica and other breeds and examine the relationship between triglyceride and fat development in Mangalica.

These results in this study indicated that the specific gene expressions may contribute to slow development and accumulation of dorsal fat tissue in Mangalica. Previous research has shown that dietary conditions and gender may influence the composition of fatty acids and the expression of fatty acid synthesis-related factors. Therefore, to further investigate the mechanism of fat development in Mangalica, standardization of condition such as sex, diet and shipping status of domestic animals will resolve the issue for more comprehensive analysis.

In conclusion, this study sheds light on the unique mechanisms of fat development in Mangalica, offering valuable insights that can be beneficial for livestock breeding and management.

Figure and captions

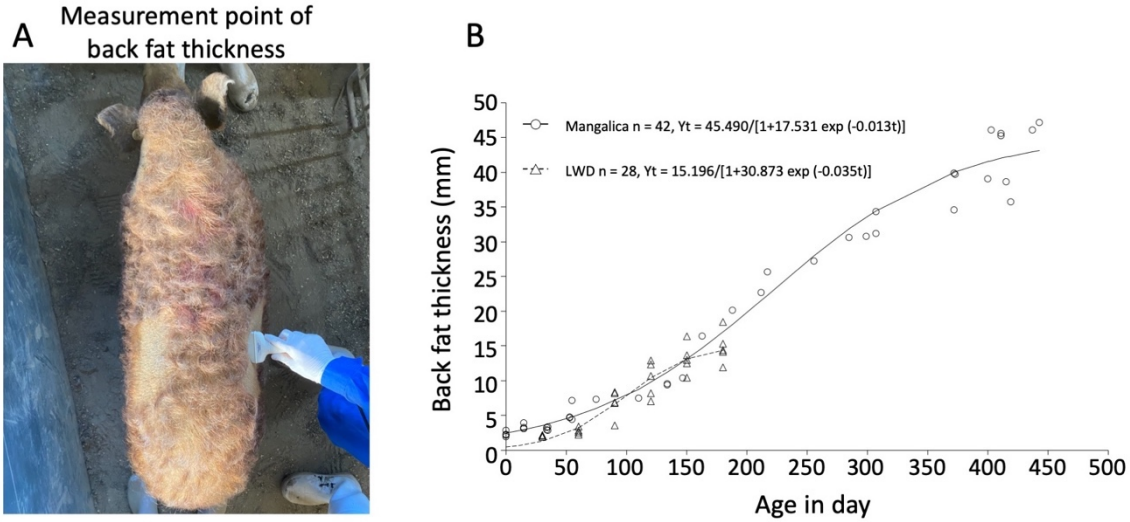

FIGURE 1. Measurement of dorsal fat tissue thickness in Mangalica and Camborough. (A) the measurement of dorsal fat tissue thickness using echo, and the measurement point of dorsal fat tissue thickness. (B) the change of dorsal fat tissue thickness with age in day: (-◯-) Mangalica and (--△--) LWD.

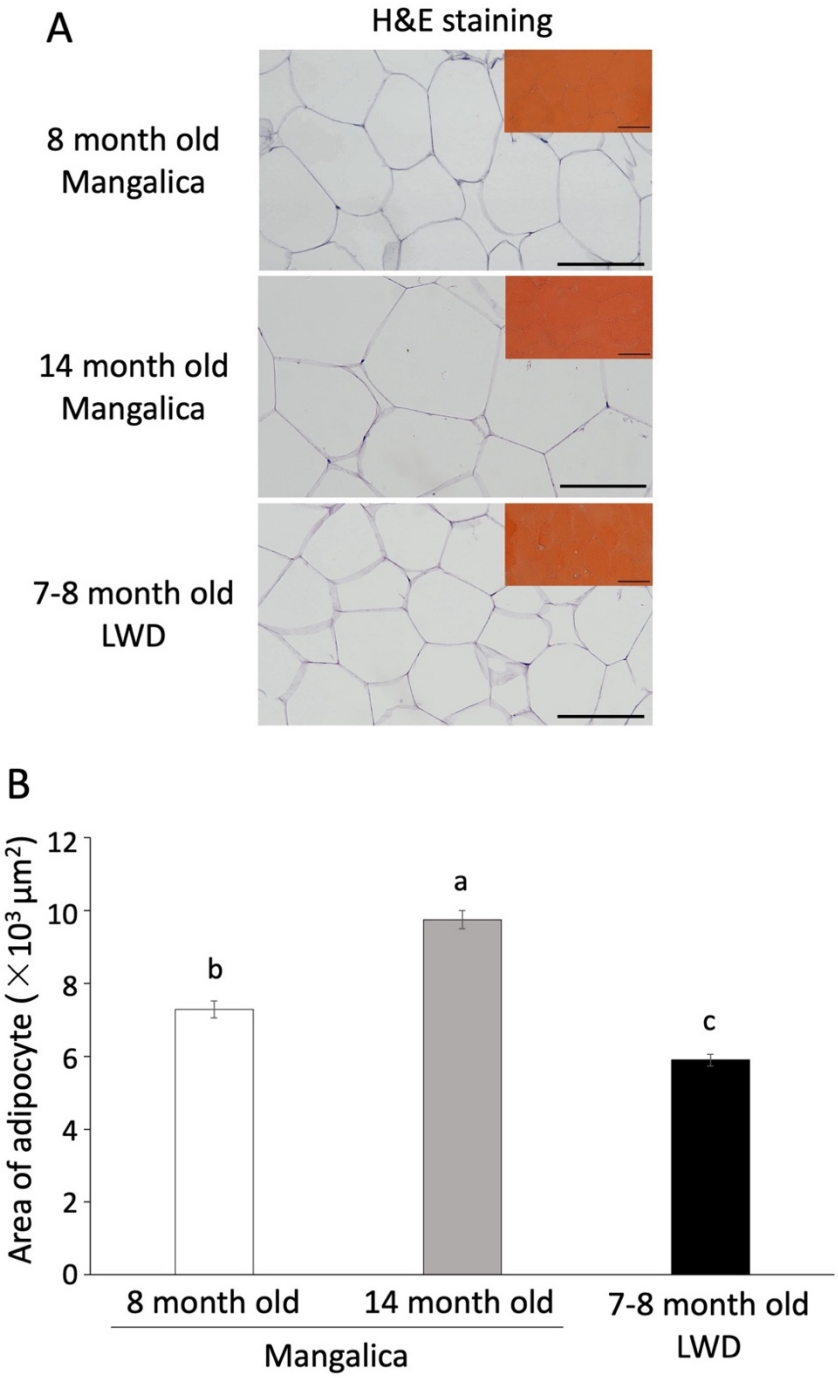

FIGURE 2. Measurement of area of adipocyte and compered between Mangalica and LWD. (A) Images of hematoxylin and eosin (H&E) and Oil Red O staining (bar 100 μm). (B) Comparison of area of adipocyte with 8 (n = 3, white square) and 14 (n = 3, gray square) months old Mangalica and LWD (n = 3, black square). Values are shown as mean ± SEM. and significantly difference was indicated between different signs.

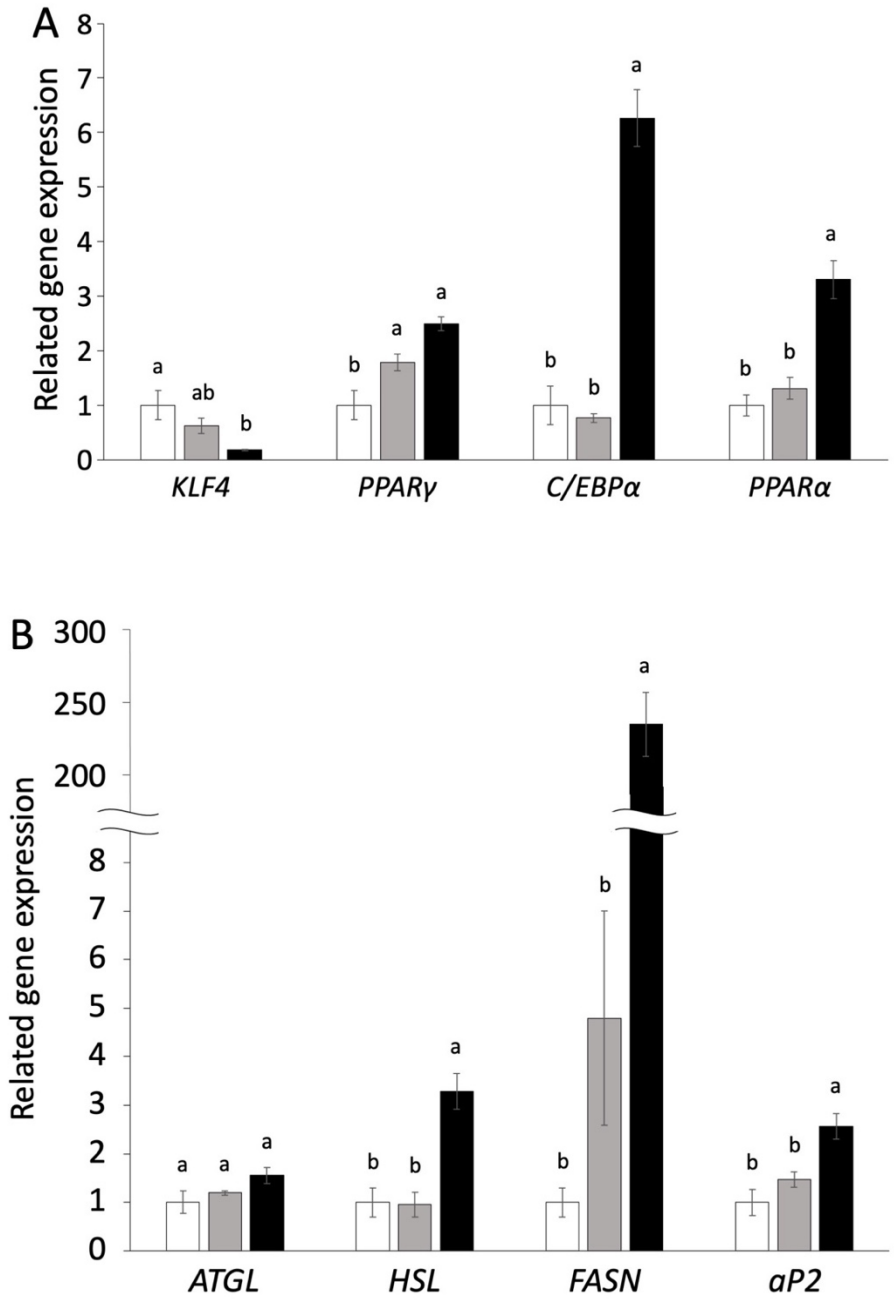

FIGURE 3. Gene expressions of fat tissue of Mangalica and LWD. (A) Gene expression of *KLF4*, *PPARγ*, *C/EBPα* and *PPARα* related to differentiation and maturation of adipocyte. (B) Gene expression of *ATGL*, *HSL*, *FASN* and *aP2* related to lipolysis and lipogenesis. Gene expressions were compared to 8 (n = 3, white square) and 14 (n = 3, gray square) months old Mangalica and LWD (n = 3, black square). The values are shown as mean ± SEM., and significantly difference was indicated between different signs.

TABLE 1. Nonlinear formula model of development curve of fat tissue in Mangalica

	Models
Brody	$Yt = A[1-B\ (-Kt)]$
Logistic	$Yt = A[1+B \exp (-Kt)]^{-1}$
Gompertz	$Yt = A \exp[-B \exp (-Kt)]$
Bertalanffy	$Yt = A[1-B \exp (-Kt)]^{3}$

t: age in day, Yt: fat thickness in a day, A: value of maturation
B: constant of integration, K: speed of maturation

Production of regression equation from formula model of Brody, Logistic, Gompertz and Bertalanffy

TABLE 2. Sequence of primer using RT-PCR

Genes		Primer sequence	Product length (bp)	Annealing temperature (°C)	Accession number
KLF4	F	CCTCTCCAACTCACTGTCT	377	60	NM_001031782
	R	GCGATGCCTTCAACACAA			
PPARγ	F	AGGACTACCAAAGTGCCATCAAA	142	60	NM_214379
	R	GAGGCTTTATCCCCACAGACAC			
C/EBPα	F	GCACAGCGACGAGTACAAGA	98	60	XM_003127015.4
	R	TATGCTGCGTCTCCAGGTTG			
PPARα	F	CAGCCTCCAGCCCCTCGTC	382	60	NM_001044526
	R	GCGGTCTCGGCATCTTCTAGG			
ATGL	F	CCTAGTGGCCAACGCCAAG	115	60	NM_001098605.1
	R	CGACACCTCGATGATGCTGG			
HSL	F	TTCCTGCGCGAGTATGTCAC	140	60	NM_214315.3
	R	TTGCGTTTGTAATGCTCCCC			
FASN	F	CAAGCAGGCGAACACGATG	141	60	NM_001099930.1
	R	GCATCAGAACTGCTCACACC			
aP2	F	GTAGGTACCTGGAAACTTGTCT	118	60	NM_001002817.1
	R	CAGTGATGATCAGGTTGGGTTTG			
ACTB	F	CCAGGTCATCACCATCGG	158	60	DQ845171.1
	R	CCGTGTTGGCGTAGAGGT			

TABLE 3. Suitability of parameter in formula model

Mangalica	A	B	K	RMSE
Brody	53.985	1.034	0.003	5.003
Logistic	45.490	17.531	0.013	3.043
Gompertz	48.254	3.890	0.008	3.291
Bertalanffy	49.446	0.831	0.006	3.595
LWD				
Brody	232.577	1.008	0.0004	1.863
Logistic	15.758	27.137	0.033	1.721
Gompertz	18.923	4.609	0.017	1.777
Bertalanffy	22.094	0.885	0.011	1.799

A: value of maturation, B: constant of integration, K: speed of maturation
RMSE: root mean square error

The lower the RMSE was consider to be suitable

Chapter 3

SEASONAL ADAPTATION OF MANGALICA PIGS IN TERMS OF MUSCLE MORPHOLOGY AND METABOLISM

3.1. Introduction

The skeletal muscle plays an important role in maintaining body temperature through shivering. Especially, the function of thermogenesis is associated with cold tolerance in muscle metabolic activity (Periasamy *et al.* 2017).

The Mangalica is a lard-type, native Hungarian pig (Sus scrofa domesticus). Mangalica is thought to have evolved from Alföldi, Bakonyi and Szalontai, which are much older breeds that originated from domesticated Slovenian pigs and wild boars (Egerszegi *et al.* 2003). Mangalica shared part of its genetic background with Hungarian wild boars and had characteristic features similar to those of wild boars compared to commercial breeds (Frank *et al.* 2017; Bâlteanu *et al.* 2019; Kaltenbrunner *et al.* 2019). Mangalica is classified by the colour of curly hair: red, blond and swallow belly. Furthermore, Mangalica has a unique fat tissue with a high rate of unsaturated fatty acids (Egerszegi *et al.* 2003; Tomović *et al.* 2016). Previous studies have reported that the developmental rate of Mangalica slowly increases compared to that of commercial breeds (Egerszegi *et al.* 2003; Takatani *et al.* 2021). However, Mangalica has cold tolerance and can be placed in a grazing environment throughout the year. When kept in cold conditions, the daily gain in body weight of Mangalica did not decrease compared to that of commercial breeds (Pârvu *et al.* 2012, 2012).

In general, commercial pig breeds are sensitive to environmental changes, and seasonal changes in temperature reduced their physiological functions such as development rate, metabolism and fertility (Claus & Weiler 1994; Carroll *et al.* 2012; Guo *et al.* 2018; Choi *et al.* 2019; Yu *et al.* 2021; Liu *et al.* 2022). Furthermore, heat and cold stresses induce several

diseases such as pneumonia and hypothermia, and increase the mortality rate in the commercial pig (Carroll *et al.* 2012; Liu *et al.* 2022). On the contrary, hibernators that live in a cold environment such as squirrels change their muscle metabolism based on the decrease in the ambient temperature (Cotton 2016). Some non-hibernating wild animals, such as deer, wild boars and pheasants, also changed their muscle characteristics, such as components of muscle, abundance of protein and fat, and gene expression related to fatty acid synthesis, between each season (Wiklund *et al.* 2010; Sales & Kotrba 2013; Stanisz *et al.* 2019; Liang *et al.* 2022). The muscle produces heat using two types of muscle fibres, and thus, it is an important organ for the maintenance of temperature (Frontera & Ochala 2015). The muscle fascicles are formed by individual muscle fibres, which are made of myofibrils contained within the sarcomeres (Frontera & Ochala 2015). The muscle has two types of muscle fibres with different metabolic functions: Type 1 (slow-twitch fibre) has a high lipid metabolism and expresses MYH7; type 2 (fast-twitch fibre) has a high glucose metabolism and expresses MYH1, MYH2 and MYH4 (Blaauw *et al.* 2013; Schiaffino 2018). Furthermore, a muscle fibre can shift to the other fibre type (that is fast → slow and slow → fast) by nerve stimulation, such as exercise, fasting and ageing (Schiaffino & Reggiani 2011; Wilson *et al.* 2012; Ciciliot *et al.* 2013). Wild animals change the characteristics of their muscles based on seasonal changes, leading to physiological adaptation to ambient environments.

We hypothesized that Mangalica alters its muscle metabolisms and composition in response to seasonal changes to increase heat and cold tolerance to survive in grazing environments. However, there are few studies associated with the development of the muscle in Mangalica. It is unclear whether there are seasonal changes in body development, muscle tissue structure and muscle metabolism in Mangalica. The aim of this study was to perform a histological analysis and examine the expression of genes involved in the metabolism of the muscle tissue of Mangalica to reveal its seasonal adaptation.

3.2. Materials and Methods

3.2.1. Seasonal experimental setting for Mangalica

The experimental setting of seasons was based on weather records of the Nukanai station of the Japan Meteorological Agency (https://www.data.jma.go.jp/obd/stats/etrn/index.php?prec_no. =20&block_no = 1286&year = &month = &day = &view=), which is located approximately 12 km from the Tokachi Royal Mangalica Farm in Japan (42°47.2' N). The season was determined based on the average temperature. Each season was determined as follows: winter from December to March (−8.5 to −0.4°C), spring from April to June (7.1 – 15.0°C), summer from July to September (16.6 – 20.4°C) and autumn from October to November (3.5 – 9.2°C).

3.2.2. Animals

Mangalica animals that were raised at the Tokachi Royal Mangalica Farm during 2020–2022 were used for the experiment. Body weight (BW) was measured at various stages such as birth (Day 0), weaning (Day 30), growing (Days 30 to 300) and before slaughter (Days 300 to 480). The BW was measured 149 Mangalica pigs (13-15 months old) and the calculation of BW/day (BW/d) in each stage used BW data that are recorded in the farm. The body temperature was measured before slaughter (n = 143). The muscle tissues were kept at −30°C until experiments were performed. To perform histological and genetic analyses, muscle tissues were collected from the thoracic longissimus muscle of 8 months old Mangalica, which was slaughtered after electrical stunning, in summer (n = 3) and winter (n = 3).

3.2.3. Preparation of muscle tissue for histological analysis

For hematoxylin and eosin (H&E) staining, muscle tissues were collected from more than three locations on the longissimus muscle, fixed in 10% formalin, dehydrated in an ethanol series and embedded in paraffin. Multiple sections (4 μm) were prepared using an SM2000R microtome (Leica) and stained with H&E. Images were obtained using an Optiphot-2 stereomicroscope (Nikon) with a Digital Sight 1000 camera (Nikon), and the cross-sectional area (CSA) of skeletal muscle cells was calculated using more than 150 cells in more than three visual fields of each sample using ImageJ Fiji (https://imagej.net/software/fiji/). To prepare fresh-frozen muscle tissue samples, the longissimus muscle was fixed with isopentane and liquid nitrogen. Then, the frozen sections were prepared using a Leica CM1900 Cryostat (Leica) and stained with Oil Red O and ATPase staining. ATPase staining was performed using the conventional method to distinguish between type 1 and type 2 fibres (Lefaucheur *et al.* 2002; Westwood *et al.* 2005). Briefly, frozen sections (15 μ) were pre-incubated in pH 10.3-10.8 solution containing 0.1 M sodium barbital (021-00032, Fujifilm Wako) and 0.18 M $CaCl_2$ (07057-00, KANTO CHEMICAL CO., INC., Tokyo, Japan) for 15 minutes at room temperature. In turn, frozen sections were placed in pH 9.4-9.7 solution containing 0.1 M sodium barbital, 0.18 M $CaCl_2$ and 50 mg ATP disodium salt (10127523001, Roche) for 45 minutes. After reaction at pH 9.4-9.7 solution, frozen sections were washed for 3 time with 1% $CaCl_2$, and reacted in 2% $CoCl_2$ (036-03682, Fujifilm Wako) for 3 minutes. Following reaction in $CoCl_2$, the slides were washed 8 time with 0.01% sodium barbital and transferred to 1% ammonium sulfide solution (018-03466, Fujifilm Wako) for 1 minutes. Microscopic images were obtained using the Optiphot-2 stereomicroscope with a Digital Sight 1000 camera for the measurement of muscle fibre types. The fibre type composition was calculated using 100 muscle cells of each sample.

3.2.4. Preparation of muscle tissue for transmission electron microscopy

The muscle samples were cut into 2 mm 3 blocks and placed in 10% formalin overnight. The muscle blocks were then fixed with 2.5% glutaraldehyde fixative (079-00533, Fujifilm Wako) for 2 h at room temperature and post fixed with 1% osmium tetroxide (30,202, Nisshin-EM) for 1 h at room temperature. The fixed samples were dehydrated using an ethanol series and embedded in LR White resin (14,381, Electron Microscopy Sciences). Ultrathin sections (70 nm) were prepared with Reichert Ultracut S (Leica), and images were obtained using a transmission electron microscope Hitachi TEM system Model HT7700 (Hitachi). To evaluate the length of sarcomere and the thicknesses of myofibril and Z-line, over 20 myofibrils of the muscle sample were analysed using the ImageJ Fiji software.

3.2.5. Analysis of gene expression in muscle tissue

Total RNA was extracted from longissimus muscle samples using TRIzol reagent (Thermo Fisher Scientific). The total RNA concentration was measured using a NanoDrop spectrophotometer (Thermo Fisher Scientific). Total RNA (1 μg) was treated with DNase and converted to cDNA using Random Primers (48,190,011, Thermo Fisher Scientific) and SuperScript II (18,064,022, Thermo Fisher Scientific) on a GeneAtlas thermal cycler (4,990,902, ASTEC, Fukuoka, Japan).

Real-time PCR was performed using the SsoAdvanced Univer- sal SYBR Green Supermix (1,725,271, Bio-Rad) and LightCycler 96 (05815916001, Roche), according to the manufacturers' instructions. Each PCR reaction was performed at 95°C for 30 s for denaturation, 95°C for 10 s and 60°C for 60 s for 35 cycles for amplification. Table 1 lists the primer sequences used. We used 18S ribosomal RNA (18S) for internal control, and the relative expression levels of genes were calculated using the $2^{-\Delta\Delta CT}$ method.

3.2.6. Statistical analyses

All statistical analyses were performed using R version 4.2.2 (https://www.r-project.org/). The results of BW/day for each season were compared to the annual average using Dunnett's test. T test, U test and chi-squared test were used to compare summer and win- ter. All data are presented as the mean ± standard error of the mean (SEM.). $p < 0.05$ was considered significant (* $p < 0.05$, ** $p < 0.01$, *** $p < 0.001$).

3.2.7. Animal ethics

The study and management of all animals used in this study were conducted in accordance with the Guidelines for the Care and Use of Animals of the Obihiro University of Agriculture and Veterinary Medicine (approval numbers 21-19 and 22-165).

3.3. Results

3.3.1. Body weight of Mangalica in each season

To investigate the effect of seasonal changes on Mangalica development, we examined body temperature and weight. The ambient temperature was obtained from weather records, and the body temperatures of the Mangalica are indicated in Table 2. The minimum ambient temperature in winter was −14.6 to −26.2°C, the maximum ambient temperature in summer was 30.5–33.1°C, and the average ambient temperature in a year was −8.5 ± 0.8 to 20.4 ± 0.4°C. On the contrary, the body temperature of Mangalica was 38.35 ± 0.12 – 39.06 ± 0.18°C (Table 2).

The measurements of body weight during each season are shown in Figure 1. The BW/d from birth to weaning did not change between the average of 1 year (0.195 ± 0.004 kg/day) and each season (Figure 1A). The BW/d from the growing to slaughter period of spring (0.343 ± 0.014 kg/day) was significantly increased compared to the average of the year (0.284 ± 0.007 kg/day), and the BW/d in autumn (0.228 ± 0.011 kg/day) was significantly decreased compared to the average of the year ($p < 0.01$ and $p < 0.001$, respectively, Figure 1B). Although differences of ambient temperature between summer and winter were largest changes in the year, Mangalica could not be observed the changes BW/d during these seasons. I considered that Mangalica obtains tolerance to heat stress through metabolic functions related to thermogenesis. Thus, I focused on the changes in physiological functions during summer and winter.

3.3.2. Histological analysis of muscle tissue

To examine the muscle morphology in each season, we performed histological analysis using tissue staining and electron microscopy. The histological results of H&E, Oil Red O and ATPase staining are shown in Figure 2 and Supplemental figure. In Oil Red O staining,

the number of adipocytes may be increased in winter compared to summer in the muscles (Figure 2A). The CSA of skeletal muscle cells in summer and winter were 3.00 ± 0.05 and 2.52 ± 0.04 × 10^3 μm^2, respectively, and the CSA in summer was significantly larger than that in winter (Figure 2B, $p < 0.001$). The ratio of muscle fibre was 11.00 ± 1.53% and 89.00 ± 1.53% for types 1 and 2, respectively, in summer. The ratio of muscle fibre was 17.33 ± 3.53% and 82.67 ± 3.53% for types 1 and 2, respectively, in winter (Figure 2C and Figure 3). In winter, the type 1 muscle fibre was significantly increased and type 2 muscle fibre was significantly decreased compared to those in summer.

We measured the length of the sarcomere and thickness of myofibrils and the Z-line (Figure 4). The length of sarcomere in summer and winter was not different (Figure 4A and B), while the thickness of myofibril in summer and winter were 0.94 ± 0.03 and 0.66 ± 0.02 μm, respectively, and it was significantly higher in summer than that in winter (Figure 4A and C, $p < 0.001$). The thickness of the Z-line in summer and winter were 49.84 ± 1.27 and 67.44 ± 1.42 nm, respectively, and it was significantly higher in winter than that in summer (Figure 4A and B, $p < 0.001$).

3.3.3. Gene expression in muscle tissue

We compared the gene expression in the muscle between summer and winter (Figure 5). The expressions of *MYH4*, which is related to the formation of myosin heavy chain in the muscle fibre, and *GLUT4*, which is related to the uptake of glucose into cells, were decreased in winter compared to those in summer ($p < 0.001$ and $p < 0.05$, respectively, Figure 5). The expression levels of *MYH1*, *MYH2* and *MYH7* did not vary between summer and winter.

3.4. Discussion

This study indicates that the seasonal change between summer and winter in the metabolism of the muscle leads to Mangalica's gain in tolerance for heat and cold stresses. Very few studies on the muscle of Mangalica are available to date. To the best of our understanding, this is the first study that demonstrates seasonal changes in fibre type and gene expression relating to muscle metabolism function of muscle change seasonally in Mangalica. These results provide valuable insights on the mechanism of tolerance for heat and cold stresses in Mangalica.

It is known that cold environments decrease BW to maintain body temperature (Morrison *et al.* 2008; Bal *et al.* 2016), and heat stress reduces the accretion of muscle protein and developmental rate (Guo *et al.* 2018; Liu *et al.* 2022). Neonatal pigs need to maintain a high temperature: a thermoneutral zone of 30–34°C, and the early period is extremely affected by temperature conditions; for example, heat and cold shock, because they do not have adequate muscle and fat tissue to adapt to the ambient environment (Herpin *et al.* 2002; Carroll *et al.* 2012). However, in this study, weight gain in neonatal Mangalica did not differ between the seasons. We previously reported that neonatal Mangalica have thicker dorsal fat tissue compared to the commercial breed (Kim *et al.* 2022). These results suggest that neonatal Mangalica endures cold and heat shock conditions owing to the thickness of its fat tissue. On the contrary, before slaughter, weight significantly increased in spring and decreased in autumn compared to the annual average. Studies of wild animals such as rodents, deer and wild boars, which are not hibernators, have reported that their body weights are higher in spring and summer compared to autumn and winter because of seasonal factors such as temperature and food intake (Heldmaier 1988; Suttie & Webster 1995; Li & Wang 2005; Skubis *et al.* 2009). The BW/d of Mangalica indicated an increase in the growth rate in spring, which was consistent with that of wild animals.

During summer, the CSA of skeletal muscle cells and the thickness of the Z-line in Mangalica pigs increased. Increased muscle mass is associated with muscle fibre hypertrophy in mammals (Duclos *et al.* 2007; Watanabe *et al.* 2019). Thus, the increase in CSA suggests that the gain of weight in Mangalica is due to an increase in muscle mass during warm seasons. It has been reported that the CSA of the fast-twitch fibre is more than that of the slow-twitch fibre (Schiaffino & Reggiani 2011; Wilson *et al.* 2012). The Z-line of the slow-twitch fibre is thicker than that of the fast-twitch fibre, which is related to the number of mitochondria (Schiaffino & Reggiani 2011). In this study, the gene expression of *MYH4* and *GLUT4* was significantly decreased in winter compared to summer. The changes in these gene expressions were consistent with the results of CSA and Z-line, suggesting the shift in muscle fibre caused by seasonal changes in Mangalica. ATPase staining of the longissimus muscle in Mangalica indicates a significant increase in type 1 muscle fibre in winter.

Previous studies have reported that hibernators such as hamsters, black bears and white-tailed prairie dogs have rich type 1 muscle; the decreased CSA in muscle fibre and the shifting of muscle fibre type from type 2 to type 1 is accompanied by a decrease in temperature (Egginton *et al.* 2001; Rourke *et al.* 2006; Gao *et al.* 2012; Kawata *et al.* 2022). Furthermore, the metabolism of hibernators shifts from the glucose metabolism to lipolysis during winter (Cotton 2016), and unsaturated fatty acid such as oleic acid in fat tissue changed during pre-hibernation to post-hibernation (Florant 1998; Falkenstein *et al.* 2001). In this study, Oil Red O staining did not indicate morphological changes in intermuscular fat; however, oleic acid was significantly increased in winter compared to summer in the muscle of Mangalica (data not shown). Previous studies have revealed that the fat tissue of Mangalica was different and contained a high concentration of oleic acid compared to the commercial breed (Takatani *et al.* 2021; Kim *et al.* 2022). These results on Mangalica are

consistent with the changes in the muscle physiology of hibernators in winter. Hence, the gain in heat and cold tolerance by Mangalica may be related to the alterations of muscle based on seasonal change and the inter- action between muscle and fat tissue.

In summary, Mangalica has gained tolerance to the seasonal heat stress owing to changes in muscle fibre type and metabolic function. These results may contribute to elucidating the mechanism of thermogenetic adaptation in cold and heat environments in mammals.

Figure and captions

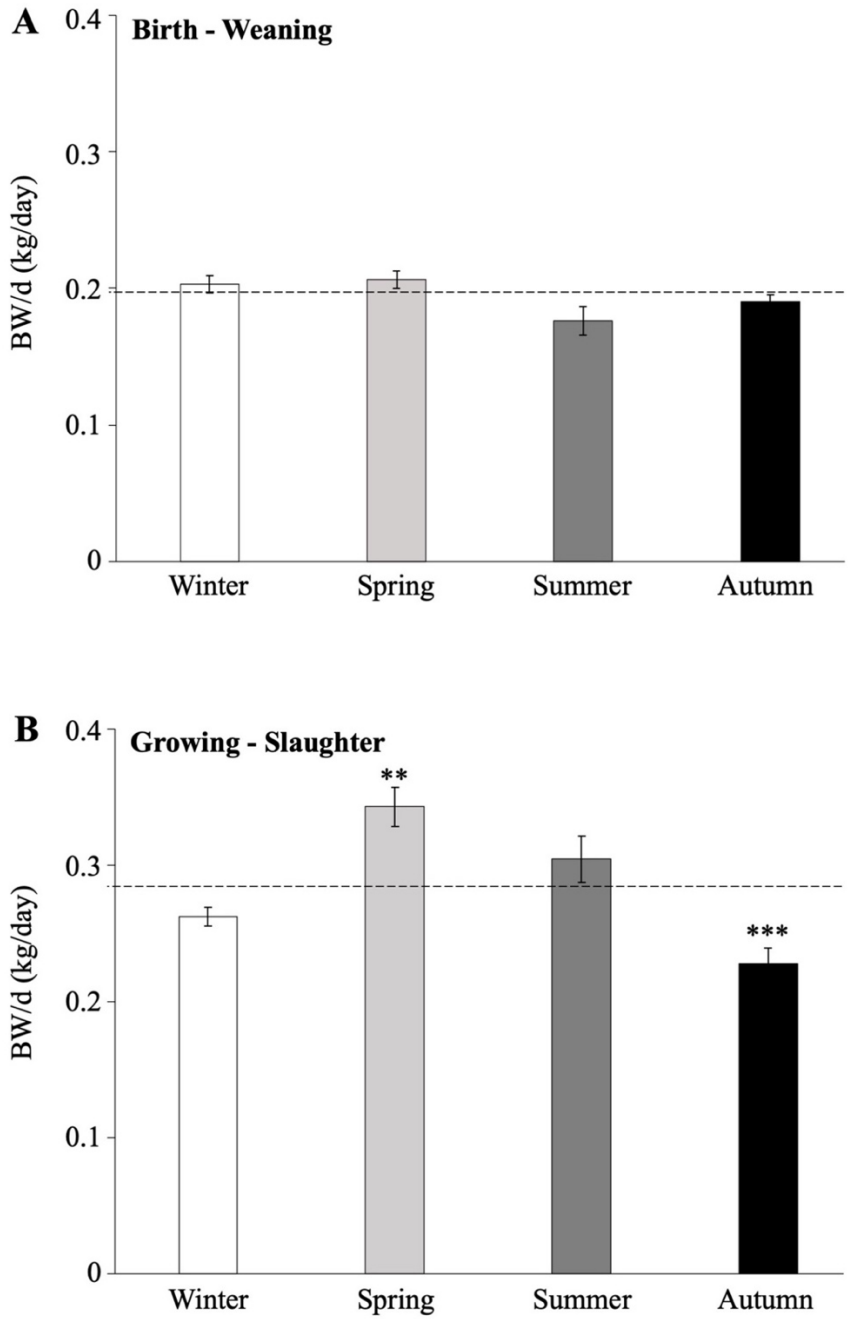

FIGURE 1. Daily gain of body weight (BW/d) in Mangalica (total n = 149). (A) BW/d from birth stage to weaning (n = 137). (B) BW/d from growing period and before slaughter period (n = 149). The line on the graph indicates the average of a year. The values of each season were compared to the average of a year. Values are shown as mean ± SEM. and $^{**}p < 0.01$, $^{***}p < 0.001$

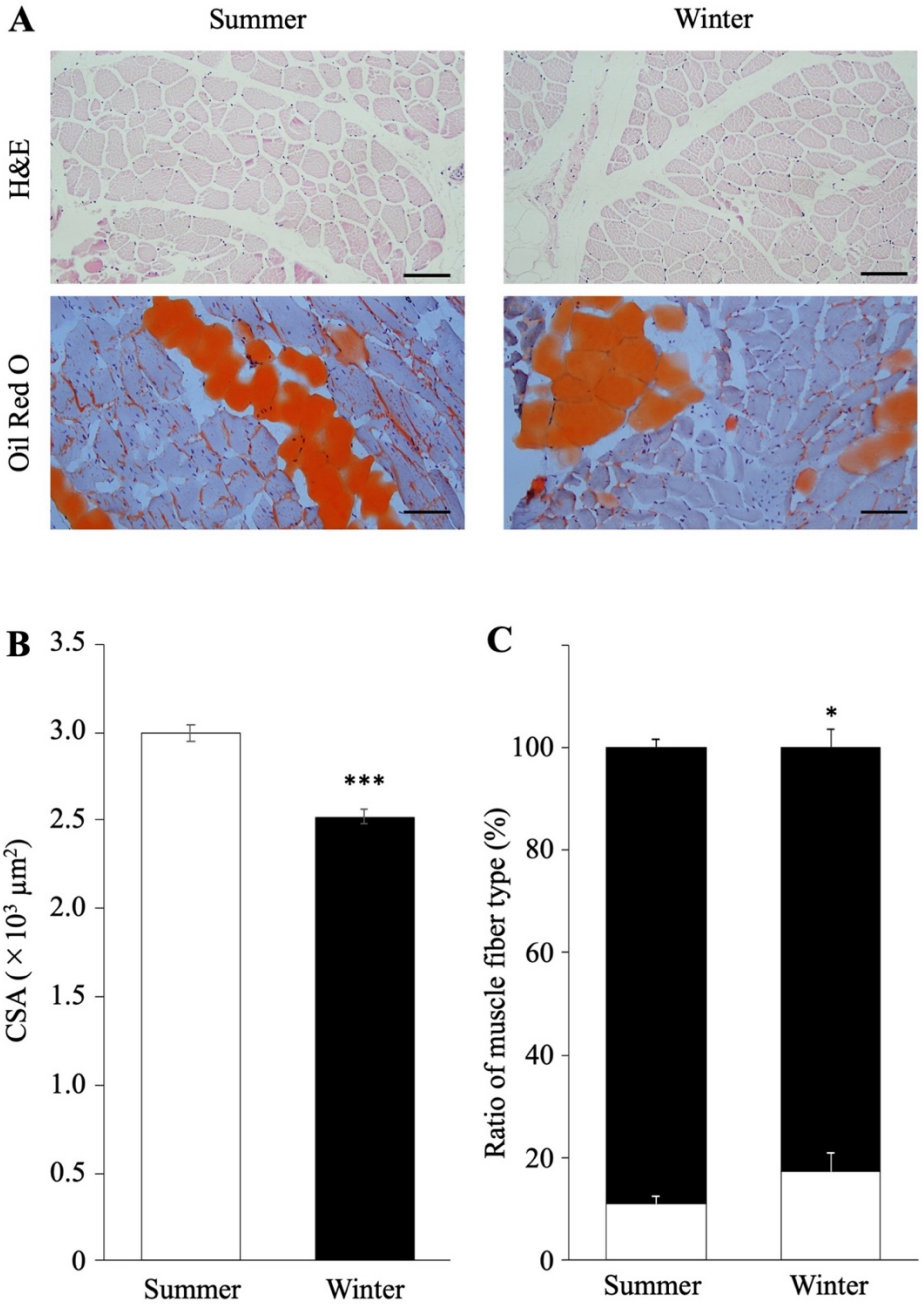

FIGURE 2. Comparison of muscle morphology between summer and winter. (A) Images of hematoxylin and eosin (H&E) and Oil Red O staining (bar 100 μm). (B) Comparison of cross-sectional area (CSA) of skeletal muscle cells between summer (n = 3, black square) and winter (n = 3, white square). (C) Comparison of ratio of muscle fiber type 1 (white square) and type 2 (black square) between summer and winter. Values are shown as mean ± SEM. and * $p < 0.05$, *** $p < 0.001$

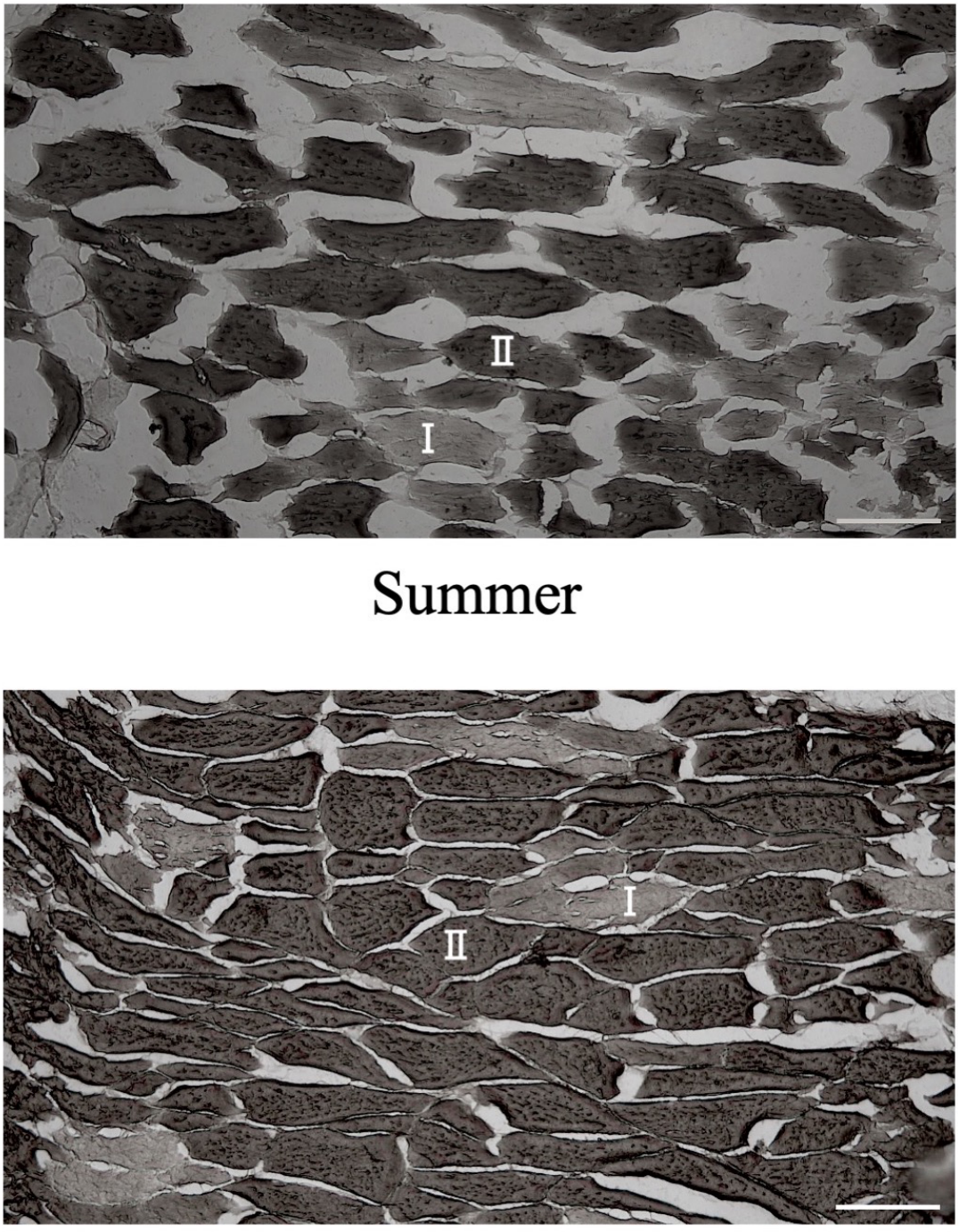

FIGURE 3. Image of ATPase staining of longissimus muscle of Mangalica during summer and winter (bar 100 μm). I: type 1 muscle fiber, II: type 2 muscle fiber.

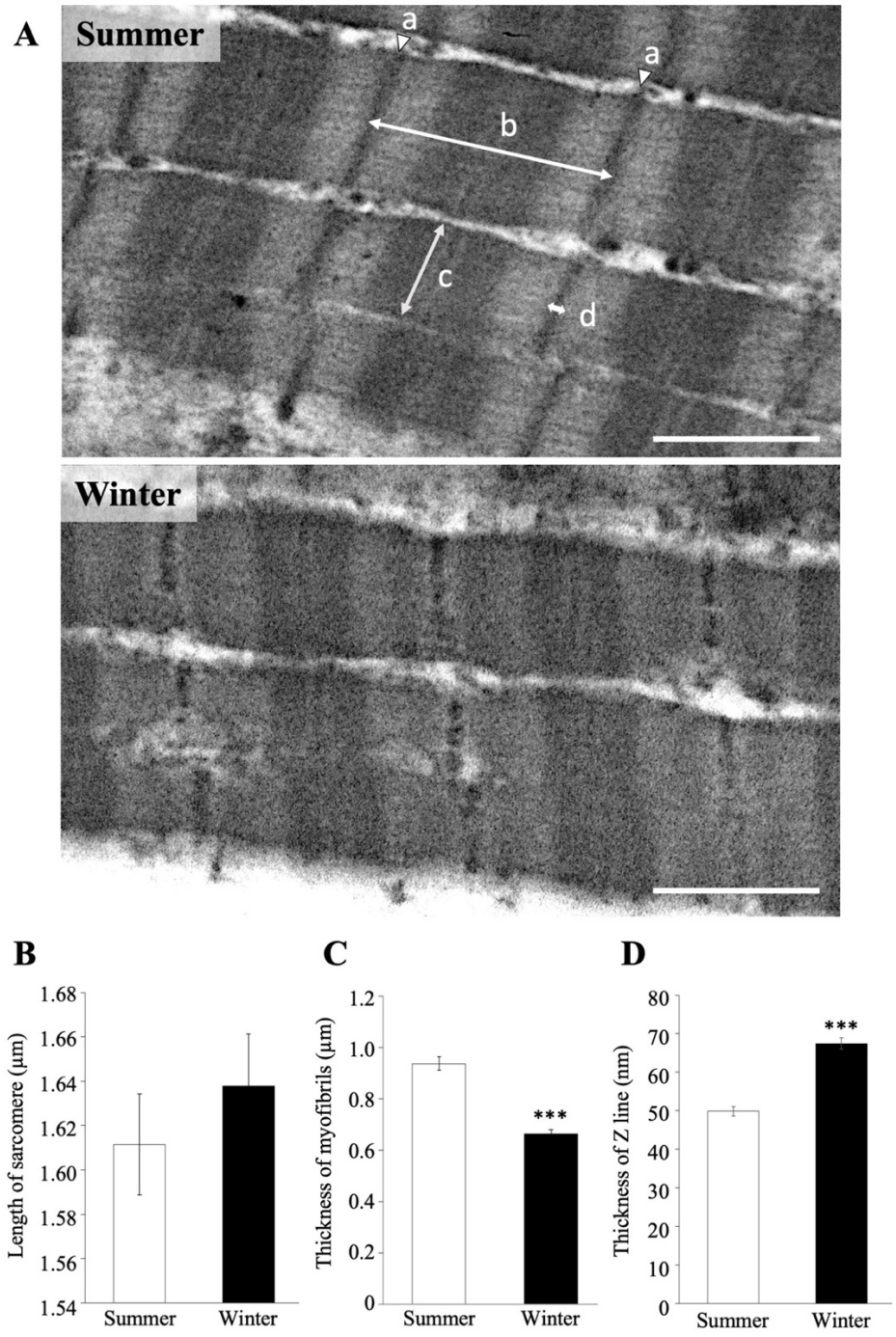

FIGURE 4. Comparison of sarcomere between summer (n = 3, white square) and winter (n = 3, black square). (A) Transmission electron microscope image of myofibrils, a: Z-line, b: Length of sarcomere, c: Thickness of myofibrils, d: thickness of Z-line (×3000, bar 1 μm). (B) Length of sarcomere. (C) Thickness of myofibrils. (D) Thickness of Z-line. Values are shown as mean ± SEM. and *** $p < 0.001$

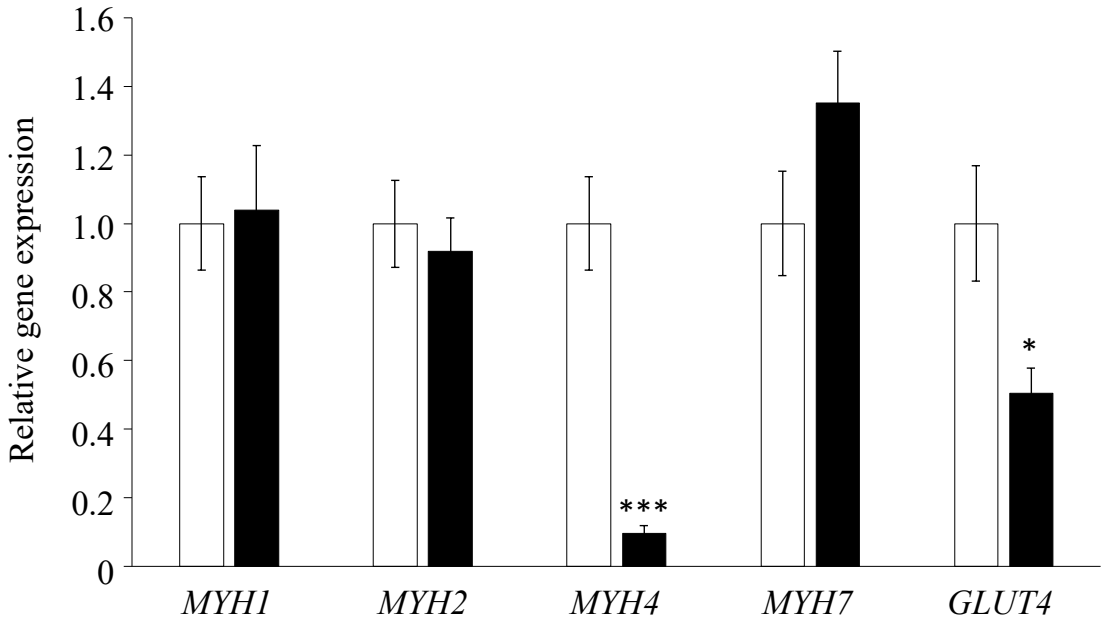

FIGURE 5. Gene expressions of muscle tissue. The muscle tissue was collected from the longissimus muscle of 8 months old Mangalica in summer (n = 3, white square) and in winter (n = 3, black square). Values are shown as mean ± SEM. and * $p < 0.05$, *** $p < 0.001$

TABLE 1. Primer pairs used in the analysis of gene expression

Gene	Primer		Product length (bp)	Annealing temperature (℃)	Accession number
MYH1	F	CTTTCCTCTTCACTGGCGCA	290	60	NM_001104951.2
	R	GATTCTGCTTGGGAAGCCCT			
MYH2	F	CCAGACGGAAGAGGATCGGA	237	60	NM_214136.1
	R	ACTTTTGTGTGAACCTCCCGG			
MYH4	F	CTGGCTTTCCTCTTTGCTGAGA	184	60	NM_001123141.1
	R	TGGTCTCATTGGGGATGATGC			
MYH7	F	GGAAGAGTGAGCGTCGCAT	290	60	NM_213855.2
	R	AATCTACTCCTCGTTCAAGCCC			
GLUT4	F	TGGGAAGGAAGAAGGCAATGCT	234	60	NM_001128433.1
	R	AGAATGCCAATGACGATGGCC			
S18	F	TGCCTTTGCTATCACTGCGA	285	60	NM_213940.1
	R	CTGTGGGCCCGAATCTTCTT			

Table 2. Ambient and body temperatures in a year

	January	February	March	April	May	June	July	August	September	October	November
Ambient temperature	−8.5±0.8	−7.3±0.6	−0.4±0.5	7.1±0.6	11.8±0.5	15.0±0.8	20.4±0.4	20.0±0.4	16.6±0.5	9.2±0.7	3.5±0.5
Body temperature	39.1±0.2	39.0±0.1	38.7±0.2	38.3±0.1	38.5±0.1	38.6±0.1	38.6±0.1	38.6±0.1	38.6±0.1	38.6±0.1	38.3±0.1

Chapter 4

SEASONAL ADAPTATION OF MANGALICA PIGS IN TERMS OF METABOLIC FUNCTION RELATED TO BROWNING FROM WHITE ADIPOCYTE

4.1. Introduction

The Mangalica is a lard-type, native Hungarian pig breed and it have a genetic background and features similar to wild boars compared to commercial breeds (Frank *et al.* 2017; Bâlteanu *et al.* 2019; Kaltenbrunner *et al.* 2019). Furthermore, Mangalica has cold tolerance and it is raising in a grazing environment throughout the year in general in Hungary. It had reported that Mangalica did not decreased daily gain of body weight compared to commercial breed in cold condition (Pârvu *et al.* 2012, 2012). Previous study had been demonstrated that Mangalica change the structure and metabolic function in muscle with seasonal change, and these changes may contribute to obtain the cold tolerance in Mangalica (Kim *et al.* 2023).

Skeletal muscle constitutes a substantial physiological contributor to the basal metabolic rate, and is integral to body temperature regulation mediated shivering thermogenesis and non-shivering thermogenesis (NST) (Frontera & Ochala 2015; Nowack *et al.* 2017; Bal *et al.* 2018). The shivering thermogenesis in muscle is related to recruitment of Ca^{2+} to sarcoplasmic reticula, and Ca^{2+} is transported by sarcoendoplasmic reticulum ATPases (SERCA: ATP2A1, ATP2A2 and ATP2A3) with hydrolysis of ATP. The hydrolysis of ATP with Ca^{2+} transportation and muscle contraction result in production of heat (Fuller-Jackson & Henry 2018). The NST in muscle is related to gene expression of sarcolipin (SLN). SLN inhibited the Ca^{2+} transportation and enhance the ATP hydrolysis at SERCA, these SLN effect result in heat production (Bal *et al.* 2018).

The adipose tissue also serves as a significant metabolic tissue in the regulation of body temperature and is associated with the acquisition of cold tolerance. The adipose tissue includes 3 phenotypes, which have different metabolic functions, such as white adipocyte in white adipose tissue (WAT), brown adipocyte in brown adipose tissue (BAT) and beige adipocyte. Among 3 phenotypes, Brown adipocyte and beige adipocyte is well known to have high metabolism as it includes many mitochondria and promotes NST through the uncoupling protein (UCP) in mitochondrial membranes (Bargut *et al.* 2017; Jung *et al.* 2019). UCP has been reported to been associated with NST not only in adipose tissue but also in muscle (Fuller-Jackson & Henry 2018). Furthermore, recent research has revealed that white adipocyte transformed (browning) to beige adipocyte with adrenergic stimulation (Patsouris *et al.* 2015; Hu & Christian 2017; Xu *et al.* 2019; Pinto *et al.* 2022). Hibernators such as squirrel and hamster were reported that the browning of white adipocyte and gene expression of UCP1 were increased with decrease temperature and photoperiod, and they obtain the cold tolerance (Laursen *et al.* 2015; Ryu *et al.* 2018). Although metabolism of muscle was changed by season in Mangalica, change of fat following season is unclear. On the other hand, pigs are considered to lack the functional BAT and UCP1 (Berg *et al.* 2006; Gaudry *et al.* 2017; Hou *et al.* 2017). Previous studies reported that pigs are sensitive to cold condition, and their physiological functions, such as development rate, metabolism and fertility, were reduced with decreased temperature (Claus & Weiler 1994; Carroll *et al.* 2012; Guo *et al.* 2018; Choi *et al.* 2019; Yu *et al.* 2021; Liu *et al.* 2022). Whereas, previous study using Tibetan pigs, which is inhabiting the Qinghai-Tibetan Plateau, acute cold stimulation induces expression of UCP3 and browning of white adipocyte (Lin *et al.* 2017). These results were suggested that the adaptation to cold condition in pigs was depended to pig breed and indicated the possibility that the UCP3 has functional redundancy across UCP1 and white adipose browning is occurred without UCP1. However, the knowledge is limited that thermogenetic

function in muscle and fat tissue of Mangalica with seasonal change, and the mechanism to obtain the cold tolerance is not revealed completely in Mangalica. In particularly, there is a lack of studies on gene expression of UCP and the browning in fat tissue of Mangalica.

In this study, to revealed the mechanism of obtain the cold tolerance in Mangalica, I perform the gene expression analysis in fat tissue using RT-PCR and RNA-seq compared between Mangalica and LWD.

4.2. Materials and Methods

4.2.1. Seasonal experimental setting for Mangalica

The experimental setting of seasons was based on weather re- cords of the Nukanai station of the Japan Meteorological Agency (https://www.data.jma.go.jp/obd/stats/etrn/index.php?prec_no. =20&block_no = 1286&year = &month = &day = &view=), which is located approximately 12 km from the Tokachi Royal Mangalica Farm in Japan (42°47.2' N). The season was determined based on the average temperature. Each season was determined as follows: winter from December to March (−8.5 to −0.4°C), spring from April to June (7.1–15.0°C), summer from July to September (16.6–20.4°C) and autumn from October to November (3.5–9.2°C).

4.2.2. Animal and ethics

The study and management of all animals used in this study were conducted in accordance with the Guidelines for the Care and Use of Animals of the Obihiro University of Agriculture and Veterinary Medicine (approval numbers 19-26, 20-29, 21-19 and 22-165).

Mangalica animals that were raised at the Tokachi Royal Mangalica Farm (Makubetsu) during 2020-2021 were used for the experiment. The dorsal fat tissues and longissimus muscle tissue were collected from 8-month-old Mangalica, which was slaughtered after electrical stunning, in summer (n = 3) and winter (n = 3).

Furthermore, the fat tissue of commercial pig breed was collected LWD (cross breed) after slaughtered with electrical stunning which was raised at indoor in Obihiro University of Agriculture and Veterinary Medicine (n =1) and at outside from pig farm of Elpaso (Makubetsu) in summer (n = 6) and winter (n = 6). All fat tissue samples were kept at −80°C until experiments were performed.

4.2.3. Analysis of gene expression in fat tissue and muscle tissue

Total RNA was extracted from fat and muscle samples using TRIzol reagent (Thermo Fisher Scientific). The total RNA concentration was measured using a NanoDrop spectrophotometer (Thermo Fisher Scientific). Total RNA (1 μg) was treated with DNase and con- verted to cDNA using Random Primers (48,190,011, Thermo Fisher Scientific) and SuperScript II (18,064,022, Thermo Fisher Scientific) on a GeneAtlas thermal cycler 482 (4,990,902, ASTEC, Fukuoka, Japan).

Real-time PCR was performed using the SsoAdvanced Univer- sal SYBR Green Supermix (1,725,271, Bio-Rad) and LightCycler 96 (05815916001, Roche), according to the manufacturers' instructions. Each PCR reaction was performed at 95°C for 30 s for denaturation, 95°C for 10 s and 60°C for 60 s for 35 cycles for amplification. Table 1 lists the primer sequences used. We used 18S ribosomal RNA (18S) for internal control, and the relative expression levels of genes were calculated using the $2^{-\Delta\Delta CT}$ method. Furthermore, total RNA of fat from Mangalica and LWD raising indoor were used to global analysis of gene expression with RNA-seq.

4.2.4. Determination of mitochondrial function and copy number

Total DNA, comprising both genomic and mitochondrial DNA (mtDNA), was extracted from the browning adipocytes. DNA concentration was determined using Nanodrop (Thermo Fisher Scientific). To quantify the relative mtDNA copy number compared to genomic DNA, real-time PCR was performed using the LightCycler® 96 system. The primers used for amplification were as follows: COX-II: forward GGCTTACCCTTTCCAACTAGG, reverse AGGTGTGATCGTGAAAGTGTAG; β-globin: forward GGGGTGAAAAGAGCGCAAG, reverse CAGGTTGGTATCCAGGGCTTCA.

4.2.5. RNA-seq

The RNA samples from Mangalica and LWD raising indoor were sent to Novogene (Novogene, Beijing, China) for RNA-seq analysis. The integrity of the RNA samples was measured to obtain the sequencing information using the bioanalyzer and sequenced on Illumina platforms. The sequencing performed in the NovaSeq 6000 (Illumina, San Diego, CA, USA) resulted in 150 bp paired-end sequences, around 20M raw reads (around 4 G raw data) in each library. The adapter sequences were removed with the Fastp (version 0.23.4) and the sequence length (default: 50-60 bp). The quality analysis of the reads was carried out using FastQC (version 0.12.1). The trimmed reads were mapped on the pig reference genome (Sscrofa 11.1.110) using HISAT-3n (version 2.2.1-3n-0.0.3), and the mapped reads were sorted and converted from SAM to BAM files using SAMtools (version 1.18). Read count was conducted with converted BAM files and the GTF file (Sscrofa 11.1.110) using featureCounts (version 2.0.1). The counted CSV files were uploaded to Calculate and draw custom Venn diagrams (https://bioinformatics.psb.ugent.be/webtools/Venn/) and produced venn diagram comparing fat tissue of Mangalica in summer and winter, and fat tissue of LWD raising indoor. Furthermore, the counted CSV files were uploaded to TCC-GUI (https://infinityloop.shinyapps.io/TCC-GUI/) and normalizing with TMM. I integrated Differential Expression and produced MA-plot (FDR Cut-off: 0.1) and Volcano plot (Fold Change Cut-off: under -15 and over 1.5, P-value Cut-off: 0.05). The top 100 of DEGs upregulated in Mangalica was uploaded to Metascape (https://metascape.org/gp/index.html #/main/step1) and the upregulated genes are first converted into their corresponding Homo sapiens Entrez gene IDs using the latest version of the database (last updated on 2023-09-01). And, Metascape Gene List was produced using converted data.

4.2.6. Statistical analyses

All statistical analyses were performed using R version 4.2.2 (https://www.r-project.org/). *T* and *U* test were used to compare summer and winter. All data are presented as the mean ± standard error of the mean (SEM). $p < 0.05$ was considered significant († $p < 0.1$, * $p < 0.05$, ** $p < 0.01$, *** $p < 0.001$).

4.3. Results

4.3.1. Gene expression related thermogenesis in fat and muscle tissue

We compared the gene expression in the muscle and fat tissue between summer and winter in Mangalica and LWD raising outside (Figure 1 and 2). In muscle tissue, the gene expressions of *PGC-1α*, and *UCP3* were significantly increased and SLN was significantly decreased in winter compared to summer at LWD (Figure 1A). In Mangalica, the gene expression of *PGC-1α* and *UCP3* were significantly decreased and *ATP2A1* and *SLN* were significantly increased in winter compared to summer (Figure 1B). In fat tissue, the gene expression of *UCP2* was significantly increased and *UCP3* was significantly decreased in winter compared to summer at LWD (Figure 2A). However, in Mangalica, the gene expression of *PGC-1α*, *UCP1*, *UCP2* and *UCP3* were significantly increased in fat at winter compared to summer (Figure 2B).

In Mangalica, the expression of COX2 was significantly increased in muscle tissue ($p < 0.05$, Figure 3A) and the gene expression of COX1 tended to increase in fat tissue ($p < 0.1$, Figure 3B).

4.3.2. RNA-seq

The gene expression related to thermogenesis of Mangalica fat tissue was significantly increased in winter compared to summer. Hence, RNA-seq was performed with fat tissue of Mangalica in summer (n = 1) and winter (n = 2) and LWD raising indoor (n = 1) and specific gene expression in Mangalica was identified. I produced Venn diagram compared to Mangalica in summer, winter and LWD, and analysed Differentially Expressed Genes (DEGs) between Mangalica and LWD. Mangalica expressed 445 specific genes in summer and 3969 specific genes in winter compered to LWD (Figure 4). The number of genes were 35,670 before normalizing with TMM and 18,595 (52.13%) genes were removed by

normalizing with TMM. After normalizing, the differentiated genes (DGEs) were shown 6541 from the MA-plot (Figure 5) and Mangalica had 2258 upregulated DGEs from the Volcano-plot (Figure 6). From Metascape Gene List, the most upregulated genetic pathway is “regulation of secretion by cell” (GO:1903530) and the pathway of “positive regulation of cold-induced thermogenesis” (GO:0120162) was involved (Figure 7).

4.4. Discussion

This study indicates that the seasonal change between summer and winter in the metabolism of the fat tissue leads to Mangalica's gain in tolerance for cold stresses. Very few studies which is the thermogenic functions of Mangalica are available to date. To the best of our understanding, this is the first study that demonstrates seasonal changes in gene expression relating to thermogenesis of fat tissue in Mangalica. These results provide valuable insights on the mechanism to gain cold tolerance in Mangalica and mechanism of browning of white adipocyte.

The interaction between SERCA and SLN have been reported to relate the thermogenesis in muscle (Fuller-Jackson & Henry 2018; Bal *et al.* 2018). In mouse, cold stimulation was upregulated the SLN expression (Bal *et al.* 2017). Furthermore, in wild boar, gene expression of SERCA and SLN was increased by cold exposure and it obtain cold adaptation (Nowack *et al.* 2019). The increase of *ATP2A1* and *SLN* expression in Mangalica is similar to the animals which have cold adaptation ability, and this genetic change in muscle may be related to obtain cold adaptation in Mangalica.

Previous studies using hamster reported that cold stimulation affected gene expression of UCP1 in fat tissue and enhanced browning of white adipocyte (Bal *et al.* 2017). Within the UCP family, UCP1 is recognized as principal protein related to thermogenesis. In contrast, UCP2 and UCP3, which expressed multiple tissues such as muscle, have been reported that these proteins were lacked the function of thermogenesis in mouse (Gong *et al.* 2000; Vidal-Puig *et al.* 2000; Erlanson-Albertsson 2003; Kim *et al.* 2022). On the other hand, in pig lacking UCP1, the cold stimulation induced lipolysis following upregulation of UCP3 expression depending on pig breed (Lin *et al.* 2017). Furthermore, previous study demonstrated that the adipose browning and upregulation of UCP1 enhanced mitochondrial function (Chouchani *et al.* 2016). In this study, gene expression of UCP family was increased in winter compared

to summer in fat tissue of Mangalica, and COX expression indicated the tendency to increase with upregulation of UCP similar to previous studies. However, these seasonal changes did not indicate in LWD raising outside which is a similar environment to Mangalica. From these results, it was suggested that fat tissue of Mangalica may be browning in winter, and browning of white adipocyte in pig is not influenced by raising environment and it affected depending on breed. Although gene expression of UCP1 was increased in winter in fat tissue of Mangalica, protein of UCP1 could not be detected to expression using Western blotting with mouse monoclonal antibody in prior experiment (data is not shown). In whale which do not have UCP1 similar to pig, protein of UCP1 have been detected in third layer in fat tissue near the muscle layer using Western blotting with rabbit polyclonal antibody (Zhou *et al.* 2022). The browning of white adipocyte was suggested to occur the specificity of the layer in fat tissue. To determine the layer to construct browning cells, I will perform the experiment of fat physiology using each fat layers.

In this study, RNA-seq detected 4414 specific genes and 6541 DEGs in fat tissue of Mangalica. Previous study comparing between Iberian pig and Duroc, RNA-seq detected 837-1435 DEGs with software of Cufflinks pipeline and DESeq2 (Benítez *et al.* 2019). Furthermore, cross breed of Meishan (Meishan × LWD) pig had been detected 214 DEGs compared to cross breed of Landrace (Landrace × LWD) using microarray (Kojima *et al.* 2018). Mangalica have been reported that genome of Mangalica is near to wild boar in Hungary and Romania than commercial breed such as Duroc, Landrace and Large White with RNA-seq using blood sample (Bâlteanu *et al.* 2019). Thus, the RNA-seq result of Managalica fat in this study was in accord with previous study and it is suggested that Mangalica has many specific gene expressions more than other lard-type breeds. The gene sets of RNA-seq was containing gene expression of *PRDM16*, *UCP1* and *UCP2*, which indicate genetic ontology “positive regulation of cold-induced thermogenesis”. These genes

were detected with Real-time PCR in fat tissue of winter Mangalica. Furthermore, *PRDM16* and *UCP2* were involved the genetic pathway of “brown fat cell differentiation” in human, and hence white adipocyte of Mangalica may be suggested to occur the browning in winter.

In summary, Mangalica may gained the cold tolerance owing to occur the browning with upregulation of UCP expression. These results may contribute to elucidating the mechanism of browning of white adipocyte and thermogenetic adaptation in cold environments in mammals lacking BAT or UCP1.

Figure and captions

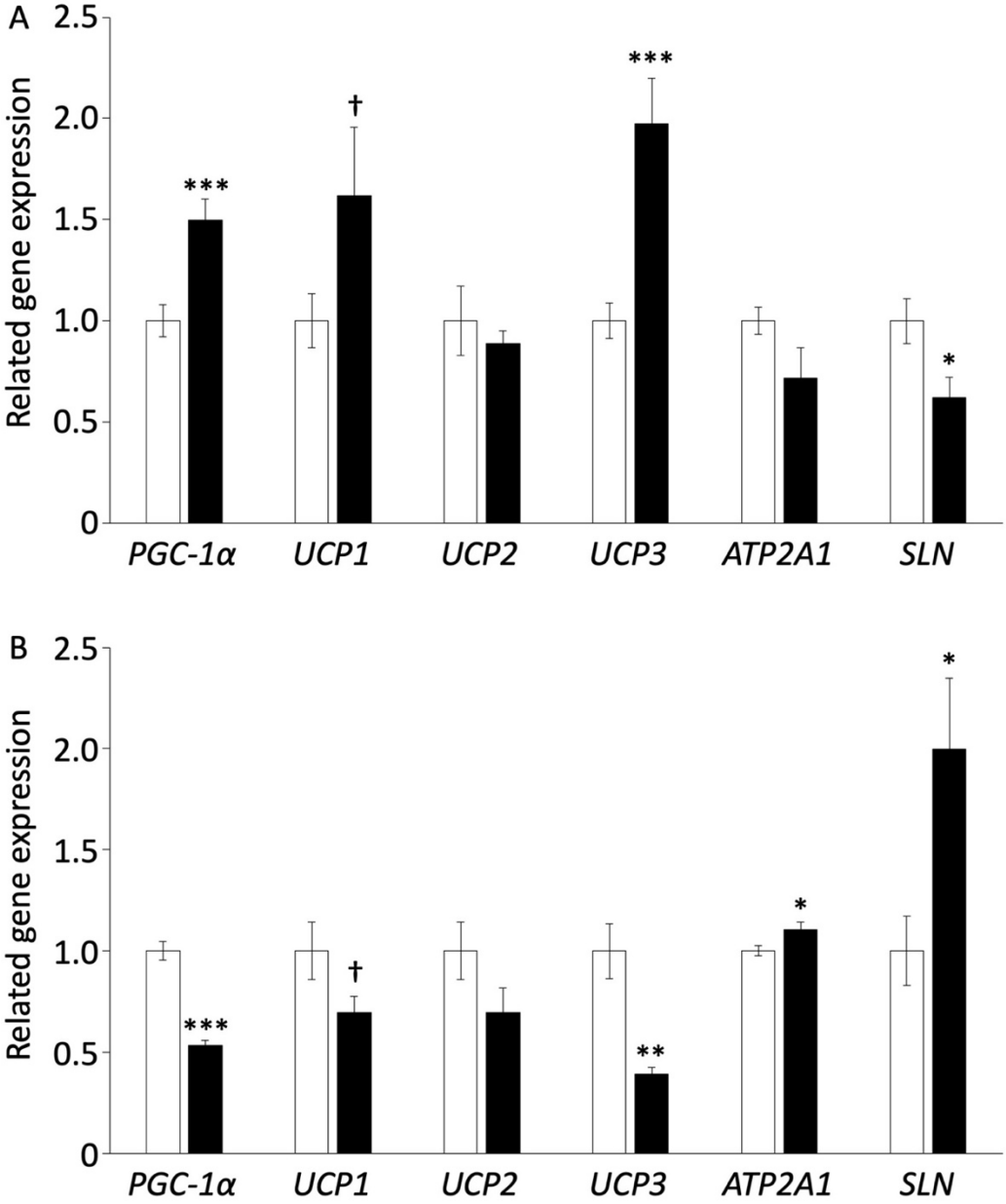

FIGURE 1. Gene expressions of muscle tissue in LWD and Mangalica. The muscle samples were collected from the longissimus muscle of LWD and Mangalica in summer (white square, LWD: n = 6, Mangalica: n = 3) and winter (black square, LWD: n = 6, Mangalica: n = 3). (A) the gene expression of muscle sample in LWD. (B) the gene expression of muscle sample in Mangalica. Values are shown as mean ± SEM. and † $p < 0.1$, * $p < 0.05$, ** $p < 0.01$, *** $p < 0.001$

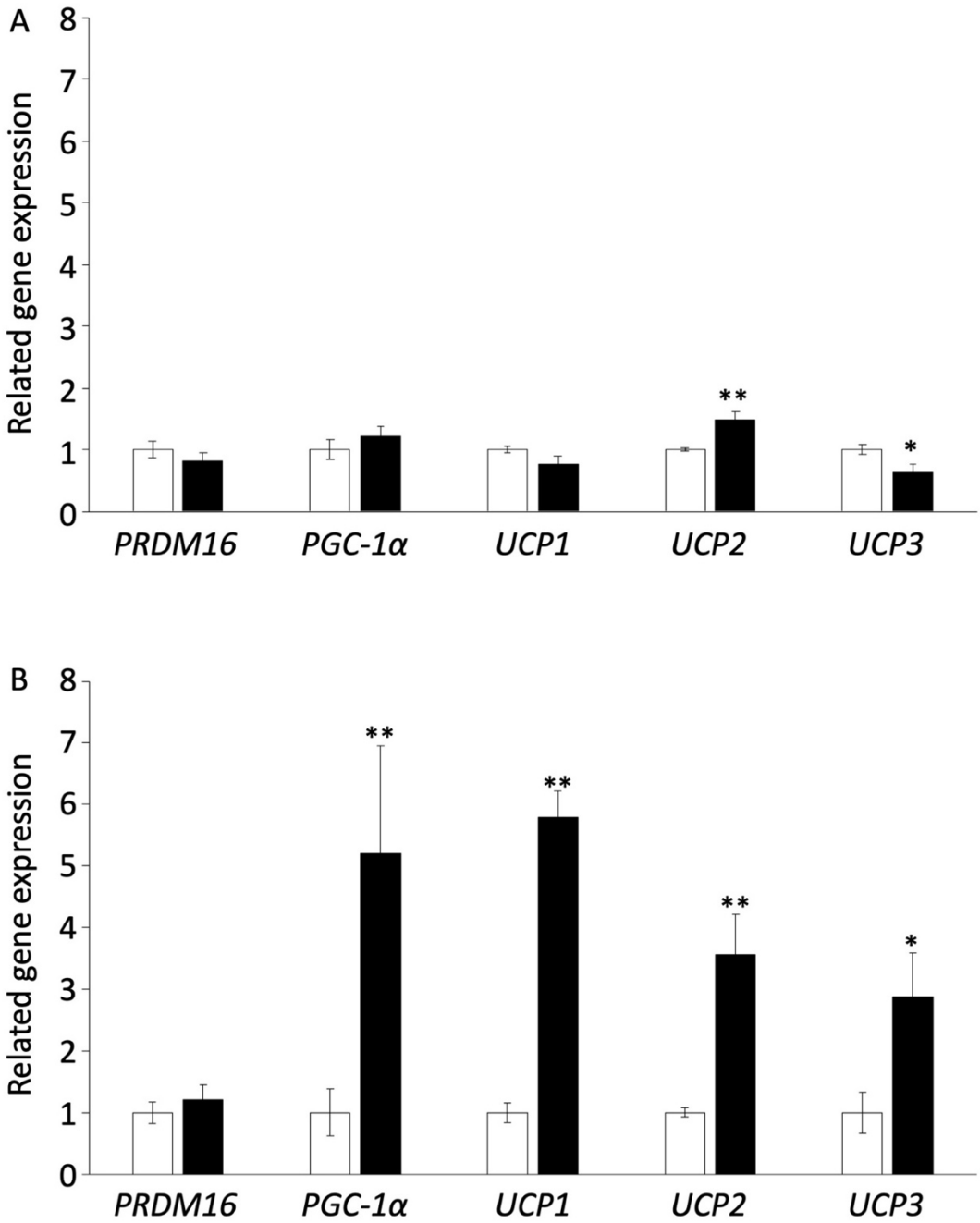

FIGURE 2. Gene expressions of fat tissue in LWD and Mangalica. The fat samples were collected from the dorsal fat tissue of LWD and Mangalica in summer (white square, LWD: n = 6, Mangalica: n = 3) and winter (black square, LWD: n = 6, Mangalica: n = 3). (A) the gene expression of fat sample in LWD. (B) the gene expression of fat sample in Mangalica. Values are shown as mean ±SEM. and † $p < 0.1$, * $p < 0.05$, ** $p < 0.01$, *** $p < 0.001$

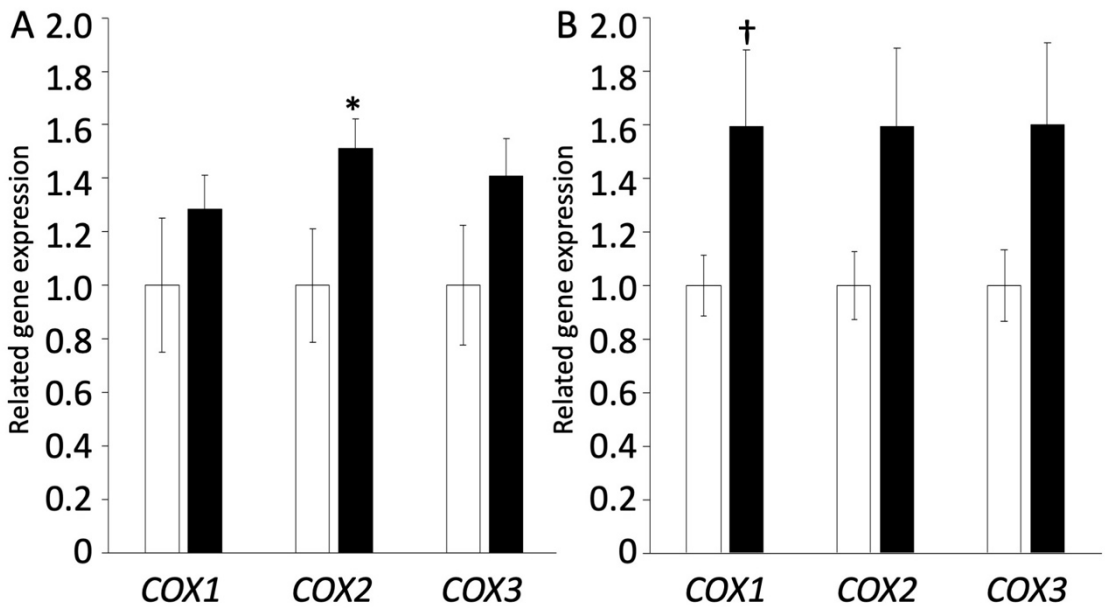

FIGURE 3. Gene expressions of COX family using total DNA in muscle and fat sample of Mangalica. The muscle and fat samples were collected from the longissimus muscle and dorsal fat tissue of Mangalica in summer (white square, n = 3) and winter (black square, n = 3). (A) the gene expression of COX family in muscle sample. (B) the gene expression of COX family in fat sample. Values are shown as mean ±SEM. and † $p < 0.1$, * $p < 0.05$, ** $p < 0.01$, *** $p < 0.001$

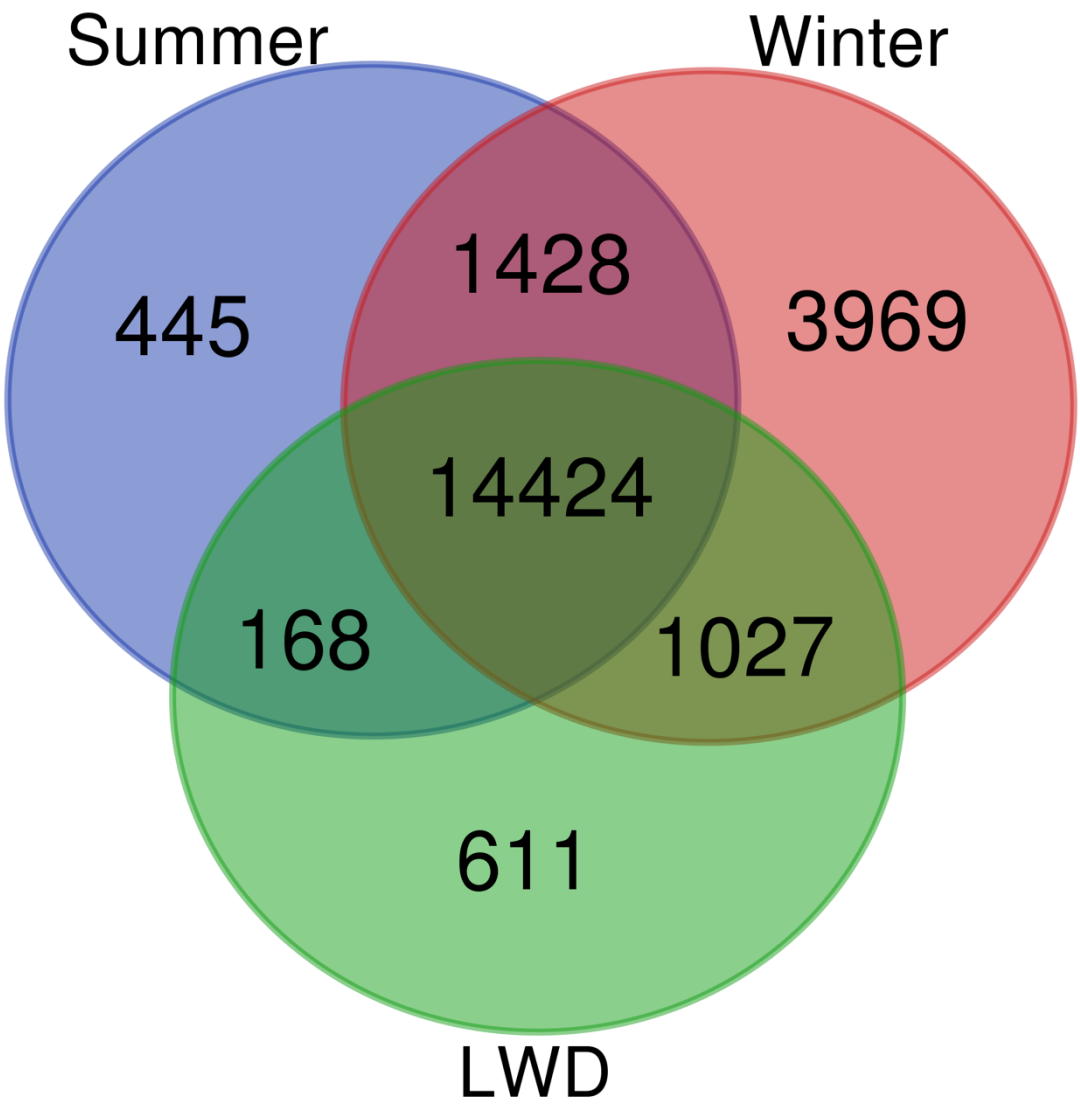

FIGURE 4. The Venn diagram compared to Mangalica in summer, winter and LWD. The venn diagram was produced by Mangalica in summer (n = 1), in winter (n = 1) and LWD raising indoor (n = 1) with Calculate and draw custom Venn diagrams (https://bioinformatics .psb.ugent.be/webtools/Venn/)

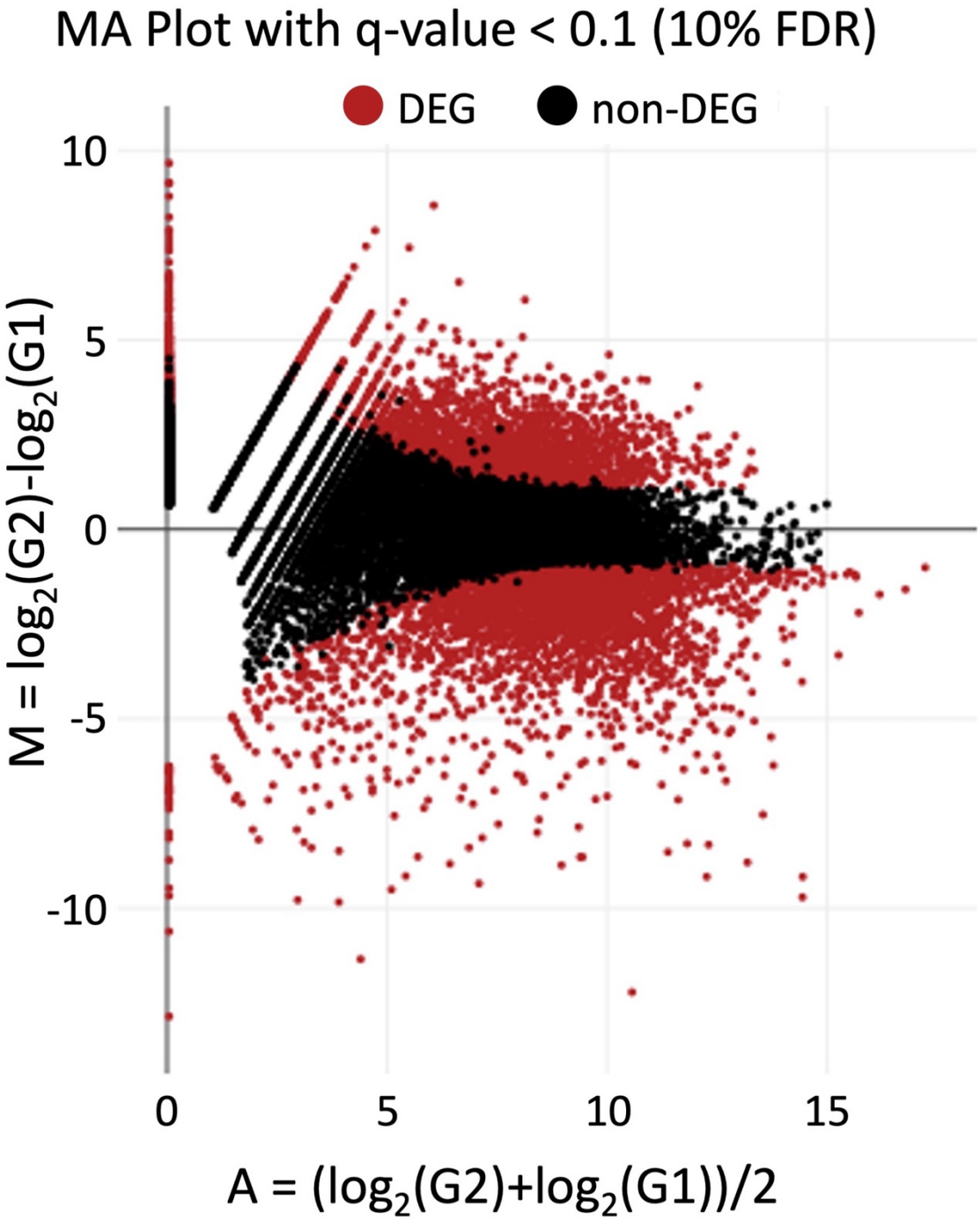

FIGURE 5. The MA plot compared to Mangalica and LWD. The MA plot was produced by RNA-seq data after normalized wit TMM of Mangalica (n = 3) and LWD raising indoor (n = 1) using TCC-GUI (https://infinityloop.shinyapps.io/TCC-GUI/).

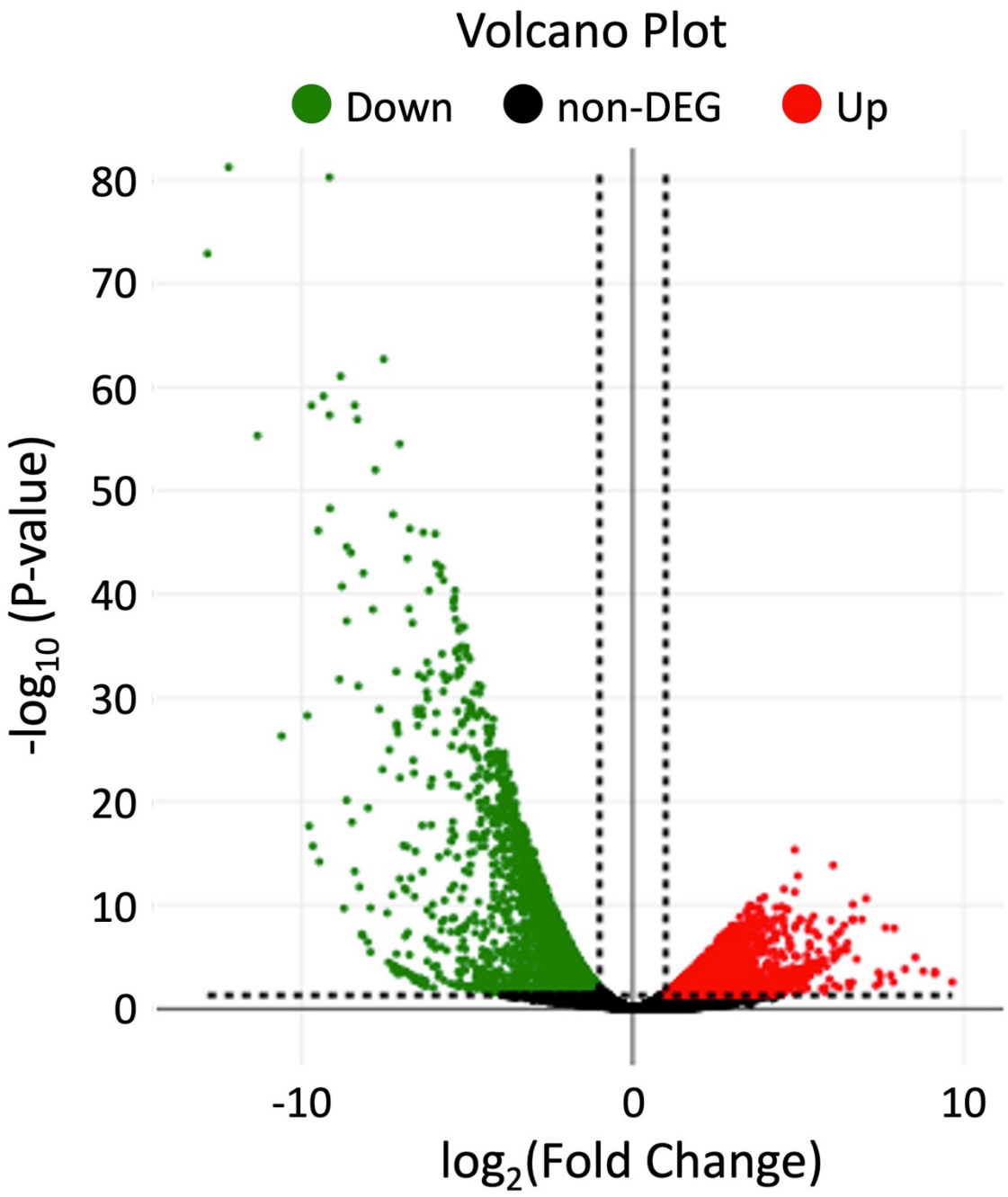

FIGURE 6. The Volcano plot compared to Mangalica and LWD. The Volcano plot was produced by RNA-seq data after normalized with TMM of Mangalica (n = 3) and LWD raising indoor (n = 1) using TCC-GUI (https://infinityloop.shinyapps.io/TCC-GUI/).

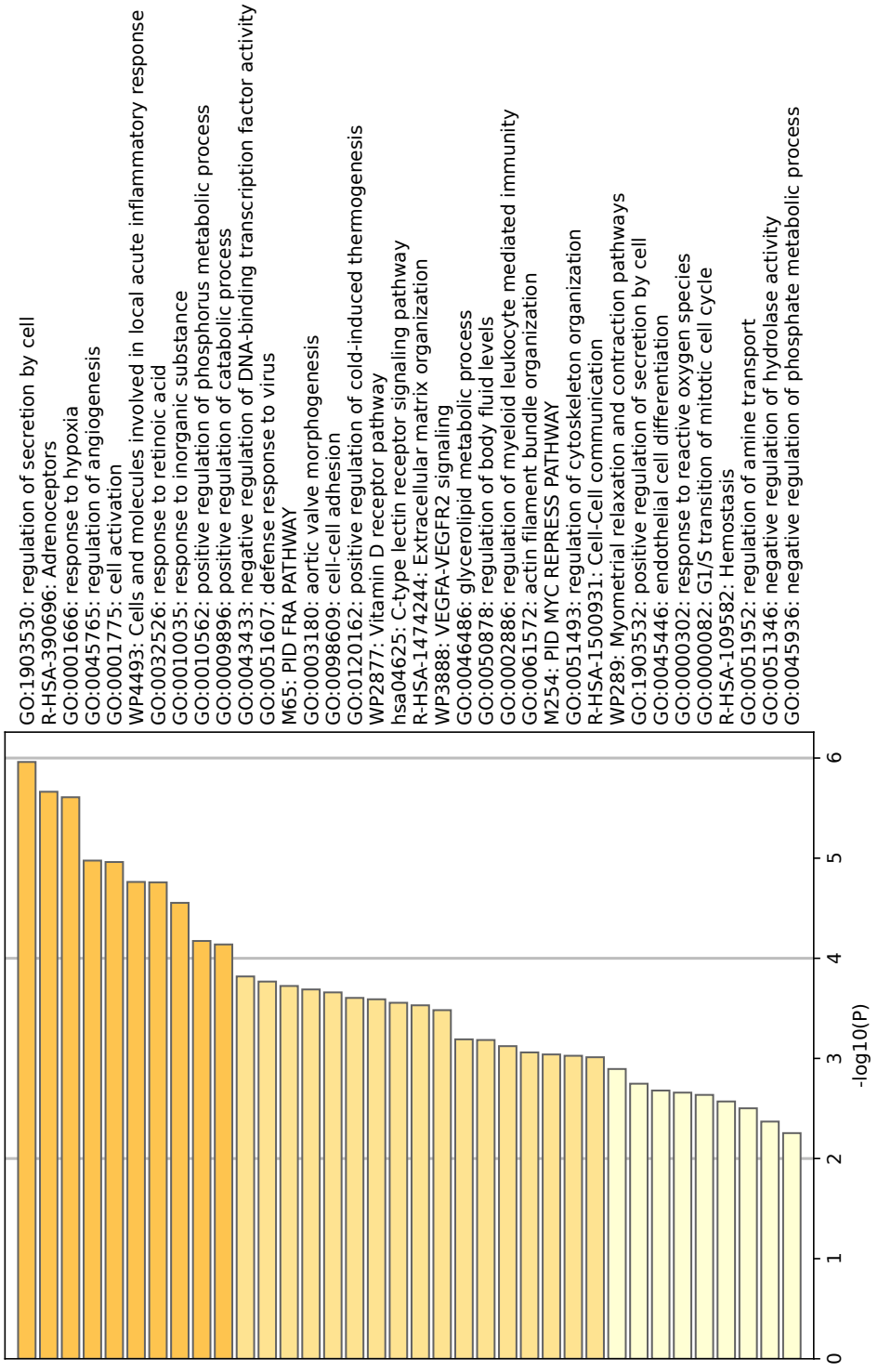

FIGURE 7. The Metascape Gene List indicated upregulated genetic pathway in Mangalica compared to LWD. Metascape Gene List was produced by top 100 DEGs upregulated in Mangalica (n = 3) using Metascape (https://metascape.org/gp/index.html#/main/step1).

TABLE 1. Primer pairs used in the analysis of gene expression

Gene		Primer	Product length (bp)	Annealing temperature (°C)	Accession number
PRDM16	F	CCCGCCTGGTGTAGGAATTT	83	60	XM_021095209.1
	R	TGGGGTGTTTGTAACGGAGG			
PGC-1α	F	CATGTGCAACCAGGACTCTG	133	60	NM_213963
	R	GCTGTCTGTATCCAAGTCGTTC			
UCP1	F	GCAGGGCAGACAGGTAAGC	134	60	XM_021100543.1
	R	CAAATAGTCCCGCCAAACCA			
UCP2	F	CCTCAGTGTGAGACCTGACGAA	148	60	NM_214289
	R	CTGTGGCCTTGAATCCAACCA			
UCP3	F	ATTCCAGGCCAGCATACACG	165	60	NM_214049
	R	GTCACCATCTCGGCACAGTT			
ATP2A1	F	TGAAGACCTCCTAGTGCGGA	268	60	NM_001204393.1
	R	GACAATGTCTCGGGCCTTGA			
SLN	F	CTGTGTGTCCTTGACGCTGT	255	60	NM_001044566.2
	R	GACAGCAATGGGATTGAAGGC			
18S	F	TGCCTTTGCTATCACTGCGA	285	60	NM_213940.1
	R	CTGTGGGCCCGAATCTTCTT			

GENERAL DISCUSSION

This study indicated a potential of the browning from white adipocyte in pig which is the mammal lacked UCP1 and revealed the mechanism of browning mediated through upregulation of UCP3.

In chapter 1, the adrenergic stimulation using isoproterenol investigated change of the gene expression related to thermogenesis and mitochondrial function in pig DFAT. Furthermore, administration of isoproterenol induced fragmentation of the lipid droplets to small particle, and these results discovered the browning potential from white adipocyte in pig without UCP1. In chapter 2-4 explained the fat development and seasonal changes of metabolic function between muscle and fat tissue in Mangalica. In particular, chapter 4 discovered that specific changes of gene expression in Mangalica were indicated non-shivering thermogenesis function including UCP family between muscle and fat tissue compered to LWD. Therefore, this research provides insights that contribute to the understanding of important physiological functions following seasonal change, serving as valuable knowledge for transformation leading to the browning of adipose tissue.

I demonstrated that exposure of ambient environment influenced the thermogenic function of muscle and fat tissue in pig which lack the functional UCP and BAT, and depend on pig breed significantly influenced thermogenic function of muscle and fat tissue between Mangalica and LWD. Furthermore, the upregulated genes of Mangalica fat in winter were accorded to gene expression in browning transformation of DFAT in chapter 1 and these results suggested that Mangalica fat has browning ability exposure cold stimulation, for example winter season. Because pigs lack the UCP1 gene and the physiological similarities were known between humans and pigs, Mangalica may be an optimal animal model for studying the mechanism of browning in humans.

This study is the first report to demonstrate that pig adipocyte can be induced the browning using adrenergic stimulation, and highlighting the potential for browning in the fat tissue of Mangalica. These findings offer valuable insights into the mechanism of browning in white adipocytes and have the potential to contribute to obesity therapy in humans.

ACKNOWLEDGMENTS

I would like to sincerely thank Dr. Yuki Muranishi, my doctoral supervisor and the principal investigator of our Laboratory of Animal Physiological Function at Obihiro University of Agriculture and Veterinary Medicine, Obihiro, Japan. She has provided constructive guidance for all my experiments, critically reviewed manuscripts, and guided me in my doctoral philosophy. I am also grateful to Prof. Masafumi Tetsuka, who imparts scientific advice and the philosophy of a researcher's life for the future. Dr. Hiroyuki Watanabe has generously provided experimental equipment and taken the time to discuss my doctoral experiments with me. A special thanks to Prof. Takehiro Nishida, who offered kind encouragement throughout my doctoral journey, from the entrance examination to job hunting. I also want to express my gratitude to everyone at the Tokachi Royal Mangalica Farm. They generously supported the measurement of body weight and dorsal fat tissue thickness of Mangalica and provided Mangalica pig samples. Their assistance was crucial to the success of my doctoral work, and without their support, I would not have been able to conduct the research for my doctoral thesis. I am truly thankful for their support and acknowledge the invaluable contributions they made to my doctoral studies.

I would like to express my gratitude to Dr. Motoki Sasaki, a professor, and Dr. Daisuke Kondoh, an associate professor at Obihiro University of Agriculture and Veterinary Medicine, Obihiro, Japan. They provided guidance and assistance with histological experiments and analyses, such as H&E and ATPase staining of muscle, as well as the use of transmission electron microscopy and techniques of TEM. I am also thankful to Dr. Kayano Mitsunori, who provided excellent advice on statistical analysis for my studies. Additionally, I appreciate the guidance of Dr. Yoshikage Muroi in writing application documents for research grants and his lectures on neuroscience experiments. Special thanks

to Dr. Nana Mikami, who advised on the measurement of fatty acid components in fat tissue in Mangalica. I am also grateful to Dr. Tomas Acosta, who shared valuable insights from the perspective of veterinary science and offered a global perspective through his life experiences. These experiences have broadened my mind and will be useful for my philosophy as a researcher.

Furthermore, I would like to express my gratitude to Dr. Takashi Yazawa at Asahikawa Medical University, Asahikawa, Japan. He assisted in the analysis of promoter activity in UCP3 through luciferase assays for my study and provided instruction on genetic engineering techniques, including gene transfer. Additionally, I extend my thanks to Dr. Sho Nishikawa at Teikyo University of Science, Tokyo, Japan. He provided valuable guidance on my study of adipose browning and conducted analyses on the expression of UCP proteins in the fat tissue of Mangalica.

I express my sincere gratitude to the members of my laboratory, including Miss Akari Koide, Mr. Keigo Yamane, Miss Erina Yoneda, Mr. Tatsuki Okazaki, Miss Chisato Nakayama, Miss Kisaki Tomita, Miss Misuzu Hashimoto, Miss Kaho Eguchi, Miss Miho Sekiguchi, and Miss Kana Shimada. Their invaluable assistance in conducting experiments contributed significantly to the success of my research. I am also thankful to all other students in the Laboratory of Animal Physiological Function for their collaborative support throughout my study.

Finally, I extend my deepest appreciation to my family in Osaka for their unwavering warmth and support.

REFERENCES

1. ALBUQUERQUE A., ÓVILO C., NÚÑEZ Y., BENÍTEZ R., LÓPEZ-GARCIA A., GARCÍA F., FÉLIX M.D.R., LARANJO M., CHARNECA R. & MARTINS J.M. 2020. — Comparative transcriptomic analysis of subcutaneous adipose tissue from local pig breeds. *Genes* 11 (4). https://doi.org/10.3390/genes11040422

2. ALI A.T., HOCHFELD W.E., MYBURGH R. & PEPPER M.S. 2013. — Adipocyte and adipogenesis. *European Journal of Cell Biology* 92 (6–7): 229–236. https://doi.org/10.1016/j.ejcb.2013.06.001

3. ANDRÉ R. SIMON, ANTHONY N. WARRENS & MEGAN S. 1999. — Efficacy of adhesive interactions in pig-to-human xenotransplantation. *Immunol Today.* 20 (7): 323–329

4. BAL N.C., MAURYA S.K., SINGH S., WEHRENS X.H.T. & PERIASAMY M. 2016. — Increased Reliance on Muscle-based Thermogenesis upon Acute Minimization of Brown Adipose Tissue Function. *Journal of Biological Chemistry* 291 (33): 17247–17257. https://doi.org/10.1074/jbc.M116.728188

5. BAL N.C., SAHOO S.K., MAURYA S.K. & PERIASAMY M. 2018. — The Role of Sarcolipin in Muscle Non-shivering Thermogenesis. *Frontiers in Physiology* 9. https://doi.org/10.3389/fphys.2018.01217

6. BAL N.C., SINGH S., REIS F.C.G., MAURYA S.K., PANI S., ROWLAND L.A. & PERIASAMY M. 2017. — Both brown adipose tissue and skeletal muscle thermogenesis processes are activated during mild to severe cold adaptation in mice. *Journal of Biological Chemistry* 292 (40): 16616–16625. https://doi.org/10.1074/jbc.M117.790451

7. BÂLTEANU V.A., CARDOSO T.F., AMILLS M., EGERSZEGI I., ANTON I., BEJA-PEREIRA A. & ZSOLNAI A. 2019. — The footprint of recent and strong demographic decline in the genomes of Mangalitza pigs. *Animal* 13 (11): 2440–2446. https://doi.org/10.1017/S1751731119000582

8. Bargut T.C.L., Souza-Mello V., Aguila M.B. & Mandarim-De-Lacerda C.A. 2017. — Browning of white adipose tissue: Lessons from experimental models. *Hormone Molecular Biology and Clinical Investigation* 31 (1). https://doi.org/10.1515/hmbci-2016-0051

9. Benítez R., Fernández A., Isabel B., Núñez Y., De Mercado E., Gómez-Izquierdo E., García-Casco J., López-Bote C. & Óvilo C. 2018. — Modulatory effects of breed, feeding status, and diet on adipogenic, lipogenic, and lipolytic gene expression in growing iberian and duroc pigs. *International Journal of Molecular Sciences* 19 (1). https://doi.org/10.3390/ijms19010022

10. Benítez R., Trakooljul N., Núñez Y., Isabel B., Murani E., De Mercado E., Gómez-Izquierdo E., García-Casco J., López-Bote C., Wimmers K. & Óvilo C. 2019. — Breed, diet, and interaction effects on adipose tissue transcriptome in iberian and duroc pigs fed different energy sources. *Genes* 10 (8). https://doi.org/10.3390/genes10080589

11. Berg F., Gustafson U. & Andersson L. 2006. — The uncoupling protein 1 gene (UCP1) is disrupted in the pig lineage: A genetic explanation for poor thermoregulation in piglets. *PLoS Genetics* 2 (8): 1178–1181. https://doi.org/10.1371/journal.pgen.0020129

12. Blaauw B., Schiaffino S. & Reggiani C. 2013. — Mechanisms modulating skeletal muscle phenotype. *Comprehensive Physiology* 3 (4): 1645–1687. https://doi.org/10.1002/cphy.c130009

13. Boström P., Wu J., Jedrychowski M.P., Korde A., Ye L., Lo J.C., Rasbach K.A., Boström E.A., Choi J.H., Long J.Z., Kajimura S., Zingaretti M.C., Vind B.F., Tu H., Cinti S., Højlund K., Gygi S.P. & Spiegelman B.M. 2012. — A PGC1-α-dependent myokine that drives brown-fat-like development of white fat and thermogenesis. *Nature* 481 (7382): 463–468. https://doi.org/10.1038/nature10777

14. Bouillaud F., Alves-Guerra M.C. & Ricquier D. 2016. — UCPs, at the interface between bioenergetics and metabolism. *Biochimica et Biophysica Acta - Molecular Cell Research* 1863 (10): 2443–2456. https://doi.org/10.1016/j.bbamcr.2016.04.013

15. Carroll J.A., Burdick N.C., Chase C.C., Coleman S.W. & Spiers D.E. 2012. — Influence of environmental temperature on the physiological, endocrine, and immune responses in livestock exposed to a provocative immune challenge. *Domestic Animal Endocrinology* 43 (2): 146–153. https://doi.org/10.1016/j.domaniend.2011.12.008

16. Chen C.C., Kuo C.H., Leu Y.L. & Wang S.H. 2021. — Corylin reduces obesity and insulin resistance and promotes adipose tissue browning through SIRT-1 and β3-AR activation. *Pharmacological Research* 164. https://doi.org/10.1016/j.phrs.2020.105291

17. Choi J., Kwon K., Lee Y., Ko E., Kim Y. & Choi Y. 2019. — Characteristics of pig carcass and primal cuts measured by the autofom III depend on seasonal classification. *Food Science of Animal Resources* 39 (2): 332–344. https://doi.org/10.5851/kosfa.2019.e30

18. Choi M., Mukherjee S. & Yun J.W. 2021. — Trigonelline induces browning in 3T3-L1 white adipocytes. *Phytotherapy Research* 35 (2): 1113–1124. https://doi.org/10.1002/ptr.6892

19. Chouchani E.T., Kazak L., Jedrychowski M.P., Lu G.Z., Erickson B.K., Szpyt J., Pierce K.A., Laznik-Bogoslavski D., Vetrivelan R., Clish C.B., Robinson A.J., Gygi S.P. & Spiegelman B.M. 2016. — Mitochondrial ROS regulate thermogenic energy expenditure and sulfenylation of UCP1. *Nature* 532 (7597): 112–116. https://doi.org/10.1038/nature17399

20. Ciciliot S., Rossi A.C., Dyar K.A., Blaauw B. & Schiaffino S. 2013. — Muscle type and fiber type specificity in muscle wasting. *International Journal of Biochemistry and Cell Biology* 45 (10): 2191–2199. https://doi.org/10.1016/j.biocel.2013.05.016

21. CLAUS R. & WEILER U. 1994. — Endocrine regulation of growth and metabolism in the pig: a review*

22. COOPER D.K.C., GASTON R., ECKHOFF D., LADOWSKI J., YAMAMOTO T., WANG L., IWASE H., HARA H., TECTOR M. & TECTOR A.J. 2018. — Xenotransplantation - The current status and prospects. *British Medical Bulletin* 125 (1): 5–14. https://doi.org/10.1093/bmb/ldx043

23. CORTES DE OLIVEIRA C., NICOLETTI C.F., PINHEL M.A. DE S., DE OLIVEIRA B.A.P., QUINHONEIRO D.C.G., NORONHA N.Y., FASSINI P.G., MARCHINI J.S., DA SILVA JÚNIOR W.A., SALGADO JÚNIOR W. & NONINO C.B. 2018. — Influence of expression of UCP3, PLIN1 and PPARG2 on the oxidation of substrates after hypocaloric dietary intervention. *Clinical Nutrition* 37 (4): 1383–1388. https://doi.org/10.1016/j.clnu.2017.06.012

24. COTTON C.J. 2016. — Skeletal muscle mass and composition during mammalian hibernation. *Journal of Experimental Biology* 219 (2): 226–234. https://doi.org/10.1242/jeb.125401

25. CRISTANCHO A.G. & LAZAR M.A. 2011. — Forming functional fat: A growing understanding of adipocyte differentiation. *Nature Reviews Molecular Cell Biology* 12 (11): 722–734. https://doi.org/10.1038/nrm3198

26. CYPESS A.M., WEINER L.S., ROBERTS-TOLER C., ELÍA E.F., KESSLER S.H., KAHN P.A., ENGLISH J., CHATMAN K., TRAUGER S.A., DORIA A. & KOLODNY G.M. 2015. — Activation of human brown adipose tissue by a β3-adrenergic receptor agonist. *Cell Metabolism* 21 (1): 33–38. https://doi.org/10.1016/j.cmet.2014.12.009

27. DRIDI S., ONAGBESAN O., SWENNEN Q., BUYSE J., DECUYPERE E. & TAOUIS M. 2004. — Gene expression, tissue distribution and potential physiological role of uncoupling protein in avian species. *Comparative Biochemistry and Physiology - A Molecular and Integrative Physiology* 139 (3): 273–283. https://doi.org/10.1016/j.cbpb.2004.09.010

28. DUCHARME N.A. & BICKEL P.E. 2008. — Minireview: Lipid droplets in lipogenesis and lipolysis. *Endocrinology* 149 (3): 942–949. https://doi.org/10.1210/en.2007-1713

29. DUCLOS M.J., BERRI C. & LE BIHAN-DUVAL E. 2007. — Muscle Growth and Meat Quality. *J. Appl. Poult. Res.* 16 (107–112)

30. DUFAU J. EMY, SHEN J.X., COUCHET M., DE CASTRO BARBOSA T., MEJHERT N., MASSIER L., GRISETI E., MOUISEL E., AMRI E.Z., LAUSCHKE V.M., RYDEN M. & LANGIN D. 2021. — In vitro and ex vivo models of adipocytes. *American Journal of Physiology - Cell Physiology* 320 (5): C822–C841. https://doi.org/10.1152/ajpcell.00519.2020

31. EGERSZEGI I., RÁTKY J., SOLIT L. & BRÜSSOW K. 2003. — Mangalica - an indigenous swine breed from Hungary. *Archives fur Tierzucht* 46 (3): 245–256

32. EGGINTON S., FAIRNEY F. & BRATCHER J. 2001. — Differential Effects of Cold Exposure on Muscle Fibre Composition and Capillary Supply in Hibernator and Non-Hibernator Rodents. *Experimental Physiology* 86 (5): 629–639

33. EMRE Y., HURTAUD C., RICQUIER D., BOUILLAUD F., HUGHES J. & CRISCUOLO F. 2007. — Avian UCP: The killjoy in the evolution of the mitochondrial uncoupling proteins. *Journal of Molecular Evolution* 65 (4): 392–402. https://doi.org/10.1007/s00239-007-9020-1

34. ERLANSON-ALBERTSSON C. 2003. — The role of uncoupling proteins in the regulation of metabolism. *Acta Physiologica Scandinavica* 178 (4): 405–412

35. FALKENSTEIN F., KÖRTNER G., WATSON K. & GEISER F. 2001. — Dietary fats and body lipid composition in relation to hibernation in free-ranging echidnas. *Journal of Comparative Physiology - B Biochemical, Systemic, and Environmental Physiology* 171 (3): 189–194. https://doi.org/10.1007/s003600000157

36. FLORANT G.L. 1998. — Lipid Metabolism in Hibernators: The Importance of Essential Fatty Acids 1. *American Zoologist* 38 (2): 331–340

37. FRANK K., MOLNÁR J., BARTA E. & MARINCS F. 2017. — The full mitochondrial genomes of Mangalica pig breeds and their possible origin. *Mitochondrial DNA Part B: Resources* 2 (2): 730–734. https://doi.org/10.1080/23802359.2017.1390415

38. FRONTERA W.R. & OCHALA J. 2015. — Skeletal Muscle: A Brief Review of Structure and Function. *Behavior Genetics* 45 (2): 183–195. https://doi.org/10.1007/s00223-014-9915-y

39. FULLER-JACKSON J.P. & HENRY B.A. 2018. — Adipose and skeletal muscle thermogenesis: Studies from large animals. *Journal of Endocrinology* 237 (3): R99–R115. https://doi.org/10.1530/JOE-18-0090

40. GAO Y.F., WANG J., WANG H.P., FENG B., DANG K., WANG Q. & HINGHOFER-SZALKAY H.G. 2012. — Skeletal muscle is protected from disuse in hibernating dauria ground squirrels. *Comparative Biochemistry and Physiology - A Molecular and Integrative Physiology* 161 (3): 296–300. https://doi.org/10.1016/j.cbpa.2011.11.009

41. GARCÍA-MARTÍNEZ C., SIBILLE B., SOLANES G., DARIMONT C., MACÉ K., VILLARROYA F. & GÓMEZ-FOIX A.M. 2001. — Overexpression of UCP3 in cultured human muscle lowers mitochondrial membrane potential, raises ATP/ADP ratio, and favors fatty acid versus glucose oxidation. *The FASEB Journal* 15 (11): 2033–2035. https://doi.org/10.1096/fj.00-0828fje

42. GAUDRY M.J., JASTROCH M., TREBERG J.R., HOFREITER M., PAIJMANS J.L.A., STARRETT J., WALES N., ANTHONY ‡, SIGNORE V., SPRINGER M.S. & CAMPBELL K.L. 2017. — Inactivation of thermogenic UCP1 as a historical contingency in multiple placental mammal clades. *Sci. Adv.* 3 (7)

43. GONG D.W., MONEMDJOU S., GAVRILOVA O., LEON L.R., MARCUS-SAMUELS B., CHOU C.J., EVERETT C., KOZAK L.P., LI C., DENG C., HARPER M.E. & REITMAN M.L. 2000. — Lack of obesity and normal response to fasting and thyroid hormone in mice lacking uncoupling

protein-3. *Journal of Biological Chemistry* 275 (21): 16251–16257. https://doi.org/10.1074/jbc.M910177199

44. GOOSSENS G.H. 2017. — The Metabolic Phenotype in Obesity: Fat Mass, Body Fat Distribution, and Adipose Tissue Function. *Obesity Facts* 10 (3): 207–215. https://doi.org/10.1159/000471488

45. GOTO T., LEE J.Y., TERAMINAMI A., KIM Y. IL, HIRAI S., UEMURA T., INOUE H., TAKAHASHI N. & KAWADA T. 2011. — Activation of peroxisome proliferator-activated receptor-alpha stimulates both differentiation and fatty acid oxidation in adipocytes. *Journal of Lipid Research* 52 (5): 873–884. https://doi.org/10.1194/jlr.M011320

46. GUO Z., LV L., LIU D. & FU B. 2018. — Effects of heat stress on piglet production/performance parameters. *Tropical Animal Health and Production* 50 (6): 1203–1208. https://doi.org/10.1007/s11250-018-1633-4

47. HASS D.T. & BARNSTABLE C.J. 2021. — Uncoupling proteins in the mitochondrial defense against oxidative stress. *Progress in Retinal and Eye Research* 83. https://doi.org/10.1016/j.preteyeres.2021.100941

48. HEATON J.M. 1972. — The distribution of brown adipose tissue in the human 35–39 p.

49. HELDMAIER G. 1988. — Seasonal Acciimatization of Energy Requirements in Mammals: Functional Significance of Body Weight Control, Hypothermia, Torpor and Hibernation. *10th European Society for Comparative Physiology and Biochemistry*: 130–139

50. HERPIN P., DAMON M. & LE DIVIDICH´UNITE J. 2002. — Development of thermoregulation and neonatal survival in pigs 25–45 p.

51. HOU L., SHI J., CAO L., XU G., HU C. & WANG C. 2017. — Pig has no uncoupling protein 1. *Biochemical and Biophysical Research Communications* 487 (4): 795–800. https://doi.org/10.1016/j.bbrc.2017.04.118

52. HU J. & CHRISTIAN M. 2017. — Hormonal factors in the control of the browning of white adipose tissue. *Hormone Molecular Biology and Clinical Investigation* 31 (1). https://doi.org/10.1515/hmbci-2017-0017

53. IBRAHIM Z., BUSCH J., AWWAD M., WAGNER R., WELLS K. & COOPER D.K.C. 2006. — Selected physiologic compatibilities and incompatibilities between human and porcine organ systems. *Xenotransplantation* 13 (6): 488–499. https://doi.org/10.1111/j.1399-3089.2006.00346.x

54. IRIE M. & NISHIMURA K. 1987. — B モード゛リニア電子スキャナーによる豚生体の背脂肪厚の測定. 日畜会報 58 (1): 44–52

55. JOUBERT R., COUSTARD S.M., SWENNEN Q., SIBUT V., CROCHET S., CAILLEAU-AUDOUIN E., BUYSE J., DECUYPERE E., WRUTNIAK-CABELLO C., CABELLO G., TESSERAUD S. & COLLIN A. 2010. — The beta-adrenergic system is involved in the regulation of the expression of avian uncoupling protein in the chicken. *Domestic Animal Endocrinology* 38 (2): 115–125. https://doi.org/10.1016/j.domaniend.2009.08.002

56. JUNG S.M., SANCHEZ-GURMACHES J. & GUERTIN D.A. 2019. — Brown adipose tissue development and metabolism. *Handbook of Experimental Pharmacology* 251: 3–36. https://doi.org/10.1007/164_2018_168

57. KAISANLAHTI A. & GLUMOFF T. 2019. — Browning of white fat: agents and implications for beige adipose tissue to type 2 diabetes. *Journal of Physiology and Biochemistry* 75 (1). https://doi.org/10.1007/s13105-018-0658-5

58. KALTENBRUNNER M., MAYER W., KERKHOFF K., EPP R., RÜGGEBERG H., HOCHEGGER R. & CICHNA-MARKL M. 2019. — Differentiation between wild boar and domestic pig in food by targeting two gene loci by real-time PCR. *Scientific Reports* 9 (1). https://doi.org/10.1038/s41598-019-45564-7

59. KAWATA M., LUZIGA C., MIYATA H., SUGIURA T. & WADA N. 2022. — Differential expression of myosin heavy chain isoforms type II in skeletal muscles of polar and black bears. *Journal of Veterinary Medicine Series C: Anatomia Histologia Embryologia*. https://doi.org/10.1111/ahe.12893

60. KIM D.H., KIM H.J. & SEONG J.K. 2022. — UCP2 KO mice exhibit ameliorated obesity and inflammation induced by high-fat diet feeding. *BMB Reports* 55 (10): 500–505. https://doi.org/10.5483/BMBRep.2022.55.10.056

61. KIM I.H. & NAM T.J. 2017. — Enzyme-Treated Ecklonia cava extract inhibits adipogenesis through the downregulation of C/EBPα in 3T3-L1 adipocytes. *International Journal of Molecular Medicine* 39 (3): 636–644. https://doi.org/10.3892/ijmm.2017.2869

62. KIM S., NAKAYAMA C., KONDOH D., OKAZAKI T., YONEDA E., TOMITA K., SASAKI M. & MURANISHI Y. 2023. — Seasonal adaptation of Mangalica pigs in terms of muscle morphology and metabolism. *Anatomia Histologia Embryologia*: 1–8. https://doi.org/10.1111/ahe.12982

63. KIM S., TANIGUCHI K., SASAKI M., YAMANE K., TAKATANI R., KOIDE A., YONEDA E., HAGIYA K., SASAKI M. & MURANISHI Y. 2022. — Study on fat development and the unique feature of genes related to lipogenesis with the growth of Mangalica. 北海道畜産草地学会 10: 39–46

64. KIM S., YONEDA E., TOMITA K., KAYANO M., WATANABE H., SASAKI M., SHIMIZU T. & MURANISHI Y. 2023. — LPS Administration during Fertilization Affects Epigenetic Inheritance during Embryonic Development. *Animals* 13 (7). https://doi.org/10.3390/ani13071135

65. KOJIMA M., NAKAJIMA I., ARAKAWA A., MIKAWA S., MATSUMOTO T., UENISHI H., NAKAMURA Y. & TANIGUCHI M. 2018. — Differences in gene expression profiles for subcutaneous adipose, liver, and skeletal muscle tissues between Meishan and Landrace

pigs with different backfat thicknesses. *PLoS ONE* 13 (9). https://doi.org/10.1371/journal.pone.0204135

66. LAMPIDONIS A.D., ROGDAKIS E., VOUTSINAS G.E. & STRAVOPODIS D.J. 2011. — The resurgence of Hormone-Sensitive Lipase (HSL) in mammalian lipolysis. *Gene* 477 (1–2): 1–11. https://doi.org/10.1016/j.gene.2011.01.007

67. LAURSEN W.J., MASTROTTO M., PESTA D., FUNK O.H., GOODMAN J.B., MERRIMAN D.K., INGOLIA N., SHULMAN G.I., BAGRIANTSEV S.N. & GRACHEVA E.O. 2015. — Neuronal UCP1 expression suggests a mechanism for local thermogenesis during hibernation. *Proceedings of the National Academy of Sciences of the United States of America* 112 (5): 1607–1612. https://doi.org/10.1073/pnas.1421419112

68. LEFAUCHEUR L., ECOLAN P., PLANTARD L. & GUEGUEN N. 2002. — New Insights into Muscle Fiber Types in the Pig. *The Journal of Histochemistry & Cytochemistry* 50 (5): 719–730

69. LI J., ZHAO T., GUAN D., PAN Z., BAI Z., TENG J., ZHANG Z., ZHENG Z., ZENG J., ZHOU H., FANG L. & CHENG H. 2023. — Learning functional conservation between human and pig to decipher evolutionary mechanisms underlying gene expression and complex traits. *Cell Genomics*: 100390. https://doi.org/10.1016/j.xgen.2023.100390

70. LI M., CHEN L., TIAN S., LIN Y., TANG Q., ZHOU X., LI D., YEUNG C.K.L., CHE T., JIN L., FU Y., MA J., WANG X., JIANG A., LAN J., PAN Q., LIU Y., LUO Z., GUO Z., LIU H., ZHU L., SHUAI S., TANG G., ZHAO J., JIANG Y., BAI L., ZHANG S., MAI M., LI C., WANG D., GU Y., WANG G., LU H., LI Y., ZHU H., LI Z., LII M., GLADYSHEV V.N., JIANG Z., ZHAO S., WANG J., LI R. & LI X. 2017. — Comprehensive variation discovery and recovery of missing sequence in the pig genome using multiple de novo assemblies. *Genome Research* 27 (5): 865–874. https://doi.org/10.1101/gr.207456.116

71. LI X.S. & WANG D.H. 2005. — Regulation of body weight and thermogenesis in seasonally acclimatized Brandt's voles (Microtus brandti). *Hormones and Behavior* 48 (3): 321–328. https://doi.org/10.1016/j.yhbeh.2005.04.004

72. LIANG F., YAN L., LI Y., JIN Y., ZHANG J., CHE H., DIAO J., GAO Y., HE Z., SUN R., HE Y. & ZHOU C. 2022. — Effect of season on slaughter performance, meat quality, muscle amino acid and fatty acid composition, and metabolism of pheasants (Phasianus colchicus). *Animal Science Journal* 93 (1). https://doi.org/10.1111/asj.13735

73. LIN J., CAO C., TAO C., YE R., DONG M., ZHENG Q., WANG C., JIANG X., QIN G., YAN C., LI K., SPEAKMAN J.R., WANG Y., JIN W. & ZHAO J. 2017. — Cold adaptation in pigs depends on UCP3 in beige adipocytes. *Journal of Molecular Cell Biology* 9 (5): 364–375. https://doi.org/10.1093/jmcb/mjx018

74. LIU F., ZHAO W., LE H.H., COTTRELL J.J., GREEN M.P., LEURY B.J., DUNSHEA F.R. & BELL A.W. 2022. — Review: What have we learned about the effects of heat stress on the pig industry? *Animal* 16. https://doi.org/10.1016/j.animal.2021.100349

75. LONGO M., ZATTERALE F., NADERI J., PARRILLO L., FORMISANO P., RACITI G.A., BEGUINOT F. & MIELE C. 2019. — Adipose tissue dysfunction as determinant of obesity-associated metabolic complications. *International Journal of Molecular Sciences* 20 (9). https://doi.org/10.3390/ijms20092358

76. LONGO M., ZATTERALE F., NADERI J., PARRILLO L., FORMISANO P., RACITI G.A., BEGUINOT F. & MIELE C. 2019. — Adipose tissue dysfunction as determinant of obesity-associated metabolic complications. *International Journal of Molecular Sciences* 20 (9). https://doi.org/10.3390/ijms20092358

77. LSHIBASHI J. & SEALE P. 2010. — Beige can be slimming. *Science* 328 (5982): 1113–1114. https://doi.org/10.1126/science.1190816

78. LUNNEY J.K., VAN GOOR A., WALKER K.E., HAILSTOCK T., FRANKLIN J. & DAI C. 2021. — Importance of the pig as a human biomedical model. *Sci. Transl. Med* 13 (621)

79. MARKUSSEN L.K., ISIDOR M.S., BREINING P., ANDERSEN E.S., RASMUSSEN N.E., PETERSEN L.I., PEDERSEN S.B., RICHELSEN B. & HANSEN J.B. 2017. — Characterization of immortalized human brown and white pre-adipocyte cell models from a single donor. *PLoS ONE* 12 (9). https://doi.org/10.1371/journal.pone.0185624

80. MATTSSON C.L., CSIKASZ R.I., CHERNOGUBOVA E., YAMAMOTO D.L., HOGBERG H.T., AMRI E.-Z., HUTCHINSON D.S. & BENGTSSON T. 2011. — β1-Adrenergic receptors increase UCP1 in human MADS brown adipocytes and rescue cold-acclimated β3-adrenergic receptor-knockout mice via nonshivering thermogenesis. *Am J Physiol Endocrinol Metab* 301 (6): 1108–1118. https://doi.org/10.1152/ajpendo.00085.2011.-With

81. MEURENS F., SUMMERFIELD A., NAUWYNCK H., SAIF L. & GERDTS V. 2012. — The pig: A model for human infectious diseases. *Trends in Microbiology* 20 (1): 50–57. https://doi.org/10.1016/j.tim.2011.11.002

82. MILLER C.N., YANG J.Y., ENGLAND E., YIN A., BAILE C.A. & RAYALAM S. 2015. — Isoproterenol increases uncoupling, glycolysis, and markers of beiging in mature 3T3-L1 adipocytes. *PLoS ONE* 10 (9). https://doi.org/10.1371/journal.pone.0138344

83. MORRISON S.F., NAKAMURA K. & MADDEN C.J. 2008. — Central control of thermogenesis in mammals. *Experimental Physiology* 93 (7): 773–797. https://doi.org/10.1113/expphysiol.2007.041848

84. MOTTILLO E.P., BALASUBRAMANIAN P., LEE Y.H., WENG C., KERSHAW E.E. & GRANNEMAN J.G. 2014. — Coupling of lipolysis and de novo lipogenesis in brown, beige, and white adipose tissues during chronic β3-adrenergic receptor activation. *Journal of Lipid Research* 55 (11): 2276–2286. https://doi.org/10.1194/jlr.M050005

85. MUKHERJEE S. & YUN J.W. 2022. — Prednisone stimulates white adipocyte browning via β3-AR/p38 MAPK/ERK signaling pathway. *Life Sciences* 288. https://doi.org/10.1016/j.lfs.2021.120204

86. NABBEN M., VAN BREE B.W.J., LENAERS E., HOEKS J., HESSELINK M.K.C., SCHAART G., GIJBELS M.J.J., GLATZ J.F.C., DA SILVA G.J.J., DE WINDT L.J., TIAN R., MIKE E., SKAPURA D.G., WEHRENS X.H.T. & SCHRAUWEN P. 2014. — Lack of UCP3 does not affect skeletal muscle mitochondrial function under lipid-challenged conditions, but leads to sudden cardiac death. *Basic Research in Cardiology* 109 (6). https://doi.org/10.1007/s00395-014-0447-4

87. NAKAJIMA I., KOJIMA M., OE M., OJIMA K., MUROYA S. & CHIKUNI K. 2019. — Comparing pig breeds with genetically low and high backfat thickness: differences in expression of adiponectin, its receptor, and blood metabolites. *Domestic Animal Endocrinology* 68: 54–63. https://doi.org/10.1016/j.domaniend.2019.01.002

88. NAKAJIMA I., OE M., OJIMA K., MUROYA S., SHIBATA M. & CHIKUNI K. 2011. — Cellularity of developing subcutaneous adipose tissue in Landrace and Meishan pigs: Adipocyte size differences between two breeds. *Animal Science Journal* 82 (1): 144–149. https://doi.org/10.1111/j.1740-0929.2010.00810.x

89. NG S.P., NOMURA W., TAKAHASHI H., INOUE K., KAWADA T. & GOTO T. 2021. — Methylglyoxal attenuates isoproterenol-induced increase in uncoupling protein 1 expression through activation of JNK signaling pathway in beige adipocytes. *Biochemistry and Biophysics Reports* 28. https://doi.org/10.1016/j.bbrep.2021.101127

90. NOWACK J., GIROUD S., ARNOLD W. & RUF T. 2017. — Muscle non-shivering thermogenesis and its role in the evolution of endothermy. *Frontiers in Physiology* 8 (NOV). https://doi.org/10.3389/fphys.2017.00889

91. Nowack J., Vetter S.G., Stalder G., Painer J., Kral M., Smith S., Le M.H., Jurcevic P., Bieber C., Arnold W. & Ruf T. 2019. — Muscle nonshivering thermogenesis in a feral mammal. *Scientific Reports* 9 (1). https://doi.org/10.1038/s41598-019-42756-z

92. Ohno H., Shinoda K., Spiegelman B.M. & Kajimura S. 2012. — PPARγ agonists induce a white-to-brown fat conversion through stabilization of PRDM16 protein. *Cell Metabolism* 15 (3): 395–404. https://doi.org/10.1016/j.cmet.2012.01.019

93. Ooishi H., Saka N. & Miyabe takumi 2006. — 豚の飼養環境が゛生産性に及ぼ゛す影響（ストレス軽減環境の検討）. 茨城県畜産センター研究報告: 67–72

94. Pan Z., Yao Y., Yin H., Cai Z., Wang Y., Bai L., Kern C., Halstead M., Chanthavixay G., Trakooljul N., Wimmers K., Sahana G., Su G., Lund M.S., Fredholm M., Karlskov-Mortensen P., Ernst C.W., Ross P., Tuggle C.K., Fang L. & Zhou H. 2021. — Pig genome functional annotation enhances the biological interpretation of complex traits and human disease. *Nature Communications* 12 (1). https://doi.org/10.1038/s41467-021-26153-7

95. Parunovic N., Petrovic M., Djordjevic V., Petronijevic R., Lakicevic B., Petrovic Z. & Savic R. 2015. — Cholesterol Content and Fatty Acids Composition of Mangalitsa Pork Meat. *Procedia Food Science* 5: 215–218. https://doi.org/10.1016/j.profoo.2015.09.021

96. Pârvu M., Bogdan A.T., Andronie I.C., Simion V.E. & Amfim A. 2012. — The Bioproductive Effect of Thermic Stress at Mangalica Pigs 45 p.

97. Pârvu M., Bogdan A.T., Andronie I.C., Simion V.E. & Amfim A. 2012. — Influence of Cold Stress on the Chemical Composition of Carcass to Mangalica pigs. *Scientific Papers: Animal Science and Biotechnologies* 45 (2): 394–396

98. Patsouris D., Qi P., Abdullahi A., Stanojcic M., Chen P., Parousis A., Amini-Nik S. & Jeschke M.G. 2015. — Burn Induces Browning of the Subcutaneous White Adipose

Tissue in Mice and Humans. *Cell Reports* 13 (8): 1538–1544. https://doi.org/10.1016/j.celrep.2015.10.028

99. PERIASAMY M., HERRERA J.L. & REIS F.C.G. 2017. — Skeletal muscle thermogenesis and its role in whole body energy metabolism. *Diabetes and Metabolism Journal* 41 (5): 327–336. https://doi.org/10.4093/dmj.2017.41.5.327

100. PETROVIC N., WALDEN T.B., SHABALINA I.G., TIMMONS J.A., CANNON B. & NEDERGAARD J. 2010. — Chronic peroxisome proliferator-activated receptor γ (PPARγ) activation of epididymally derived white adipocyte cultures reveals a population of thermogenically competent, UCP1-containing adipocytes molecularly distinct from classic brown adipocytes. *Journal of Biological Chemistry* 285 (10): 7153–7164. https://doi.org/10.1074/jbc.M109.053942

101. PIAO Z., ZHAI B., JIANG X., DONG M., YAN C., LIN J. & JIN W. 2018. — Reduced adiposity by compensatory WAT browning upon iBAT removal in mice. *Biochemical and Biophysical Research Communications* 501 (3): 807–813. https://doi.org/10.1016/j.bbrc.2018.05.089

102. PINTO Y.O., FESTUCCIA W.T.L. & MAGDALON J. 2022. — The involvement of the adrenergic nervous system in activating human brown adipose tissue and browning. *Hormones* 21 (2): 195–208. https://doi.org/10.1007/s42000-022-00361-2

103. POHL E.E., RUPPRECHT A., MACHER G. & HILSE K.E. 2019. — Important trends in UCP3 investigation. *Frontiers in Physiology* 10 (APR). https://doi.org/10.3389/fphys.2019.00470

104. POKLUKAR K., ČANDEK-POTOKAR M., LUKAČ N.B., TOMAŽIN U. & ŠKRLEP M. 2020. — Lipid deposition and metabolism in local and modern pig breeds: A review. *Animals* 10 (3). https://doi.org/10.3390/ani10030424

105. REYES-FARIAS M., FOS-DOMENECH J., SERRA D., HERRERO L. & SÁNCHEZ-INFANTES D. 2021. — White adipose tissue dysfunction in obesity and aging. *Biochemical Pharmacology* 192. https://doi.org/10.1016/j.bcp.2021.114723

106. Riis-Vestergaard M.J., Richelsen B., Bruun J.M., Li W., Hansen J.B. & Pedersen S.B. 2020. — Beta-1 and not Beta-3 adrenergic receptors may be the primary regulator of human brown adipocyte metabolism. *Journal of Clinical Endocrinology and Metabolism* 105 (4): E994–E1005. https://doi.org/10.1210/clinem/dgz298

107. Rourke B.C., Cotton C.J., Harlow H.J. & Caiozzo V.J. 2006. — Maintenance of slow type I myosin protein and mRNA expression in overwintering prairie dogs (Cynomys leucurus and ludovicianus) and black bears (Ursus americanus). *Journal of Comparative Physiology B: Biochemical, Systemic, and Environmental Physiology* 176 (7): 709–720. https://doi.org/10.1007/s00360-006-0093-8

108. Ryu V., Zarebidaki E., Albers H.E., Xue B. & Bartness T.J. 2018. — Short photoperiod reverses obesity in Siberian hamsters via sympathetically induced lipolysis and Browning in adipose tissue. *Physiology and Behavior* 190: 11–20. https://doi.org/10.1016/j.physbeh.2017.07.011

109. Sales J. & Kotrba R. 2013. — Meat from wild boar (Sus scrofa L.): A review. *Meat Science* 94 (2): 187–201. https://doi.org/10.1016/j.meatsci.2013.01.012

110. Schiaffino S. & Reggiani C. 2011. — Fiber Types In Mammalian Skeletal Muscles. *Physiol Rev* 91: 1447–1531. https://doi.org/10.1152/physrev.00031.2010.-Mammalian

111. Schiaffino S. 2018. — Muscle fiber type diversity revealed by anti-myosin heavy chain antibodies. *FEBS Journal* 285 (20): 3688–3694. https://doi.org/10.1111/febs.14502

112. Schott M.B., Weller S.G., Schulze R.J., Krueger E.W., Drizyte-Miller K., Casey C.A. & McNiven M.A. 2019. — Lipid droplet size directs lipolysis and lipophagy catabolism in hepatocytes. *Journal of Cell Biology* 218 (10): 3320–3335. https://doi.org/10.1083/JCB.201803153

113. Scimè A., Grenier G., Huh M.S., Gillespie M.A., Bevilacqua L., Harper M.E. & Rudnicki M.A. 2005. — Rb and p107 regulate preadipocyte differentiation into white

versus brown fat through repression of PGC-1α. *Cell Metabolism* 2 (5): 283–295. https://doi.org/10.1016/j.cmet.2005.10.002

114. SEALE P., CONROE H.M., ESTALL J., KAJIMURA S., FRONTINI A., ISHIBASHI J., COHEN P., CINTI S. & SPIEGELMAN B.M. 2011. — Prdm16 determines the thermogenic program of subcutaneous white adipose tissue in mice. *Journal of Clinical Investigation* 121 (1): 96–105. https://doi.org/10.1172/JCI44271

115. SEALE P., CONROE H.M., ESTALL J., KAJIMURA S., FRONTINI A., ISHIBASHI J., COHEN P., CINTI S. & SPIEGELMAN B.M. 2011. — Prdm16 determines the thermogenic program of subcutaneous white adipose tissue in mice. *Journal of Clinical Investigation* 121 (1): 96–105. https://doi.org/10.1172/JCI44271

116. SHEN J., SUGAWARA A., YAMASHITA J., OGURA H. & SATO S. 2011. — Dedifferentiated fat cells: An alternative source of adult multipotent cells from the adipose tissues. *International Journal of Oral Science* 3 (3): 117–124. https://doi.org/10.4248/IJOS11044

117. SHI S., HIRAKATA T., SUZUKI M., MIYOSHI S. & MITSUMOTO T. 1985. — 非線形成長曲線モデ゛ルを用いたホルスタイン雌牛の成長に関する研究. 畜大研報 14: 163–173

118. SKUBIS J., ŁABUDZKI L., GÓRECKI G. & WLAZEŁKO M. 2009. — Analysis of Selected Biometric Features and Population Attributes of Wild Boar in The Zielonka Game Investigation Centre. *Acta Sci. Pol. Silv. Colendar. Rat. Ind. Lignar* 8 (3): 45–54

119. SONG T. & KUANG S. 2019. — Adipocyte dedifferentiation in health and diseases. *Clinical Science* 133 (20): 2107–2119. https://doi.org/10.1042/CS20190128

120. SOTOME R., HIRASAWA A., KIKUSATO M., AMO T., FURUKAWA K., KURIYAGAWA A., WATANABE K., COLLIN A., SHIRAKAWA H., HIRAKAWA R., TANITAKA Y., TAKAHASHI H., WU G., NOCHI T., SHIMMURA T., WARDEN C.H. & TOYOMIZU M. 2021. — In vivo emergence of beige-like fat in chickens as physiological adaptation to cold environments. *Amino Acids* 53 (3): 381–393. https://doi.org/10.1007/s00726-021-02953-5

121. SPIEGELMAN B.M., SEALE P. & KAJIMURA S. 2009. — Transcriptional control of brown adipocyte development and physiological function-of mice and men. *Genes and Development* 23 (7): 788–797. https://doi.org/10.1101/gad.1779209

122. STANISZ M., SKORUPSKI M., ŚLÓSARZ P., BYKOWSKA-MACIEJEWSKA M., SKŁADANOWSKA-BARYZA J., STAŃCZAK Ł., KROKOWSKA-PALUSZAK M. & LUDWICZAK A. 2019. — The seasonal variation in the quality of venison from wild fallow deer (Dama dama) – A pilot study. *Meat Science* 150: 56–64. https://doi.org/10.1016/j.meatsci.2018.12.003

123. SUTTIE J.M. & WEBSTER J.R. 1995. — Are arctic ungulates physiologically unique? *The Second International Arctic Ungulate Conference* 18 (3–4): 99–118

124. SZABÓ A., BÁZÁR G., LOCSMÁNDI L. & ROMVÁRI R. 2010. — Quality alterations of four frying fats during long-term heating (conventional analysis and nirs calibration). *Journal of Food Quality* 33 (1): 42–58. https://doi.org/10.1111/j.1745-4557.2009.00285.x

125. SZABÓ A., HORN P., ROMVÁRI R., HÁZAS Z. & FÉBEL H. 2010. — Comparison of Mangalica and Hungarian Large White pigs at identical bodyweight: 2. Fatty acid regiodistribution analysis of the triacylglycerols. *Archiv Tierzucht* 53: 147–161

126. TABUCHI C. & SUL H.S. 2021. — Signaling Pathways Regulating Thermogenesis. *Frontiers in Endocrinology* 12. https://doi.org/10.3389/fendo.2021.595020

127. TAKATANI R., YAMANE K., KOSAKA K., KAYANO M., HAGIYA K., MIKAMI N., HAYASHIDA S., MIYASHITA T., KOIDE A., YAMAGUCHI Y. & MURANISHI Y. 2021. — Research on growth curve and suitable slaughter weight of the Mangalica pig. 北畜草会報 9: 25–35

128. TEMPFLI K., KISS B., SZALAI K., SIMON Z., PONGRÁCZ L. & BALI PAPP Á. 2016. — Differential expression of six genes in fat-type Hungarian Mangalica and other pigs. *Archives Animal Breeding* 59 (2): 259–265. https://doi.org/10.5194/aab-59-259-2016

129. TOMOVIĆ V.M., ŠEVIĆ R., JOKANOVIĆ M., ŠOJIĆ B., ŠKALJAC S., TASIĆ T., IKONIĆ P., POLAK M.L., POLAK T. & DEMŠAR L. 2016. — Quality traits of longissimus lumborum muscle from

White Mangalica, Duroc × White Mangalica and Large White pigs reared under intensive conditions and slaughtered at 150 kg live weight: A comparative study. *Archives Animal Breeding* 59 (3): 401–415. https://doi.org/10.5194/aab-59-401-2016

130. Vidal-Puig A.J., Grujic D., Zhang C.Y., Hagen T., Boss O., Ido Y., Szczepanik A., Wade J., Mootha V., Cortright R., Muoio D.M. & Lowell B.B. 2000. — Energy metabolism in uncoupling protein 3 gene knockout mice. *Journal of Biological Chemistry* 275 (21): 16258–16266. https://doi.org/10.1074/jbc.M910179199

131. Wang B., Chandrasekera P.C. & Pippin J.J. 2014. — Leptin-and Leptin Receptor-Deficient Rodent Models: Relevance for Human Type 2 Diabetes. *Current Diabetes Reviews* 10 (2): 131–145

132. Wang P.P., She M.H., He P.P., Chen W.J., Laudon M., Xu X.X. & Yin W.D. 2013. — Piromelatine decreases triglyceride accumulation in insulin resistant 3T3-L1 adipocytes: Role of ATGL and HSL. *Biochimie* 95 (8): 1650–1654. https://doi.org/10.1016/j.biochi.2013.05.005

133. Wang W., He W., Ruan Y. & Geng Q. 2022. — First pig-to-human heart transplantation. *Innovation* 3 (2). https://doi.org/10.1016/j.xinn.2022.100223

134. Watanabe D., Dutka T.L., Lamboley C.R. & Lamb G.D. 2019. — Skeletal muscle fibre swelling contributes to force depression in rats and humans: a mechanically-skinned fibre study. *Journal of Muscle Research and Cell Motility* 40 (3–4): 343–351. https://doi.org/10.1007/s10974-019-09521-1

135. Westwood F.R., Bigley A., Randall K., Marsden A.M. & Scott R.C. 2005. — Statin-Induced Muscle Necrosis in the Rat: DistributioN, Development, and Fibre Selectivity. *Toxicologic Pathology* 33 (2): 246–257. https://doi.org/10.1080/01926230590908213

136. WIKLUND E., DOBBIE P., STUART A. & LITTLEJOHN R.P. 2010. — Seasonal variation in red deer (Cervus elaphus) venison (M. longissimus dorsi) drip loss, calpain activity, colour and tenderness. *Meat Science* 86 (3): 720–727. https://doi.org/10.1016/j.meatsci.2010.06.012

137. WILSON J.M., LOENNEKE J.P., JO E., WILSON G.J., ZOURDOS M.C. & KIM J.-S. 2012. — The Effects of Endurance, Strength, and Power Training on Muscle Fiber Type Shifting. *The Journal of Strength & Conditioning Research* (6): 1724–1729

138. XU Z., YOU W., ZHOU Y., CHEN W., WANG Y. & SHAN T. 2019. — Cold-induced lipid dynamics and transcriptional programs in white adipose tissue. *BMC Biology* 17 (1). https://doi.org/10.1186/s12915-019-0693-x

139. YANG S.H., AHN E.K., LEE J.A., SHIN T.S., TSUKAMOTO C., SUH J.W., MEI I. & CHUNG G. 2015. — Soyasaponins Aa and Ab exert an anti-obesity effect in 3T3-L1 adipocytes through downregulation of pparγ. *Phytotherapy Research* 29 (2): 281–287. https://doi.org/10.1002/ptr.5252

140. YAZAWA T., INAOKA Y., OKADA R., MIZUTANI T., YAMAZAKI Y., USAMI Y., KURIBAYASHI M., ORISAKA M., UMEZAWA A. & MIYAMOTO K. 2010. — PPAR-γ coactivator-1α regulates progesterone production in ovarian granulosa cells with SF-1 and LRH-1. *Molecular Endocrinology* 24 (3): 485–496. https://doi.org/10.1210/me.2009-0352

141. YONESHIRO T. & SAITO M. 2015. — Activation and recruitment of brown adipose tissue as anti-obesity regimens in humans. *Annals of Medicine* 47 (2): 133–141. https://doi.org/10.3109/07853890.2014.911595

142. YU J., CHEN S., ZENG Z., XING S., CHEN D., YU B., HE J., HUANG Z., LUO Y., ZHENG P., MAO X., LUO J. & YAN H. 2021. — Effects of cold exposure on performance and skeletal muscle fiber in weaned piglets. *Animals* 11 (7). https://doi.org/10.3390/ani11072148

143. ZHAO S.M., REN L.J., CHEN L., ZHANG X., CHENG M.L., LI W.Z., ZHANG Y.Y. & GAO S.Z. 2009. — Differential expression of lipid metabolism related genes in porcine muscle tissue

leading to different intramuscular fat deposition. *Lipids* 44 (11): 1029–1037. https://doi.org/10.1007/s11745-009-3356-9

144. ZHENG Q., LIN J., HUANG J., ZHANG H., ZHANG R., ZHANG X., CAO C., HAMBLY C., QIN G., YAO J., SONG R., JIA Q., WANG X., LI Y., ZHANG N., PIAO Z., YE R., SPEAKMAN J.R., WANG H., ZHOU Q., WANG Y., JIN W. & ZHAO J. 2017. — Reconstitution of UCP1 using CRISPR/Cas9 in the white adipose tissue of pigs decreases fat deposition and improves thermogenic capacity. *Proceedings of the National Academy of Sciences of the United States of America* 114 (45): E9474–E9482. https://doi.org/10.1073/pnas.1707853114

145. ZHOU M., WU T., CHEN Y., XU S. & YANG G. 2022. — Functional Attenuation of UCP1 as the Potential Mechanism for a Thickened Blubber Layer in Cetaceans. *Molecular Biology and Evolution* 39 (11). https://doi.org/10.1093/molbev/msac230

146. ZWICK R.K., GUERRERO-JUAREZ C.F., HORSLEY V. & PLIKUS M. V. 2018. — Anatomical, Physiological, and Functional Diversity of Adipose Tissue. *Cell Metabolism* 27 (1): 68–83. https://doi.org/10.1016/j.cmet.2017.12.002

GLOSSARY OF COMMON ABBREVIATIONS

UCP	Uncoupling Protein
BAT	Brown Adipose Tissue
WAT	White Adipose Tissue
RBL1	Retinoblastoma-Like 1
LPS	Lipopolysaccharide
ADRB3	β3 Adrenergic Receptor
PPARγ	Peroxisome Proliferator-Activated Receptor γ
PGC-1α	PPARγ Coactivator 1 alpha
PRDM16	PRDI-BF1 and RIZ (PR) domain containing 16
DFAT	Dedifferentiation Fat Cell
DMEM	Dulbecco's modified Eagle medium
ACTB	Beta-actin
mtDNA	mitochondrial DNA
COX	Cytochrome c Oxidase
FBS	Fetal Bovine Serum
PKA	cyclic AMP-dependent Protein Kinase
p38	p38 mitogen-activated protein kinases
MAPK	Mitogen-activated Protein Kinase
ERK	Extracellular Signal-regulated Kinas
avUCP	avian uncoupling protein
ISO.	Isoproterenol
TRO.	Troglitazone
PRO.	Propranolol

CS	Citrate Synthase
Bax	Bcl-2-associated X protein
Bak1	Bcl-2 homologous antagonist/killer
H&E	Hematoxylin and Eosin
PBS	Phosphate-Buffered Saline
KLF4	Kruppel-Like Factor 4
C/EBPα	CCAAT-enhancer-binding protein alpha
PPARα	Peroxisome Proliferator-activated Receptor α
LWD	Landrace, Large White and Duroc
ATGL	Adipose Triglyceride Lipase
HSL	Hormone Sensitive Lipase
FASN	Fatty Acid Synthase
aP2	adipose Protein 2
MYH	Myosin Heavy Chain
BW	Body Weight
BW/d	BW/day
CSA	Cross-Sectional Area
18S	18S ribosomal RNA
SEM	Standard Error of the Mean
GLUT4	Glucose Transporter type 4
NST	Non-Shivering Thermogenesis
ATP2A1 (SERCA)	Sarcoplasmic/Endoplasmic Reticulum Ca2+-ATPase
SLN	Sarcolipin
DGEs	Differentiated Genes
FDR	False Discovery Rate